CHARACTERIZATION OF FIREBRANDS GENERATED FROM SELECTED VEGETATIVE FUELS IN WILDLAND FIRES

by

Babak Bahrani

A dissertation submitted to the faculty of
The University of North Carolina at Charlotte
in partial fulfillment of the requirements
for the degree of Doctor of Philosophy in
Infrastructure and Environmental Systems

Charlotte

2020

Approved by:

_____
Dr. Aixi Zhou

_____
Dr. Anthony L. Brizendine

_____
Dr. Stephen L. Quarles

_____
Dr. Nicole L. Braxtan

_____
Dr. Brian I. Magi

_____
Dr. Min Shin

ABSTRACT

BABAK BAHRANI. Characterization of Firebrands Generated from Selected Vegetative Fuels in Wildland Fires. (Under the direction of DR. AIXI ZHOU AND DR. ANTHONY L. BRIZENDINE)

Wildland-Urban Interface (WUI) and Wildland fires cause damages to infrastructure and the environment, resulting in loss of life, property, and an increasing cost of mitigation. Firebrands are known as one of the leading fire spread mechanisms in wildland and WUI fires. A more thorough understanding of the firebrand phenomenon and its role in wildfire spread can lead to the development of better predictive models as well as developing effective mitigation strategies for communities prone to these fires. Firebrand characterization studies to date have been limited to reporting the mean values of physical properties of firebrands based on a small number of samples without a statistical framework. This study presents an effort toward building a statistics-based structure and developing mathematical models to characterize the physical properties of firebrands from selected vegetative fuels. Full-scale firebrand production experiments were designed and carried out in a large wind tunnel facility. Firebrand collection, characterization, and data analysis were based on the statistics-based framework. Firebrand properties (including mass, projected area, and flying distance) were measured and characterized by vegetation species and wind speed.

The outcome of these data was used to find the best probability distribution function and potential correlations among random variables. Results of statistical tests indicated that the likelihood of fitting a lognormal distribution over this dataset was the highest, and

this probability density function was the best fit for this dataset Afterward, a regression model was selected and fitted based on the results of a goodness-of-fit statistical test.

A correlation study in vegetation type and species level showed a strong relationship between the mass and projected area of firebrands regardless of fuel characteristics (i.e., vegetation type and species level) and environmental conditions of the experiment. It also indicated that higher wind speeds are capable of generating firebrands with greater weight and larger projected area. This is an essential takeaway as the accumulation of firebrands on a recipient fuel may start a spot fire, depending on numerous parameters of landed firebrands, receptivity of the fuel, and environmental factors. Nevertheless, based on both factors, it can be concluded that firebrands generated in higher wind speeds are potentially more lethal. Statistical tests in this study showed that higher wind speeds affect the firebrand generation in all vegetation types, although the magnitude of the effect differs by vegetation species. Statistical comparison of the physical property values of firebrands showed that more massive firebrands were generated in higher wind speeds as well as a larger number of generated firebrands. Results also showed that with 95% confidence, the mass values of firebrands were between 0.02 and 0.33-gr, and values for the projected area were between 0.71 and 2.49-cm^2.

Methods developed in this study brought a better understanding of the firebrand phenomenon (particularly firebrand generation). Interpretation of these findings can help various stakeholders in wildland and WUI fire protection in revising the wildfire mitigation strategies. Examples include property owners, the fire/materials and standards engineering communities, government agencies, and the fire and emergency services.

DEDICATION

To my beloved spouse,

Fateme,

who brings happiness, inspiration, and support to my life.

ACKNOWLEDGMENTS

There are many people that I would like to express my gratitude to them for their time contribution during my graduate studies and dissertation writing process.

I am indebted to my dissertation co-chair and academic adviser, Dr. *Aixi Zhou*, for his support from my first day in the Graduate School. *Aixi* provided feedback and advice during all my years at *UNC Charlotte*. I appreciate his hardworking attitude and the relationship we forged over the years.

Thanks to my other dissertation committee members for their time and invaluable service: Dr. *Nicole Braxtan*, Dr. *Brian Magi*, Dr. *Min Shin*, and Dr. *Steve Quarles*. My gratitude goes to the committee co-chair, Dr. *Anthony Brizendine*, for his continuing support during my last year of Ph.D. studies. I particularly thank *Steve* for his extensive knowledge and practical suggestions for my research work.

I am genuinely thankful to all individuals at *UNC Charlotte*, who played a remarkable role during my graduate life: Dr. *Julie Goodliffe*, Dr. *Judith Krauss*, Dr. *Tracy Rock*, Dr. *Scott Rockwell*, Dr. *Lisa Russell-Pinson*, and Dr. *Jy S. Wu*. I would also like to recognize the assistance of my labmates in the *Materials Flammability Laboratory* at *UNC Charlotte* for their collaboration and contribution to this research study. Also, I extend my sincere thanks to *Masoumeh Sheikhi Kiasari* for his crucial remarks that shaped this dissertation.

I am grateful to our industrial collaborators at the *Insurance Institute for Business & Home Safety (IBHS) Research Center* for providing the opportunity to work on full-scale firebrand generation experiments during this research study.

Thanks are also due to the *Joint Fire Science Program (JFSP)* project #15-1-04-4, and at the *University of North Carolina at Charlotte*: *Department of Civil and Environmental Engineering*, *Department of Engineering Technology and Construction Management*, and the *Graduate School*, and at the *North Carolina Agricultural and Technical State University: Department of Applied Engineering Technology*, for providing financial support during my graduate studies.

Most importantly, I express my most profound appreciation and gratitude to my spouse, *Fateme*, which her continued patience, support, and love make this dissertation possible.

Table of Contents

List of Tables

List of Figures

Glossary

AIC	Akaike Information Criterion
ANOVA	Analysis of Variance
BIC	Bayesian Information Criterion
IBHS	Insurance Institute for Business & Home Safety
MC	Moisture Content
MLE	Maximum Likelihood Estimation
NCA	National Climate Assessment
PDF	Probability Density Function
USDA	United States Department of Agriculture
WUI	Wildland-Urban Interface

CHAPTER 1: RESEARCH OBJECTIVES, GOALS, AND SCOPE

1.1 Introduction

Wildland and Wildland-Urban Interface (WUI), and more generally large outdoor fires have been an increasing global problem. (Cohen 2008; Fernandez-Pello et al. 2015; Hudson and Blunck 2019). The risk of large outdoor fires exists both for civilians and infrastructures.

There are three main categories of large outdoor fires: wildfires, urban fires, and WUI fires. A wildfire originates from an unplanned ignition and can spread based on various parameters such as weather and topographical conditions and fuel characteristics.

A planned, low-intensity fire to assist with mitigating the wildfire activity and, as a result, reducing the risk of wildfire spread (Bennett et al. 2014) is called a prescribed burn, also known as a controlled, planned, vegetation management, or hazard reduction burn, or Rx fire. Fire has a potent effect on the vegetation structure, composition, and nutrient cycling, and therefore plays an essential role in grassland ecosystems (Anderson 2006), so a prescribed fire in case of an urgent need to reduce fuel for wildfire spread could assist in preventing or reducing the severity of wildfires, and keeping the grassland resilient.

The United States has a long history of large outdoor fires. Examples of the urban fires are the 1872 great Chicago fire and 1906 post-earthquake San Francisco fire, both of which resulted in massive destruction and fatalities.

The area where infrastructure or other human development meet with the undeveloped wildland fuels is called a Wildland-Urban Interface (WUI) (Fire Executive Council 2009). Most recently, some of the largest outdoor fires have occurred in California. The December

2017 Thomas fire in Ventura County (Southern California), burned more than 114,000 acres (~46,000 ha). In November 2018, the Camp fire was spread in Butte County in Northern California, resulting in 86 fatalities, destruction of nearly 19,000 structures, and burning of over 150,000 acres (~61,000 ha). The Camp fire is the 7th largest and most destructive wildfire to date in U.S. history.

Environmental factors also play an important role in the increasing number of wildfires. The latest National Climate Assessment (NCA) Report (published in 2019) showed that the average temperature in the western United States has increased by 1.9°F (1.1°C), and the average length of wildfire season has increased from 5 months to 7 months in this region (Jay et al. 2018).

Wildfire spread is a complex multi-physics phenomenon that depends on fuel characteristics, topography, and environmental conditions (meteorology or weather). There are three accepted mechanisms of wildfire spread: 1) direct flame impingement on un-burned fuels, 2) radiant and convective heat transfer from burning vegetation and structures to surrounding fuel sources, and 3) spotting from wind-blown firebrands ahead of the fire front.

While studies have shown that radiant and convective heat transfer is most commonly responsible for the destruction of forests, wind-blown firebrand showers are proven to be a significant source of heat transfer, and responsible for the majority of the structure ignitions. As Jack Cohen stated, “WUI problem is a home ignition problem, not a wildfire control problem.”

The generation and distribution of firebrands is also a very complex natural phenomenon which depends on fire characteristics, fuel characteristics, and environmental conditions.

Various models have been developed for lofting, transportation, and ignition of fuel bed initiated by firebrands. To better understand the spotting phenomenon, the characterization of firebrands from various fuels, both structural and vegetative, is necessary. Characterization has typically been performed based on the physical properties of firebrands. Previous characterization studies indicated that multiple parameters in the firebrand phenomenon, including lofting height, flying distance, combustion rate, and ignition potential of firebrands, are all correlated with the mass and shape of individual embers.

To date, there is no comprehensive study on the characterization of firebrands from various vegetation types that utilized a statistical-based framework. Previous studies were mostly focused on reporting experimental data of firebrands from vegetative fuels (Filkov et al. 2017; El Houssami et al. 2016; Manzello et al. 2008; Manzello et al. 2007; Suzuki and Manzello 2011; Thomas et al. 2017). As a result, a detailed characterization of the formation and physical properties of such fuels plus a statistical description was justified.

1.2 Objectives, Goals, and Scopes

The purpose of this dissertation is to address the gaps discussed in section 1.1 regarding the need for characterization of firebrands. This research is focused on the first sub-process of the firebrand phenomena: generation from the wildland vegetative fuels. This study was part of a 5-year project supported by the Joint Fire Science Program (JFSP) [Grant ID# 15-1-04-4] (Zhou et al. 2019).

A thorough study of the variability among these parameters could lead to a better understanding of the ignition potential of firebrands as a function of vegetation type and, consequently, spotting and wildfire spread mechanisms. Full-scale experiments were

conducted to understand better the effect of the environmental conditions and vegetative species on the firebrand generation process and to develop data regarding critical physical parameters of firebrands, mass, projected area, and flying distance were characterized.

The following objectives were defined for this research study to address the current gap in the characterization of firebrands from wildland fuels:

1. To conduct a thorough review of previous studies focused on firebrands generated from vegetative fuels
2. To utilize the largest to date dataset of generated vegetative firebrands from a laboratory-scale experiment to develop a statistical framework for firebrand characterization
3. To develop a predictive parametric model to describe physical properties of vegetative firebrands (such as area and mass) in addition to the mutual effects of each parameter
4. To perform a comparative analysis of the current dataset with other laboratory-scale experiments in the U.S.

1.3 Organization of this Dissertation

The first chapter of this dissertation is the introduction and discussion of goals, objectives, and scope of the work. In the second chapter, the previous field, laboratory-scale, and modeling studies focused on firebrands generated from vegetative fuels are reviewed.

The third chapter discusses the selection criteria and specifications of vegetative fuels, experimental design, post-test activities, initial characterization, and preparations before the start of the statistical analysis process.

Chapter four introduces a new statistical framework to characterize firebrands from wildland fuels. A thorough statistical analysis was performed, and a predictive parametric model was developed based on firebrand mass, projected area, wind speed, and interaction terms of every two physical parameters employing regression analysis.

At last, chapter five summarizes significant findings and outcomes, and focuses on the impacts and significance of this study as well as introduces organizations that could benefit from these results.

CHAPTER 2: LITERATURE REVIEW

2.1 Wildfire and Wildland-Urban Interface (WUI) Problem

Wildfires and Wildland-Urban Interface (WUI) fires caused severe damage to infrastructures and have been a threat to housing communities for decades in the United States and many other countries (Cohen 2008; Manzello et al. 2007).

WUI fire spread could be a result of both vegetative and structural fuels (Mell et al. 2010). As the initial ignition occurs, communities prone to WUI fires are potentially at risk of exposure to fire spread mechanisms such as heat exposure, direct flame attack, and generated wind-blown embers (also referred to as firebrands). WUI fire problem was defined as a structure ignition problem (Cohen 2008; Mell et al. 2010).

Data collected by the California Department of Forestry and Fire Protection indicated that fire suppression costs have dramatically increased over the past three decades, from ~$12 million in 1980 to $773 million in 2018 (CAL FIRE 2019).

Reports also show that among the ten most destructive fires in California history, five of them occurred during the past five years with an increasing amount of fatalities, structural loss, and burned areas (CAL FIRE 2018). The Camp wildfire in California burned over 150,000 acres and destroyed almost 19,000 houses (CAL FIRE 2018).

The average temperature of western states has increased by 1.9ºF (1.1ºC), and the average length of wildfire season has increased from 5 months to 7 months in this area (Climate Central 2012; Goodrick et al. 2013). Temperature rise resulted in the melting of early snow on peaks (average of 4 weeks earlier), and drier forests and vegetative areas. Consequently, wildland fires became more lethal and severe during the past decades. Both human and

natural climate contributors in the past four decades resulted in an increase of wildfire potential in the western states (Abatzoglou et al. 2016). Consequently, wildland fires became more lethal and severe during the past decades. It is expected that temperature increases between 2.5ºF- 6.5ºF (1.4ºC – 3.6ºC) will occur by the mid-century in western states (Tompkins et al. 2014).

A report published by the National Climate Assessment (NCA) indicated that how the cumulative area burned by wildfires in the western United States has increased over 30 years due to climate change, and that how climate change has driven wildfires (Abatzoglou et al. 2016; Westerling 2016). Figure 2.1 shows the impact of climate change on the severity of wildfires, in terms of acres burned, between 1984 and 2015 in the western United States.

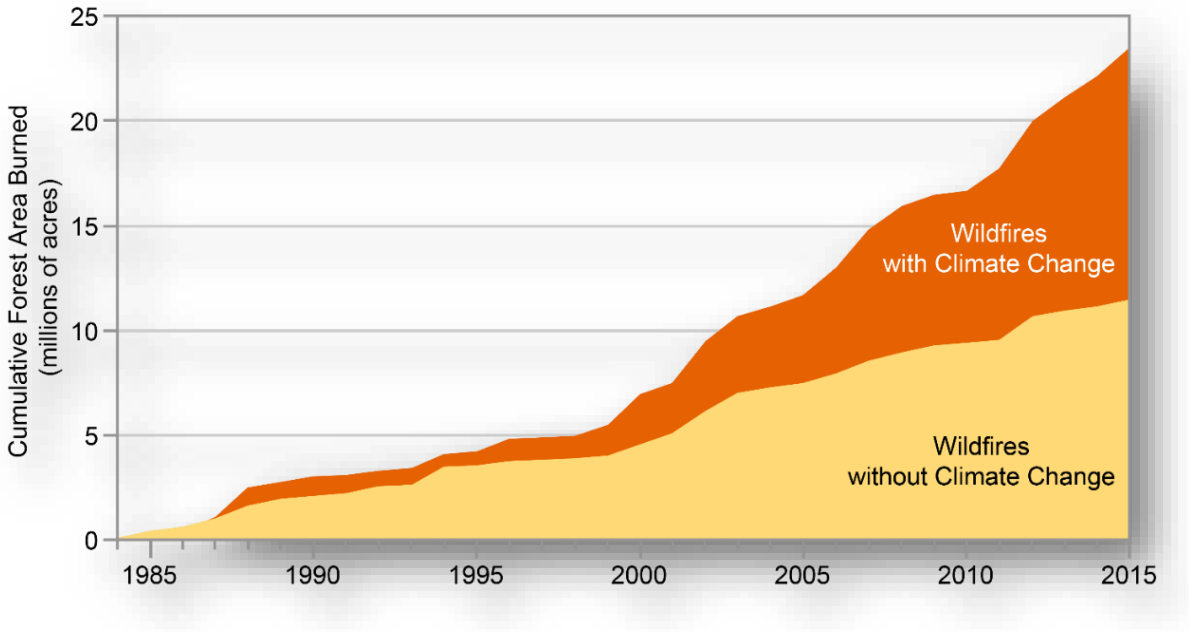

Figure 2.1. The cumulative forest area burned by wildfires has dramatically increased between 1984 and 2015. Adapted from (Abatzoglou et al. .2016; Garfin et al. 2018)

Figures 2.2 shows all wildland fires in the United States in 2019 (GeoMAC 2019). This figure indicates that most of the wildfires on the east coast were human-caused, whereas, on the west coast, they were also natural-caused (i.e., lightning). Also, despite the number of wildfires on the east coast, they have been less destructive compared to west coast fires. Data from 2019 shows that North Carolina had 3,872 wildfires, with a total of 14,548 burned acres (~5,900 ha). In comparison, the state of California had 8,194 fires, with 259,148 burned acres (~105,000) (NICC 2019). There have been few studies focused on firebrand generation from vegetative fuels (Koo et al. 2010; Manzello et al. 2008; Manzello et al. 2007; Manzello et al. 2009). The remaining studies on firebrand generation and characterization were limited to the reporting of the experimental data (Hedayati 2018; Suzuki et al. 2012; Suzuki et al. 2013; Yoshioka et al. 2004; Manzello 2014; Suzuki et al. 2016).

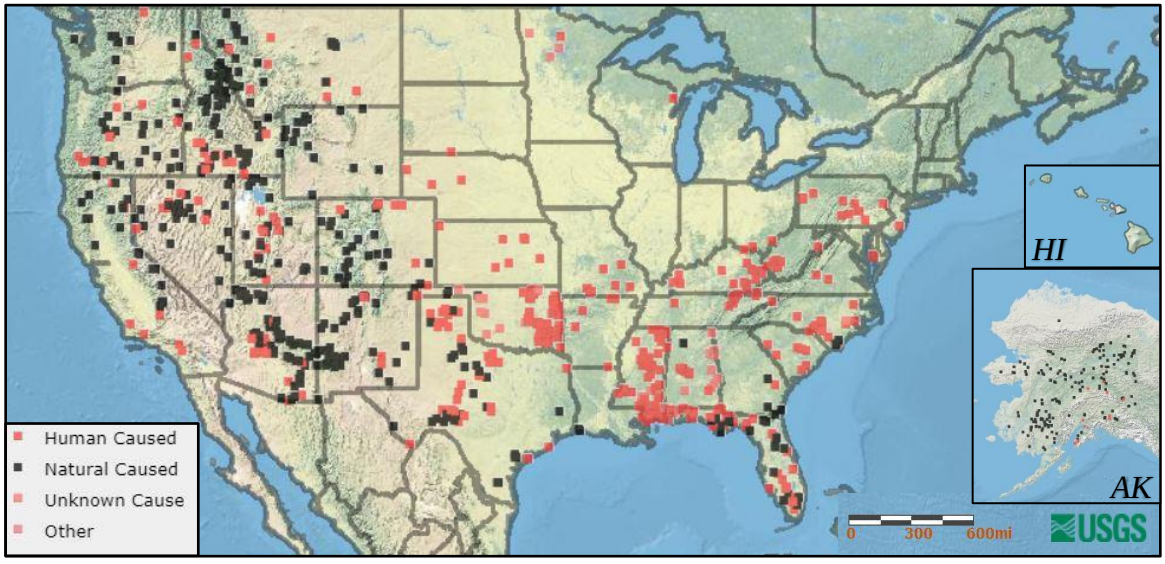

Figure 2.2. Wildland Fires in the US during 2019 2019 (GeoMAC 2019)

Most of the fires in the southeast United States are not wildfires, but prescribed fires set by federal or national agencies, where more than 5,000 fires burned a total of 323,000 acres (~131,000 ha) (Calkin et al. 2011). One recent notable exception is the 2016 Chimney Tops

2 wildfire in the Great Smoky Mountains (near Gatlinburg, Tennessee), a human-caused fire that has been one of the largest wildfires in the southeast region of the U.S. It resulted in 14 casualties, and burned nearly 17,900 acres (~7,250 ha), and burned 2,545 structures (National Park Service 2017).

A study by Jolly et al. analyzed the 35 years of meteorological data and confirmed an increase in the length of the fire season globally (Jolly et al. 2015). The authors considered four dominant parameters of fire seasons in the study, including maximum temperature, maximum wind speed, minimum relative humidity, and the number of days with no rain. Note that the study did not include the intensity or fire spread rates (Jolly et al. 2015; NASA 2018). The US National Academy of Sciences reported that the length of fire seasons in the western US has expanded by 2.5 months (Climate Signals 2018).

The wildfire problem is an increasingly global issue. The largest wildfire evacuation in Alberta, Canada, happened during the 2016 Horse River Wildfire (Fort McMurray), where more than 1.4 million acres (~590,000 ha) were burned (MNP LLP 2017). Recent wildfires in Australia started in September 2019 and lasted until February 2020, where more than 46 million acres (~18.6 million ha) and over 2,000 structures were burned. This wildfire also caused 34 casualties (Center for Disaster Philanthropy 2020).

One strategy to reduce the hazard and intensity of wildland fires is prescribed fires. Such fires are set under the control of fire service to burn the leaf litter, shrubs, and brush accumulated in wildlands (Calkin et al. 2014). This strategy is not frequently employed in western states compared to eastern states regarding the landscape size, drought problems, and vegetative area with lower moisture content; the latter could result in an uncontrollable fire if a prescribed fire is started and got out of control.

Figure 2.3 illustrates the total acres and the number of fires in the past two decades in the United States. More thorough firebrand generation and characterization studies could result in a better understanding of wildfire spread mechanisms and spotting in general, and results could assist in also better characterizing local vegetative and structural fuels. Data from the characterization of structural assemblies and dominant vegetation (e.g., Cedar and Southern Pine) could be summarized in firebrand prone areas in this region (and other parts of the United States.

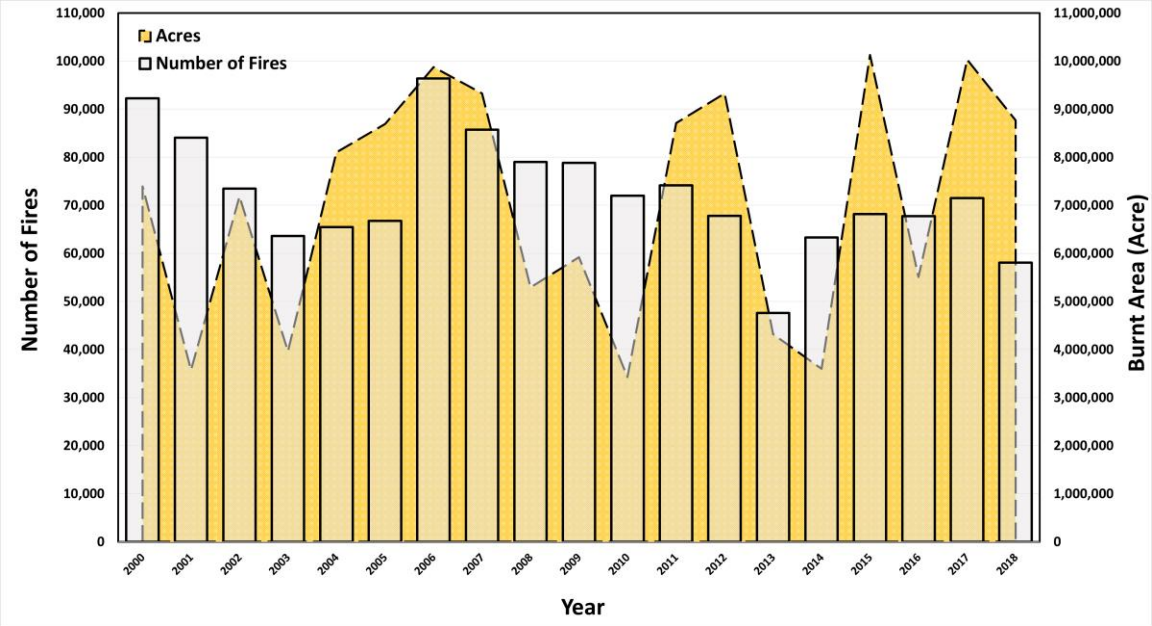

Figure 2.3. Total Wildland Fires and Acres (2000-2018)

2.2 The Firebrand Phenomenon

Studies on the firebrand phenomena in the United States goes back to the 1960s. Ignitions in wildland areas do not necessarily result in large fires. The probability of initiation of fire by firebrands is a function of 1) firebrand properties such as fine dead fuel moisture, shape,

mass, heat content, and 2) recipient fuel bed properties such as moisture content, length of contact, surface-to-volume ratio (Deeming et al. 1974; Koo et al. 2010).

As shown in Figure 2.4, the firebrand phenomena can be divided into three sequential sub-processes: 1) generation and detachment, 2) lofting and transportation, and 3) landing and ignition of the recipient fuel. Firebrands are generated from both wildland fuels and structures. Examples of wildland fuels are trees, shrubs, and grass species. Structural assemblies such as fences, roof shingles, decks, and shakes can also be a source of firebrand generation, although once a structure ignites, many interior and exterior combustible materials could produce firebrands. Numerous factors affect the generation process from a structural or wildland fuel, such as the fuel type, classification, and morphology, and climate conditions, and the intensity of the originating fire (Manzello et al. 2020). Firebrands are generated due to thermal decomposition of fuel while burning, where decomposition leads to a decrease in structural integrity and, consequently, detachment of a piece from the burning fuel. The detached part may be in smoldering or flaming state.

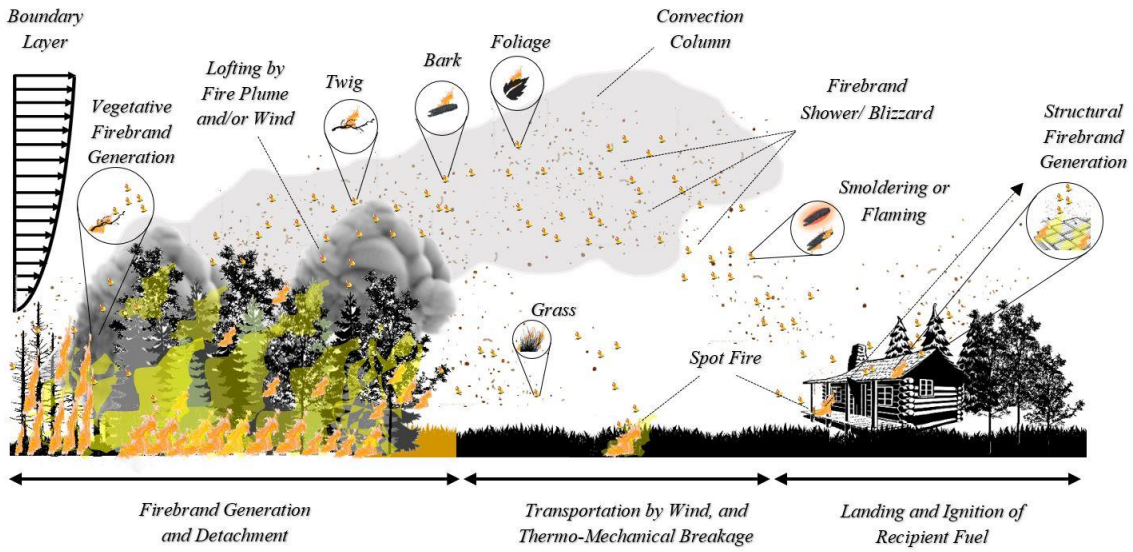

Figure 2.4. Different Processes of Firebrand Phenomenon in a Wildland Fire

Generated firebrands could then be transported by wind or fire plume. Transportation has been investigated the most among the three sub-processes of the firebrand phenomena.

Ignition by a firebrand occurs in four stages (Deeming et al. 1974).

1) Proper contact with recipient fuel bed
2) Loss of moisture content in the recipient fuel bed
3) Temperature rise to pyrolysis range
4) Heating of gas up to the ignition temperature

The ignition potential of firebrands depends on many factors such as the number and thermal inertia of firebrands, environmental conditions like wind intensity and direction, and characteristics of the recipient fuel bed such as moisture content, packing density, surface-area-to-volume ratio, and fuel size.

2.3 Summary of Previous Firebrand Generation and Characterization Studies

Firebrand characterization is a relatively new field in the wildland and wildland-urban interface (WUI) fires. As mentioned earlier, the firebrand phenomenon has three steps: 1) generation (production), 2) transportation, and 3) ignition.

Koo and others (Koo et al. 2010) studied firebrand phenomena and previous experiments and models. They focused on spotting as one of the main mechanisms of fire spread during wildland, WUI, and post-earthquake fires. They also reviewed the developed combustion models that were focused on firebrand trajectories. Although spotting plays a vital role in fire spread, it has not been appropriately modeled to date. Some empirical (McArthur 1967) and mathematical models (Albini 1979b) for vegetative fuels, accumulated vegetative fuels (Hargrove et al. 2000), and wind-driven fires (Albini 1983a) have been developed. Firebrand spread is also a function of surface smoothness; the more homogeneous a surface

is, the higher the fire spread rate is (Porterie et al. 2007). A firebrand's life span (i.e., the time between ignition and burnout) also determines the flying distance, and consequently, ignition potential and spotting (Baum and Atreya 2014). More studies are discussed in sections 3.3 and 4.1.1 of this dissertation.

2.4 Summary of Previous Statistical Analysis on Experimental Data

Studies have been performed both in and outside of the United States focusing on a statistical analysis of risk analysis, fire spread pattern and severity (Belkacem et al. 2015; Hernandez et al. 2015), fire frequency, classification based on flammability, fire spread, and wildfire modeling (Holmes et al. 2008) in wildland and WUI fires.

Muraszew suggested statistical models for both firebrand generation and ignition as they land on a recipient fuel bed (Muraszew et al. 1976). Studies on structural firebrands also recognized firebrand exposure as a critical problem in wildland and WUI fires and found statistical correlations between different assemblies (e.g., roof) and increase in structures' loss (Abt et al. 1987; Gordon 2000; Ramsay et al. 1986; Wilson et al. 1986).

A study by Ganteaume et al. (2011) reported on the development of a statistical method to model the thermal decomposition of vegetative firebrands in the Mediterranean region. The team characterized vegetative firebrands based on their physical properties (mass, surface, surface-to-volume ration), flammability properties (time-to-ignition, sustainability, ignition frequency), and mass-loss rate. Although they utilized one-way, parametric analysis of variance (ANOVA) in their study, the team did not build a PDF and/or a statistical model based on their findings.

The first characterization study in the United States characterized the mass and projected area of firebrands (Suzuki et al. 2012). The characterization method in this study was limited to utilizing a precision balance and digital image analysis. Studies after that were built upon three approaches: 1) different firebrand generation and collection methods, 2) indoor vs. outdoor tests, and 3) medium-scale (experimental) vs. full-scale setup (Suzuki et al. 2013; Yoshioka et al. 2004).

Characterization in studies to date has been limited to reporting mean values of mass and projected area (Hedayati 2018; Suzuki et al. 2012; Suzuki et al. 2013; Yoshioka et al. 2004; Manzello 2014; Suzuki et al. 2016) and flying distance (Zhou et al. 2015). Also, studies have been mostly focused on plotting histograms to characterize firebrands' physical properties. Different probability density functions (PDFs) could be created considering different possible class intervals (bin sizes) in such a method. To increase the reliability of the model, a more robust PDF is needed, where it can perform well for data withdrawn from a range of probability distributions, specifically for non-normal (non-Gaussian) ones (Huber 2004; Farcomeni 2016).

Hedayati performed statistical analysis on available firebrand data and employed the Bayesian approach to find the most suitable probability density function (PDF) models to characterize firebrands regarding their most dominant physical properties (Hedayati 2018). Three physical properties: flying distance, mass, and projected area, were used as parameters of interest in this study to characterize the structural firebrands. This characterization method could be further used to build probability functions and models on spotting and wildfire spread.

Tohidi (Tohidi et al. 2015) performed statistical analysis on experimental findings from previous studies (Koo et al. 2010; Manzello et al. 2008; Manzello et al. 2007; Manzello et al. 2009). Findings from those studies indicated that the predominant shape of firebrands generated from the coniferous trees in no wind condition could be considered as long, thin cylinders. Based on this assumption, and the length (L), diameter (D), and density (ρ) of firebrands, an aspect ratio (η = L/D) were developed to estimate the correlation between the surface area (s) and mass (M) of firebrands. A dimensional analysis study was performed, and considering the assumption that all generated firebrands have identical aspect ratios, a scaling relationship of $s \sim m^{2/3}$ was obtained. The power-law relationship was further utilized in the characterization of firebrands from the previous studies mentioned above.

CHAPTER 3: EXPERIMENTAL DESIGN

3.1 Introduction

This chapter reports on the design of the experiments of firebrands generated from selected vegetative fuels conducted under full-scale laboratory conditions. Physical properties, including mass, projected area, and flying distance of firebrands produced from burning wildland fuels under certain environmental conditions, were investigated and measured. A description of the data analysis methodology used for firebrand characterization is also included. The dataset can be used to build a best-fit statistical model to describe firebrand generation. The analyzed data presented in this research study is hosted on a public repository.

3.2 Experiment Design

The experiment design was divided into three main sections: pre-test, test, and post-test.

3.2.1 Pre-Test

This section focuses on material selection, experiment design process, and parameters selected to be monitored during the experiment.

3.2.1.1 Material Selection and Collection Sites

There were two main criteria for choosing vegetative fuels in this study:

1) Vegetative fuels should represent typical wildfire fuels in various regions of the United States that are prone to generate firebrands, and,
2) Vegetative fuels should be accessible to the research team for collection and testing purposes.

A diverse range of wildfire fuels from four states in the United States was selected, collected, and delivered to the Insurance Institute for Business & Home Safety (IBHS) Research Center in Richburg, South Carolina. The vegetation chosen is shown in Table 3-1.

Table 3-1. Specifications of Vegetative Fuels

Vegetation Level	***Vegetation Type [Scientific Name]***	***Collection State [Site]***
Grass	Little Bluestem Grass *[Schizachyrium scoparium]*	Texas
Shrubs	Chamise* *[Adenostoma fasciculatum]*	California *[North Mountain Experimental Area near Riverside]*
	Saw Palmetto *[Serenoa repens]*	South Carolina *[Victoria Bluff Heritage Preserve/ Wildlife Management in Bluffton]*
Trees	Loblolly Pine *[Pinus taeda]*	South Carolina *[IBHS Property]*
	Leyland Cypress *[Cupressus × leylandii]*	*[Tree Farm in Chester County and IBHS Property]***

** Cut into branches and reassembled into the cylindrical wired form before testing (Figure 3.4)*
*** Cypress trees collected from Tree Farm were used in Phase I (2016), and those from IBHS Property were used during Phase II of the research study (2017)*

3.2.1.2 Environmental Conditions Monitoring

Moisture content (MC) is defined as the amount of water present in a specimen. There are two main methods to calculate moisture content (ToolBox 2012):

1) Wet Basis

$$MC_w = M_{water} / m_w \qquad \text{(Eq. 3.1)}$$

$$= M_{water} / (M_{water} + m_d)$$

where:

MC_w = *Moisture Content on Wet Basis*

M_{water} = *Mass of Water [kg]*

m_w = *Total Mass of Moist (Wet) Sample - Mass of Solid and Mass of Water [kg]*

m_d = *Mass of Dry Solid [kg]*

2) Dry Basis

$$MC_d = M_{water} / m_d \qquad (Eq.\ 3.2)$$

where:

MC_d = *Moisture Content on Dry Basis*

M_{water} = *Mass of Water [kg]*

m_d = *Mass of Dry Solid [kg]*

Both wet and dry moisture content of vegetative specimens were monitored and recorded per arrival and before tests. A summary of MC levels is shown in Table 3-2.

Table 3-2. Recorded Moisture Content (MC) Level of Vegetative Samples

Vegetation Level	***Vegetation Type***	***Vegetation Part***	***Initial***		***Test Day***	
			Wet	***Dry***	***Wet***	***Dry***
Grass	Little Bluestem Grass	*Not Recorded*				
Shrubs	Chamise	*N/A*	*Not Recorded*		66.04	60.54
	Saw Palmetto	Fond	141.65	87.61	127.58	94.89
		Stem	63.77	46.40		
Trees	Loblolly Pine	Needle	18.61	15.64	58.63	56.68
		Twig	22.49	17.02		
		Branch	57.13	29.32		
	Leyland Cypress	Needle	16.47	14.61	73.77	68.97
		Twig	18.76	15.94		
		Branch	30.52	21.74		

3.2.1.3 Experimental Setup and Layout

Whole-plant experiments were conducted in the IBHS Research Center's wind tunnel test chamber in Richburg, South Carolina. A water-filled pan layout was designed to collect the firebrands in two test stations in the chamber. Sizes of testing stations, where specimens and natural gas burner or pine needle bed were located, were not uniform across vegetation types regarding the size, shape, and ignition type of the samples. Three designs for different specimens are shown in Figures 3.1, 3.3, and 3.5.

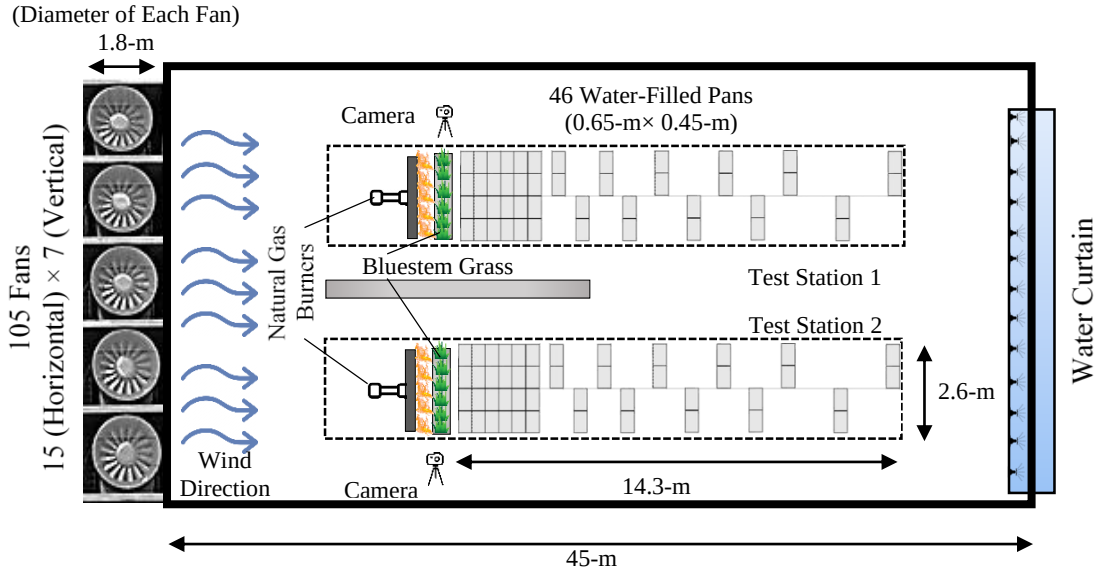

Figure 3.1. Test Station for Grass Specimen

Little Bluestem grass specimens were grouped in five rows with 18 plants per row (total of 90 plants per test). Plants were in a 2.4-m (8-ft.) wide bed (25.4-cm (1-ft.) per plant). A 2.4-m (8-ft.) line burner using natural gas, positioned at the leading edge of the vegetation, was utilized to initiate ignition for Little Bluestem grass specimens, shown in Figure 3.2.

Figure 3.2. Little Bluestem Grass Specimens and Line Burner before Test
(Photo Courtesy of IBHS)

Saw Palmetto and Chamise samples were burned using a 3-m wide × 5-m long (10×16-ft.) pine needle bed. Chamise specimens were cut into branches in the field and reassembled in the lab into cylindrical wired form (cage) before testing, as shown in Figure 3.4.

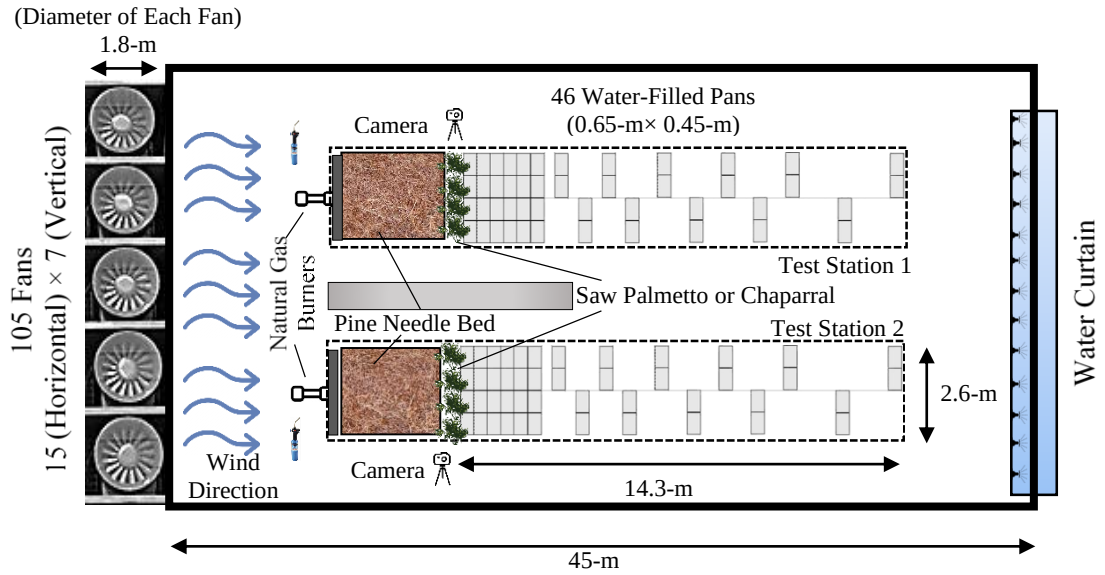

Figure 3.3. Test Station for Shrub Specimens

Figure 3.4. Pine Needle Bed and Chamise Samples before Test. Note chamise branches have been inserted into the cylindrical cage. (Photo Courtesy of IBHS)

Saw palmetto vegetation was positioned and held on a metal sample holder apparatus. For each test, four plants were used, as shown in Figure 3.5. A 3-m (10-ft.) slotted line burner was using to start ignition for palmetto and chamise specimens.

Figure 3.5. Pine Needle Bed and Saw Palmetto Samples before Test (Photo Courtesy of IBHS)

Tree samples were tested in a horizontal orientation for the series of experiments to facilitate the complete burn of the smaller branches and foliage of the tree, and to observe the maximum firebrand generation potential of tree specimens. Note, experiments were conducted with a tree in a vertical orientation, but in a wind field, only a section of the tree would ignite and burn. A tree holder was designed to allow trees as high as 2.4-m to 3.66-m (8 to 12-ft.). A star-shaped natural gas burner was used for direct flames on the tree samples. Test station design and tree specimens are shown in Figures 3.6 to 3.8.

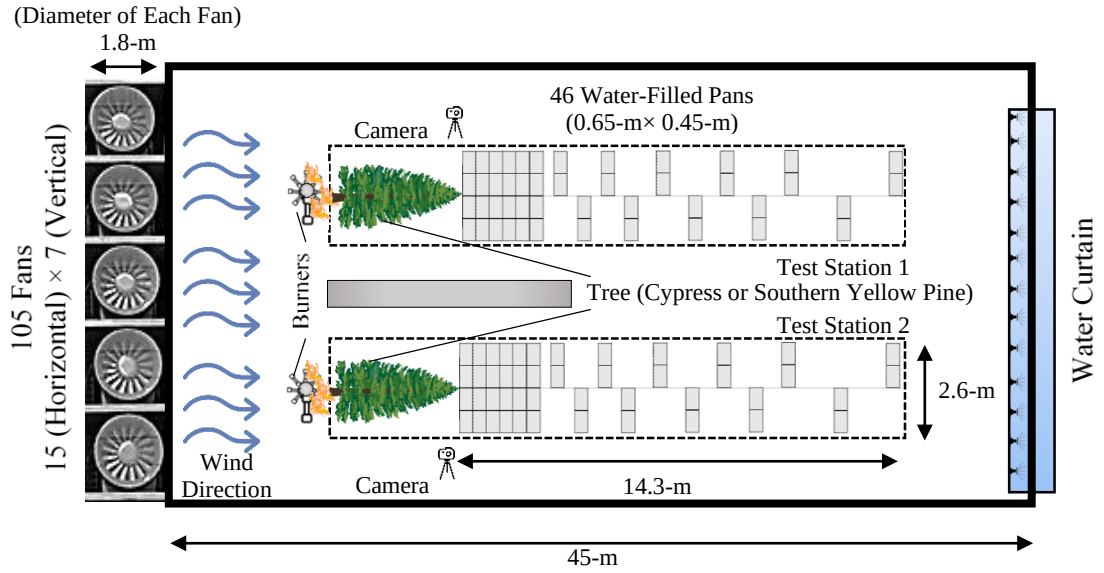

Figure 3.6. Test Station for Tree Specimens

Figure 3.7. Leyland Cypress Tree before Test (Photo Courtesy of IBHS)

Tree stations were relatively shorter comparing to shrubs, where a natural gas burner and pine needle bed were used to ignite the tree specimens and shrub specimens, respectively.

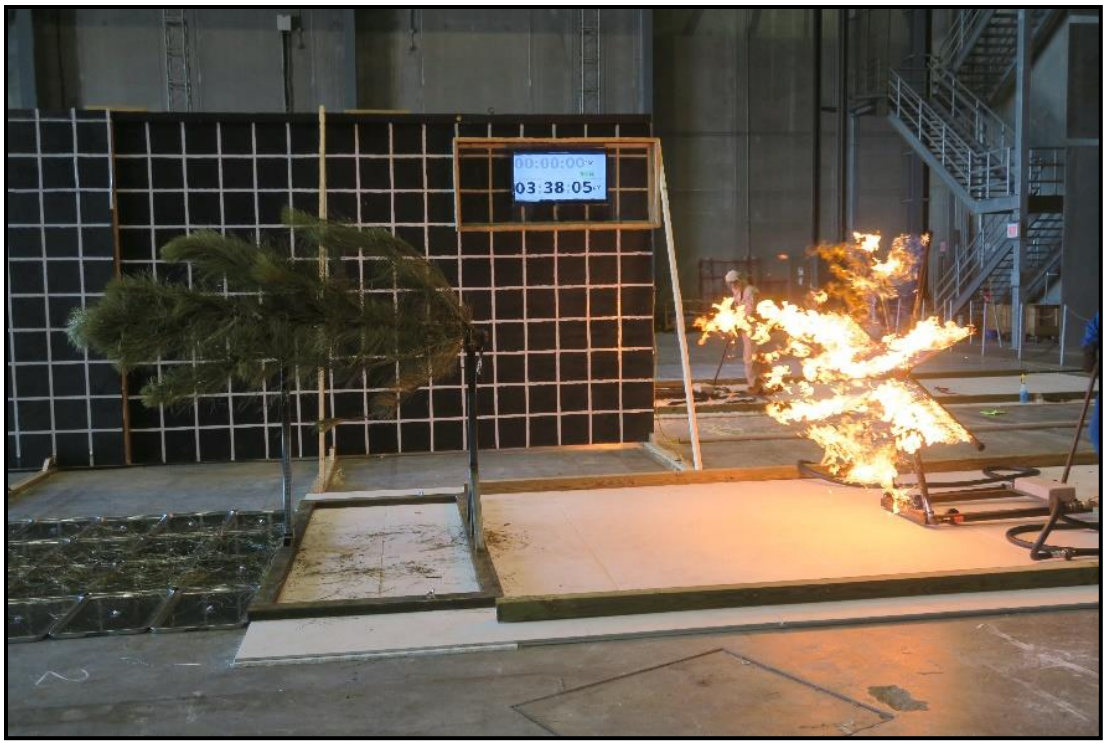

Figure 3.8. Test of Loblolly Pine Tree and natural gas “Star” burner before Ignition of the Tree (Photo Courtesy of IBHS)

A staggered water-filled pan layout was designed for this experiment to collect the lofted firebrands, assuming a symmetrical distribution of flying firebrands. Location and distance of pans from the fire source are essential since it indicated the flying range of lofted firebrands. As seen in Figure 3.9 (Hedayati et al. 2019), pans did not cover the entire floor area of test collection areas. Consequently, not all the generated firebrands from tests were collected. However, a proper statistical model can predict the landing location of firebrands in an experimental setting. Pan layout was determined based on work by Hedayati (2018).

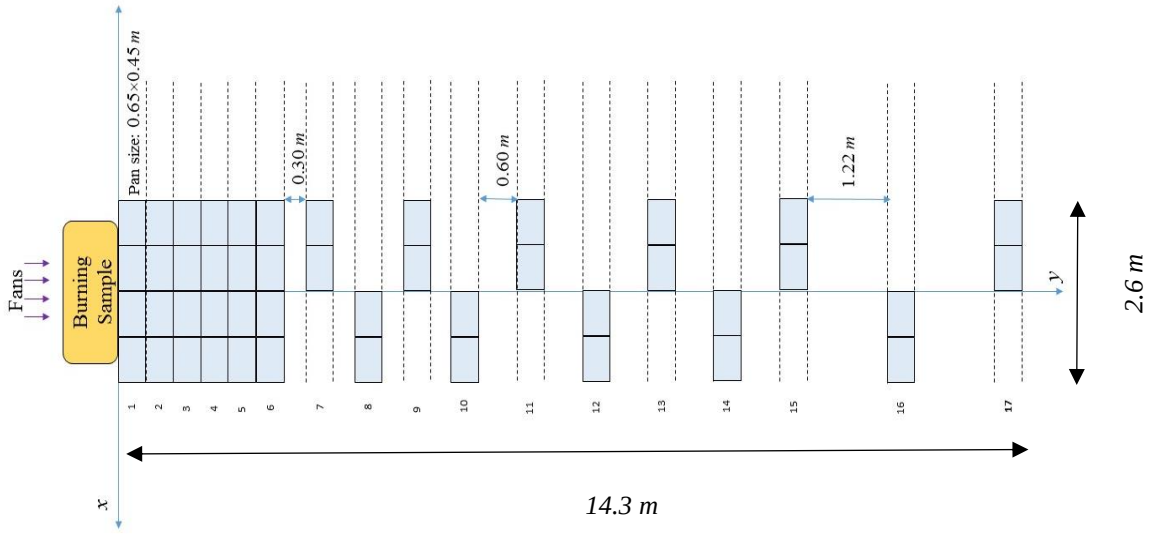

Figure 3.9. Burning Sample and Pan Layout in the IBHS Testing Chamber (*Not-to-Scale*)

For each test station, 46 aluminum pans, 0.65-m long × 0.45-m wide (2-ft. × 1.5-ft.), were used downwind of vegetation in the test chamber. A screen mesh was submerged into the water in each container to capture the landed firebrands. The mesh screen facilitated the collection of firebrands.

Considering the pressure drop downwind of the vegetation specimens due to the separation of boundary layers, a significant number of generated firebrands could land a short distance from the fire source. Hence, the first six rows of pans were placed continuously downwind of the specimen to capture the maximum possible generated firebrands.

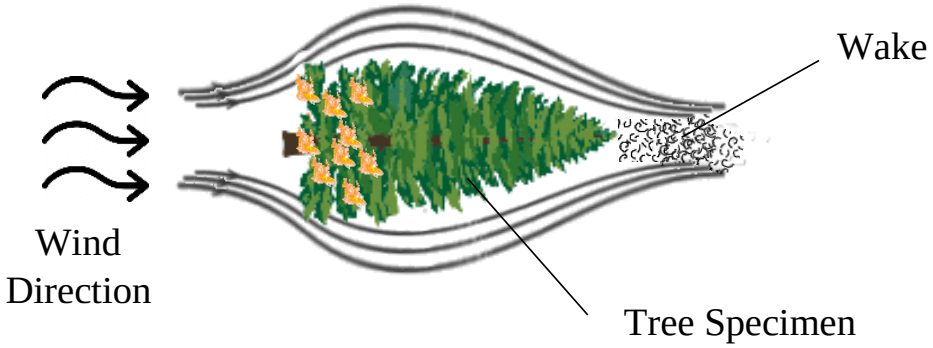

Figure 3.10. Wake Flow Formation Downwind of Vegetative Samples

3.2.2 Test

All tree samples were weighed before and immediately after the test. Experiments were conducted at three average wind speed levels: idle non-fluctuating (5.36-m/s or 12-mph), medium fluctuating (11.17-m/s or 25-mph), and high fluctuating (17.88-m/s or 40-mph). Three replicates for each species were used at each wind speed. Where the idle wind velocity was constant, the 3-s gust peaks for the fluctuating wind speeds were 14.3-m/s (32-mph), and 23-m/s (51-mph) for the fluctuating medium and high wind velocity record, respectively.

Collected firebrands were transferred from the water-filled pans by removing the screens to an oven maintained at 103°C (217.4°F) for a minimum of 24-hours. Photos of different stages of testing a Leyland cypress tree at medium wind speed are shown in Figure 3.11.

(1) Leyland Cypress Tree- Front View

(2) Leyland Cypress Tree- Side View

(3) Flame Impingement

(4) Ignition/ Firebrand Generation

(5) Tree Stem after the Test

(6) Collection Pans

Figure 3.11. Testing of Leyland Cypress Tree at Medium Wind Speed (Photo Courtesy of IBHS)

Oven-dried firebrands were carefully stored in separate sealed plastic bags, where only one layer of collected firebrands was stored in each bag, and bags were separated using multiple layers of paper towels to minimize the risk of breakage in samples during transportation. Firebrands were transferred to the *Materials Flammability Laboratory* at the *University of North Carolina at Charlotte* for initial characterization.

3.2.2.1 Vegetative Firebrand Generation

Firebrand generation tests from vegetative fuels at IBHS Research Center were performed in two phases during 2016 and 2017. Daily notes and observations from each of the tests were obtained from IBHs and are reproduced in Tables 3-3 to 3-5.

3.3.2.1.1 Grass

Table 3-3. Observations during Generation of Firebrands from Bluestem Grass

Date	***Specimen***	***Rep.***	***Wind Speed***	***Vegetation Arrivals & Notes***
11/02/2016	Little Bluestem Grass	1	Idle	▪ Test Duration: 4-min ▪ Direct flame impingement: 20-s ▪ Low firebrand generation ▪ Rapid fire spread ▪ Most of the firebrands landed in rows 1-4. ▪ The back row of live grass did not burn. ▪ 1:45 turned burner back on, live grass still not burning. 2:30 gas off
		2		▪ Test Duration: 4-min ▪ Direct flame impingement: 20-s ▪ Full open gas valve 30-s into the test for 45-s ▪ The back row of live grass did not burn
		3		▪ Test Duration: 4-min ▪ Direct flame impingement: 20-s ▪ All dead grass burned after 1.5-min
11/03/2016		1	Medium	▪ Test Duration: 4-min ▪ Direct flame impingement: 30-s ▪ All dead grass burned after 1.5-min ▪ Grass burned quickly, only stubs left of the green grass ▪ Smoldering of roots in the holder observed
		2		▪ Test Duration: 4-min ▪ Direct flame impingement: 30-s ▪ Green grass singed ▪ All dead grass burned
		3		▪ The slow progress of fire through live grass to dormant at low gas setting. ▪ Not many embers produced except in immediate vicinity Green grass singed
11/04/2016		1	High	▪ Only knubs of live grass left ▪ Some of the longer live grass stalks did not burn as completely as when the tests were at Med or Idle wind speed
		2		▪ Test Duration: 4-min ▪ Direct flame impingement: 30-s ▪ All dormant and live-dormant burned quickly
		3		▪ Dormant grass burns quickly, live grass does not, even when dried overnight ▪ Smoldering of roots observed for several minutes after the test. ▪ Once burner off, flaming was ended, not sustained

3.3.2.1.2 Shrub

Table 3-4. Observations during Generation of Firebrands from Saw Palmetto

Date	*Specimen*	*Rep.*	*Wind Speed*	*Vegetation Arrivals & Notes*
26-Oct-16	Saw Palmetto	1	Idle	▪ Test Duration: 2-min ▪ The flame reached the end of pine needle bed after 45-s ▪ Smoldering duration: 2-min ▪ Rapid-fire spread on the bed ▪ Only 1 of 4 saw palmetto samples was completely burned ▪ With the clock running, pivoted the palmetto around and piled up pine straw with a 2-m fuel bed. The fronds were positioned over the bed. ▪ The palmetto burned better after this process
		2		▪ Test Duration: 2-min ▪ The flame reached the end of pine needle bed after 25-s ▪ Palmetto holder rotated 180° for this test Stocks did not burn, but fronds did
		3		▪ Smoldering Duration: 3-min ▪ The flame reached the end of pine needle bed after 45-s and reached palmetto after 35-s ▪ Left palmetto (near the black wall) did not completely burn. Rest of palmetto had removal of most fronds
27-Oct-16		1	M	▪ Test Duration: 4-min ▪ The flame reached palmetto after 26-s ▪ 3 out of 4 palmettos burned (fronds only)
		2		▪ The flame reached the end of pine needle bed after 45-s and reached palmetto after 30-s ▪ Left 2 palmettos did not fully become involved ▪ Fronds that disconnect are very light and loft 3 to 6-m above ground. They can float out the back of the test chamber. They are not glowing, though, are black.
		3		▪ Test Duration: 5-min ▪ The flame reached palmetto after 25-s ▪ 3 of 4 palmetto fronds burned

Table 3-5, Cont'd. Observations during Generation of Firebrands from Saw Palmetto

Date	*Specimen*	*Rep.*	*Wind Speed*	*Vegetation Arrivals & Notes*
28-Oct-16		1	H	▪ Burner ignition at 0:10 ▪ The flame reached palmetto after 16-s ▪ One palmetto plant per holder location. ▪ From left to right with back to fans, facing the palmetto: • LHS plant, a complete burn of fronds; second plant from left, 4/6 fronds burned; second plant from right, 3/7 of fronds burned • RHS plant, 0/4 fronds burned
		2		▪ The flame reached palmetto after 17-s ▪ New set up: 2 palmettos per holder, but only utilizing the holders in the middle of the bed (the left most and right most are not used) ▪ Most burning was done at 2-min ▪ Several fronds left on the palmetto clump closets to the black wall
		3		▪ The flame reached palmetto after 17-s ▪ Two palmetto samples were placed in the center of two holders. The outboard holders were left empty ▪ The goal is a complete burn of palmetto fronds at high wind speed. ▪ Similar to Rep. 1 notes, with back to fans and facing palmetto holder: second to left-hand side holder, 10/10 fronds burned, second from right-hand side holder, 0/11 fronds burned. ▪ Once the burner turned off, flaming ended, not sustained.

Table 3-6. Observations during Generation of Firebrands from Chamise

Date	*Specimen*	*Rep.*	*Wind Speed*	*Vegetation Arrivals & Notes*
21-Oct-16	Chamise	1	I	▪ All foliage burned ▪ Two Twigs and branches mostly not burned (i.e., only charred) ▪ The average weight of chamise holders: 6.12-kg
		2		▪ Chaparral ignition: 50-s into the test ▪ Burning time: 15-s ▪ Smoldering of fuel bed: 1.5-min after burning time ▪ No firebrands were generated during smoldering of the fuel bed
		3		▪ Test duration: 5-min ▪ Chaparral ignition: 30-s into the test ▪ Full contact of foliage with the flame from pine straw bed ▪ Charring (and not burning) of small branches were observed
24-Oct-16		1	M	▪ Test duration: 5-min ▪ Chaparral ignition: 40-s into the test ▪ Ignition started at idle wind speed, and wind speed was increased to (fluctuating) medium after 10-s
		2		▪ Test duration: 5-min ▪ Chaparral ignition: 30-s into the test ▪ Measurements of branch diameter: • Unburned: mean 1.39-mm, std. dev. = 0.52. • Burned (end of branch): mean = 4.07-mm, std. dev. = 0.92
		3		▪ Test duration: 5-min ▪ Chaparral ignition: 30-s into the test ▪ Ignition started at idle wind speed, and wind speed was increased to (fluctuating) medium after 10-s ▪ Measured stem diameter at the end of branches (10-12 sample size) before and after the test: • Unburned: mean=1.39-mm, std. dev. = 0.20. • Burned (end of branch): mean = 4.61-mm, std. dev. = 1.12
25-Oct-16		1	H	▪ Test duration: 5-min ▪ Chaparral ignition: 20-s into the test ▪ Flame height was lower at higher wind speeds. ▪ The upper part of chamise did not burn
		2		▪ Test duration: 5-min ▪ Chaparral ignition: 30-s into the test ▪ Most flaming was finished 50-s into the test ▪ Stems of chaparral in the metal cage were burning (with flame) up until 3-min. ▪ From 3:30 to the end (5:00), the stems just smoldered, and no flames were evident
		3		N/A

3.3.2.1.3 Tree

Table 3-7. Observations during Generation of Firebrands from Loblolly Pine

Date	***Specimen***	***Rep.***	***Wind Speed***	***Vegetation Arrivals & Notes***
17-Oct-16	Loblolly Pine	1	Idle	▪ Direct flame impingement: 10-s ▪ Flames on pine not as substantial as cypress ▪ MC samples were taken from this rep.
		2		▪ Direct flame impingement: 10-s ▪ MC samples were taken from this rep.
		3		▪ Direct flame impingement: 10-s ▪ As with previous, pine tree more flattened as a result of laying in the CONEX while drying. ▪ Complete burn of tree foliage
18-Oct-16		1	Medium	▪ Test duration: 6-min ▪ Complete flaming combustion of the tree: 30-s to 45-s into the test ▪ Several larger branches and some needles were still present ▪ The sample did not smolder like Leyland cypress tree
		2		▪ Test duration: 6-min ▪ Complete flaming combustion of the tree: 40-s ▪ More branches (comparing to Leyland cypress) and few needles remained ▪ Smoldering was not observed
		3		▪ Test duration: 6-min ▪ Longer flaming combustion due to more needles on the stem of this rep. (~50-s)
19-Oct-16		1	High	▪ Test duration: 6-min ▪ Quick burn (~30-s) ▪ Incomplete burn of foliage; two parts of the tree were not burned
		2		▪ Quick and complete burn (~20-s) ▪ Only a few needles were left on the tree ▪ Smoldering was not observed
		3		▪ Quick burn (~30-s) ▪ Only a few needles were left on the tree on an upward oriented branch ▪ The tree was flat/planar ▪ Vegetation was mostly aligned with the burner leg

Table 3-8. Observations during Generation of Firebrands from Leyland Cypress

Date	*Specimen*	*Rep.*	*Wind Speed*	*Vegetation Arrivals & Notes*
17-Oct-16	Leyland Cypress	1	Idle	▪ Direct flame impingement: 10-s ▪ Complete burn ▪ MC sample from trees was taken during this test
		2		▪ Direct flame impingement: 10-s ▪ Complete burn except for the main bole ▪ MC sample from trees was taken during this test
		3		▪ Direct flame impingement: 10-s ▪ Flaming combustion: 30 – 45-s into the test ▪ Smoldering: 2 – 3-min after flaming combustion ▪ Not many branches were left ▪ The tree did fall off the front support and pivoted downward about 1:45-s into the test, but this was after the major burning
18-Oct-16		1	Medium	▪ Direct flame impingement: 10-s ▪ Flaming combustion: 30-s into the test ▪ Smoldering: 2.5-min after flaming combustion ▪ Many of smaller branches remaining on the trunk
		2		▪ Test duration: 8-min ▪ Direct flame impingement: 10-s ▪ Complete burn of foliage 50-s into the test ▪ Small branch breakage continued during the smoldering phase
		3		▪ Direct flame impingement: 10-s ▪ Complete burn of foliage 45-s into the test ▪ Some of the medium and large branches remained ▪ Branch breakage and smoldering up to 2-min into the test ▪ Up to 3:40-min into the experiment, smoldering continued 45 sec for the majority of burning…just the trunk and
19-Oct-16		1	High	▪ Direct flame impingement: 10-s ▪ Smoldering continued 2:30-mn into the test ▪ The last large branch fell off at 4:45-min into the test
		2		▪ Direct flame impingement: 10-s ▪ A tremendous heat release rate ▪ All foliage burned except for a small patch ▪ The branch with unburned foliage dropped off during smoldering
		3		▪ Direct flame impingement: 10-s ▪ Flaming combustion ended 30-s into the test ▪ Up to 2:30-min into the experiment, many breakages were observed ▪ Breakage was not observed during smoldering ▪ Some sporadic embers being generated.

3.2.2.2 Firebrand Collection and Sampling

Previous firebrand generation studies reported a sample size between 50 and 1,500. Hedayati (Hedayati 2018) utilized power analysis to determine the minimum sample size for firebrands generated from structural fuels and concluded 1,400 is a reasonable number that can represent the whole sample population in a particular test and environmental conditions. However, due to the smaller number of firebrands (9,814) in vegetative tests comparing to structural firebrands, all collected vegetative firebrands were characterized during this study.

3.2.3 Post-Test

Oven-dried firebrands were taken to the *Materials Flammability Laboratory* located at the *University of North Carolina at Charlotte*. Firebrands were characterized by evaluating three parameters: 1) flying distance (based on collection pans' rows and columns and utilizing Pythagorean Theorem to determine the distance traveled), 2) mass, and 3) projected area.

A digital balance (*SARTORIUS H51*) with a precision of 0.0001-g (3.53×10^{-6}-oz) was used to measure firebrand mass values. Firebrands were scattered over a white sheet to measure the projected area. Photos of each sheet were taken using a *Nikon D5600* and an *18-55 VR* kit lens, and digitalized information was subsequently analyzed in MATLAB utilizing an automated image analysis technique. Interested readers can find more information on the analysis of images in (Hedayati et al. 2019). The projected area was measured by performing the following steps: intensity increase, noise removal, thresholding, edge detection, and labeling. Photographs of the initial and final images are shown in Figure 3-12. There are several advantages of using an image analysis code to

calculate the projected area of the firebrands comparing to the previous methods. These advantages are discussed in section 4.1.7 of this dissertation.

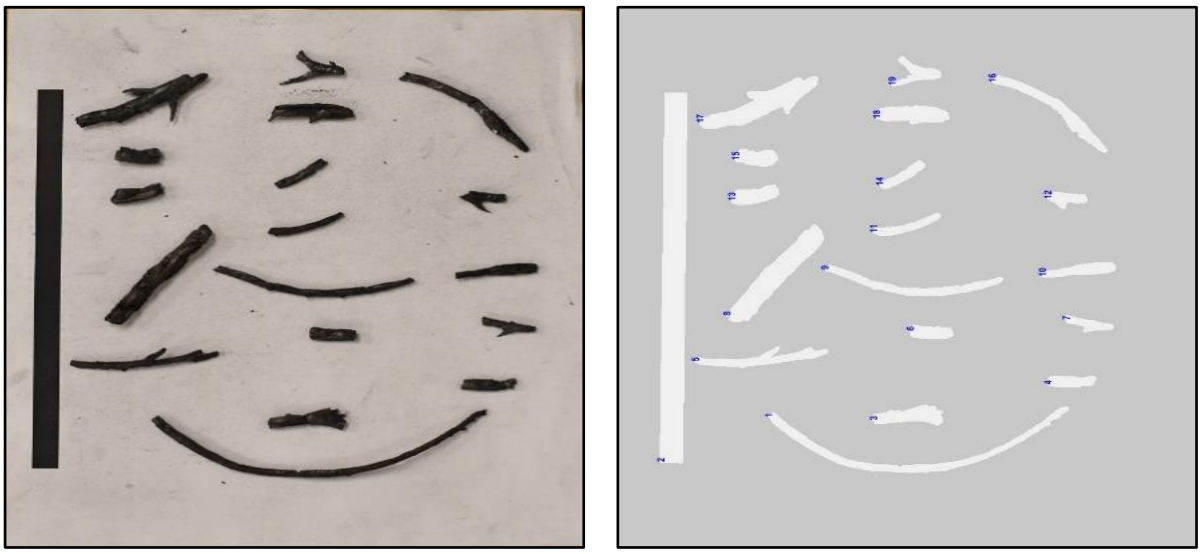

(a) (b)

Figure 3.12. Initial (a) and Final (b) Images to Measure the Projected Area of Vegetative Firebrands

The image analysis code was initially developed by Hedayati (Hedayati et al. 2019) to characterize the firebrands generated from structural assemblies. While generated firebrands from different fuels, both vegetative and structural, form different shapes, the initial code needed to be revised.

For instance, some of the firebrands generated from the Bluestem grass specimens were not wholly burned. As a result, the color scheme of these embers was different from the fully-charred firebrands from the structural assemblies (see Figure 4.1.(a)). Color thresholding assisted with the segmentation by viewing an image in various color spaces. Segmentation techniques were used to isolate firebrands for further processing, e.g., utilizing active contours to either segment a portion or the whole picture, and the physical characteristics of that segment were calculated using the region property function. In addition, the image transformation section of the code was revised. The Hough transform

was utilized to detect the lines within photos. Finding the limits assisted with the recognition of the shape and the projected area of the vegetative firebrands. Revising the elements in the object analysis section was necessary to trace the boundaries of vegetative firebrands. More information on this difference between firebrands can be read in section 4.1.1.

3.3 Preliminary Characterization

As mentioned in section 3.2.3, three physical parameters were chosen to characterize in this study: mass, projected area, and flying distance of firebrands. The flying distance models were built based on Albini's work (Albini 1983; Albini 1981; Albini 1979, 1983b). As combustion of firebrands occurs on their surface, the shape and area of firebrands play a vital role in their combustion rate (Tohidi et al. 2015). A study by Atreya (Atreya et al. 2017a) was focused on the combustion rate of firebrands based on their shape. It was previously discussed that multiple parameters affect the ignition potential of a fuel bed after the landing of firebrands, such as exposure time, the state of fuel bed (e.g., packing density), and the thermal inertia of firebrands transferred to the bed.

Consequently, the number, size, shape, and mass of firebrands play an important role in the ignition potential and spot fires. A study by Manzello examined the ignition potential of fuel bed in contact with vegetative firebrands generated from Douglas-fir trees (Manzello et al. 2008b).

As a result, previous firebrand generation studies showed that lofting height, flying distance, combustion rate, and ignition potential of firebrands are functions of their mass and shape. It is important to remember that the specimen collection, experimental design,

sample preparation, collection techniques, and report of preliminary results were different in the previous firebrand generation studies.

Characterization is typically based on the physical properties of firebrands, and it is necessary to understand the spotting phenomenon better. A statistical framework is required to describe physical properties alongside their interaction with environmental variables to fill the gap. Results from the initial characterization of selected vegetative fuels are summarized in tables 4-1 to 4-7 in Chapter 4.

CHAPTER 4: STATISTICAL FRAMEWORK FOR CHARACTERIZATION OF VEGETATIVE FIREBRANDS

4.1 Statistical Analysis

4.1.1 Introduction

Firebrand generation is a complex and stochastic phenomenon that depends on various parameters such as fuel type (structural or vegetative), morphology, fire intensity (Manzello et al. 2020), and environmental conditions such as ambient wind speed. A thorough understanding of this process is required to accurately characterize the physical parameters of generated firebrands, including mass, area, shape, and thermal inertia. As previously stated, laboratory-scale, field (i.e., prescribed fires), and studies during wildfires, as well as some modeling efforts, have been conducted on the generation of firebrands from both structural and vegetative fuels.

Most of the studies were only reported the experimental procedures, raw data, and limited data analysis. The only characterization studies to date are (Tohidi et al. 2015) and (Hedayati 2018). Also, the number of collected and characterized firebrands in previous studies have been relatively small. For example, the total number of collected specimens from an earlier study on the generation of firebrands from five Korean pine (*Pinus koraiensis*) trees was limited to 1,337 (Manzello et al. 2009b; Manzello and Maranghides 2007; Tohidi et al. 2015). More than 10,00 firebrands were generated, and a total of 9,814 vegetative firebrands were characterized during the experiments for this study, including 1,032 firebrands from grass specimens, 4,669 firebrands from the shrub species, and 4,113 firebrands from the tree species.

Previous studies also suggested that the shape of firebrands generated from vegetation can be considered as cylinders (Manzello et al. 2009; Manzello et al. 2007), but this study

showed that depending on vegetation type, species, and wind speed, firebrands can form in unlimited irregular shapes. Figure 4.1 shows the generated firebrands from various vegetative fuels.

(a) Bluestem Grass (b) Saw Palmetto (c) Chamise*

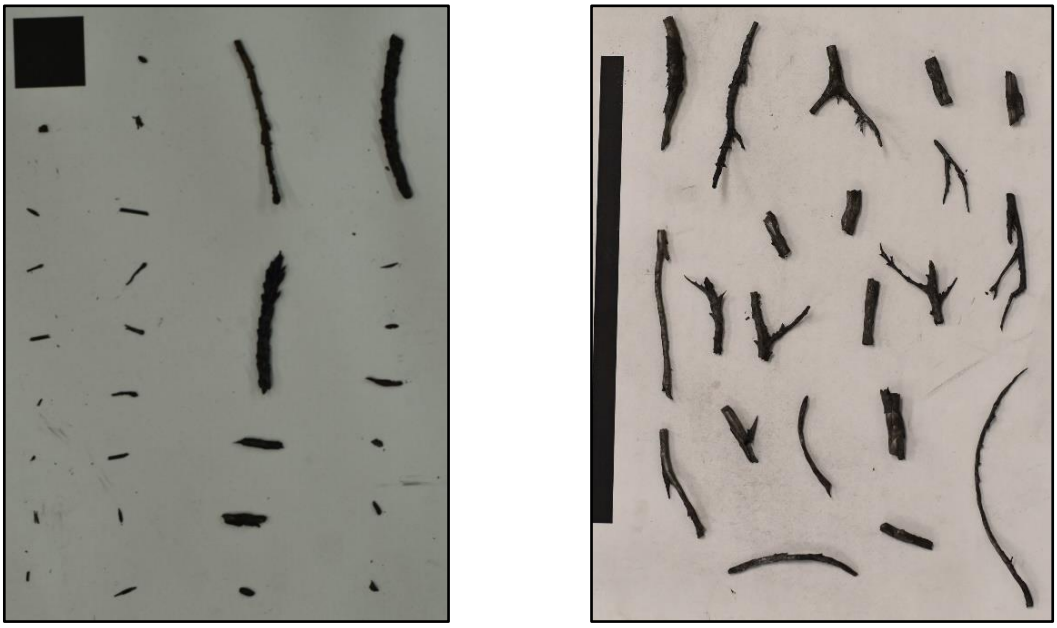

(d) Loblolly Pine (e) Leyland Cypress

Figure 4. 1. Firebrands Generated from Different Vegetative in Medium Wind Speed
(* Chamise firebrands were generated at the high wind speed level)

Physical properties of firebrands, including shape and mass, are playing a vital role in better understanding the spotting phenomenon. A predictive model for the distribution of the size of firebrands generated from a fractal tree was developed by (Barr et al. 2013). Models for lofting and transport of firebrands have been built based on research works of Albini (Albini 1979, 1981, 1983a, 1983b), and the Tachikawa (1988) who developed a model for wind-borne flying debris (Tachikawa 1988; Holmes et al. 2006). A study by (Baum and Atreya 2014) showed the effect of firebrand shape on their combustion mode. Finally, spotting was dependent on the ignition state of landed firebrand (flaming or smoldering), contact time to the recipient fuel/ bed, area, number, and thermal inertia of landed firebrands (Boonmee et al. 2002; Hakes et al. 2019), and conditions of recipient fuel (e.g., moisture content, packing density, and fuel size). Consequently, different stages of firebrand phenomena, including generation, transportation, and ignition of recipient fuel, are dependent on the physical properties, shape, and mass, of firebrands (Tohidi et al. 2015).

A common problem of all previous studies is the lack of adequate experimental data to use as input for characterization and modeling purposes. Except for (Tohidi et al., 2015), no other study is available that developed a statistical method on a large dataset of vegetative firebrands. There are limitations when it comes to using these models for validating experimental data. For instance, it was assumed that the generic shape of all the generated firebrands was thin, long cylinders. Also, the density (ρ) of all firebrands were constant, and the aspect ratio (η) of all firebrands is equal. Besides, no wind was present during the experiments, and consequently, environmental conditions were not considered

as an influential parameter in finding the derived power-law relationship between the surface (s) and the mass (m) of generated firebrands.

The methodology and statistical framework for this study can be used for further analysis of firebrands generated in full-scale experiments, as well as an input for future optimization and modification of experimental design procedures.

4.1.2 Statistical Framework

Based on the discussion in section 4.1.1, a lack of a comprehensive statistical analysis of previous vegetative firebrands, there is a need to develop a mathematical framework to proceed.

The previous study by (Hedayati et al. 2019) suggested a linear relationship based on previous studies (Manzello et al. 2014, 2017; Suzuki et al. 2016b) between the values of mass and projected area of generated firebrands, where the slope (k) is a parameter consisted of multiplying density (ρ) by the thickness (h) of firebrands. A Gaussian process regression was utilized to predict the relationship between mass and projected areas of firebrands. Based on trained data, a predictive model for mass was developed with a sample size of 1,400 firebrands that could predict the values for mean, standard deviation, and mass correlation with less than 10% error.

Although developing a supervised learning algorithm might be useful, a lack of variability in the dataset is a significant limiting parameter for further use of such a framework. In this study, the dataset was representing variables vegetative fuels based on the spatial distribution: Specimens representing overstory (tree), understory (shrub), and floor (grass), and the fuel classification. A more in-depth analysis was employed to evaluate the effects of both fuel characteristics and environmental conditions on the generation of firebrands.

Steps developed for this framework included:

1) Define dependent and independent variables
2) Display and describe data utilizing descriptive statistics
3) Find the best probability distribution functions (PDF)
4) Fit a proper regression model among variables
5) Produce a predictive model based on available data

4.1.3 Variable Definition

As stated in section 3.3, the studied parameters of this research study were firebrand mass, projected area, and flying distance. Reviewing Table 3.1, three vegetation types, grass, shrub, and tree that included five species were used. Experiments were conducted at three different wind speed levels, as stated in section 3.2.2.

Two groups of variables were evaluated considering the parameters of interest:

1) Categorical variables: those parameters without a logical order where they are part of a finite number of categories. In this study, wind speed levels, vegetation type, and vegetation species formed three, three, and five categorical variables, respectively. Based on characterization on different levels (vegetation type and species), the predictive model included eight categorical terms: three wind speed levels (idle, medium, and high), and five vegetative species (Bluestem grass, Chamise, Saw Palmetto, Leyland cypress, and Loblolly pine).
2) Quantitative variables: Parameters of interest with quantifiable numeric values. In this study, mass (m) and projected area (A_{FB}) of firebrands were discrete quantitative variables. As a result, two discrete variables, mass and projected area, were defined for statistical analysis.

As shown in Figure 3.9, collection pans in this research study were staggered in a 14.3-m long × 2.6-m (47-ft. × 8.5-ft.) wide array into 17 different locations, as defined by the rows in Figure 4.2. As stated before, the Pythagorean theorem was utilized to calculate the flying distance for the firebrands.

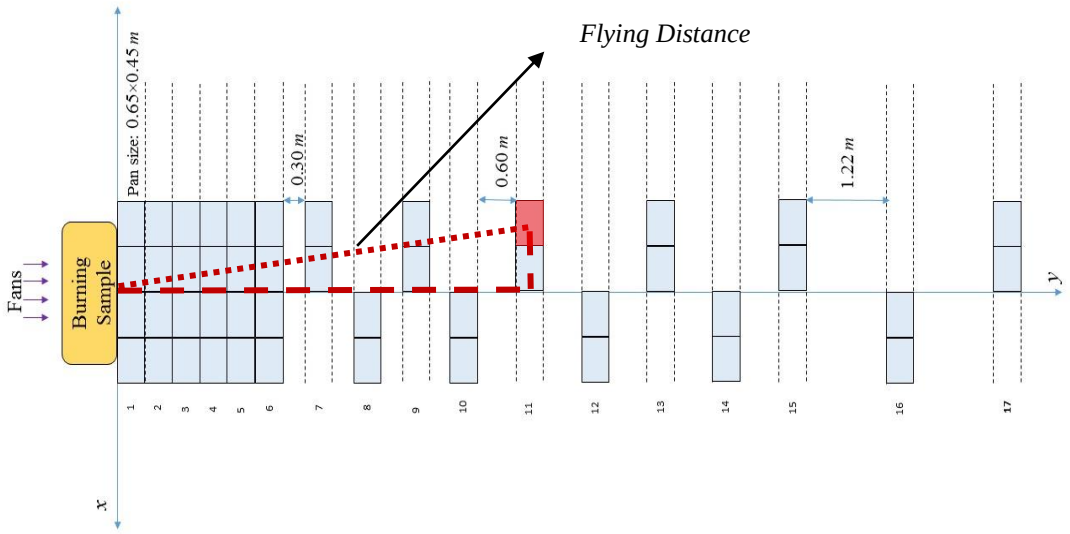

Figure 4.2. Calculation of Flying Distance of Firebrands using the Pythagorean Theorem considering their Landed Pan (Hedayati et al. 2019)

A sample flying distance for the specified pan in row 11 can be calculated using the Pythagorean theorem. In this case, the horizontal distance from the burning sample and vertical distance from the centerline (y-axis) to the center of the specified pan are 6.53-m and 0.98-m, respectively. The flying distance is equal to 6.62-m utilizing the Pythagorean theorem. Note, centers of pans were considered as the landing location of all firebrands in this method.

Regarding the design of collection pans with pre-defined landing distances, the flying distance was considered a categorical parameter in this study. The focus of this research study was on the generation and characterization of firebrands. The flying distance was considered a parameter in the second sub-process of the firebrand phenomenon:

transportation by the wind. To examine the effect of the presence of the flying distance as a categorical value in the final predictive model, a statistical test entitled *Lack-of-Fit* or *F-test* was employed. The null hypothesis for this statistical test indicates that there is no lack of fit in the proposed model.

The p-value of this test (= 0.076), using an alpha-level of 0.05, indicated that the null hypothesis failed to be rejected. This outcome means adding flying distance to the model does not explain more variability compared to the reduced model. In other words, the assumed relationship in the model is reasonable.

As a result, this parameter was eliminated in the predictive model for the characterization of firebrands in this study.

4.1.4 Descriptive and Inferential Statistics

In statistics, data need to be treated to determine whether a meaningful association among them exists or not. The discussion of the treatments is written based on the information in (Statistical Treatment 1961).

Treatment can be employed at different levels. In data analysis, treatment indicates any statistical methods that are applied to the dataset. This treatment can be divided into two groups: descriptive and inferential statistics.

During employing the descriptive analysis, statistical parameters in data are divided into three main groups:

1) the measure of location (central tendency),

2) the measure of spread (dispersion), and

3) illustration using charts and graphs.

While using the inferential statistics, hypotheses could be tested to predict any pattern or meaningful result. These treatments could include finding the error, calculating potential correlations, and utilizing statistical tests such as T-Test or Z-Test.

During treating of the dataset for this research, first, the raw data of the physical properties, including mass, projected area, flying distance, and also the number of generated embers, were gathered in separate excel sheets. By employing the descriptive statistics, the following parameters were calculated for all datapoints: mean, median, mode, skewness, and correlation. Results from this part are summarized in Tables 4-1 to 4.6. Regression analysis was performed afterward, where the five assumptions for linear regression (Poole and O'Farrell 1971), namely linear relationship, multivariate normality, no or little multicollinearity, no auto-correlation, and homoscedasticity, were examined utilizing different statistical tests and necessary transformations.

The first step in data analysis is to prepare the data so that it can be better understood. Descriptive analysis was divided into two main categories:

1) The measure of central tendency: To summarize the data in a way that shows a characteristic of the dataset using a central value. Mean, median, and mode are the three parameters measured in this category.
2) The measure of spread (dispersion): The variability indicates dispersion in the dataset. Parameters measured in this category were: standard deviation, variance, range, percentile, quartiles, skewness, kurtosis, and correlation.

For the dataset of this study, median and mode did not represent a physical explanation; however, they can assist in better understanding the variability in data by determining the skewness and showing whether the data is normally distributed or not. Although a single

firebrand may not have adequate thermal inertia to initiate a spot fire, spotting can occur in wildland and WUI fires as a result of transferring a proper amount of energy from a pile of firebrands to a recipient fuel. Assuming the energy content of firebrands is a function of their size, shape, and mass, having a clear understanding of the variability in firebrands results in more reliable characterization and the ability to build a more robust predictive model based on fuel characteristics and environmental conditions.

Table 4-1. Summary of the Measured Firebrand Parameters for Little Bluestem Grass

Physical Quantity	Statistical Quantity	Constant Wind	Variable Wind (Avg. & Gust Peak)	
		Idle (5.36-m/s)	Medium (11.17 & 14.30-m/s)	High (17.88 and 23.00-m/s)
Flying Distance (m)	Mean (μ)	1.146	1.712	3.429
	Standard Deviation (σ)	0.922	2.311	3.517
	Skewness	2.557	3.416	1.321
	Median	0.743	0.938	2.022
Projected Area (cm^2)	Mean (μ)	0.773	0.578	0.929
	Standard Deviation (σ)	0.576	0.403	0.664
	Skewness	4.150	3.631	2.856
	Median	0.657	0.509	0.735
Mass (g)	Mean (μ)	0.015	0.004	0.025
	Standard Deviation (σ)	0.021	0.007	0.037
	Skewness	2.407	6.761	4.767
	Median	0.007	0.003	0.013
Correlation	Mass and Area	0.547	0.764	0.659
	Mass and Flying Distance	-0.280	-0.047	-0.065
	Area and Flying Distance	-0.338	-0.167	-0.128
Sample Size		202	138	692

The standard deviation shows the average distance between each observation and mean value (or expected value) of a dataset, whether a segment of the population or the whole population. In other words, the standard deviation shows the dispersion of a set of values (Bland and Altman 1996). It is calculated as:

$$\sigma = \sqrt{\frac{1}{n}\sum_{i=0}^{n}(x_i - \mu)^2} \quad \text{(Eq. 4.1)}$$

Where n is the population (sample) number, x_i is the observed value, and μ is the average of observations.

Table 4-2. Summary of the Measured Firebrand Parameters for Chaparral (Chamise)

Physical Quantity	Statistical Quantity	Constant Wind	Variable Wind (Avg. & Gust Peak)	
		Idle (5.36-m/s)	Medium (11.17 & 14.30-m/s)	High (17.88 and 23.00-m/s)
Flying Distance (m)	Mean (μ)	1.403	1.205	3.318
	Standard Deviation (σ)	1.641	0.942	3.420
	Skewness	3.380	1.895	1.482
	Median	0.743	0.938	1.687
Projected Area (cm^2)	Mean (μ)	1.731	2.349	2.601
	Standard Deviation (σ)	1.923	2.460	2.568
	Skewness	4.567	4.466	3.705
	Median	1.306	1.712	1.843
Mass (g)	Mean (μ)	0.174	0.214	0.236
	Standard Deviation (σ)	0.592	0.568	0.539
	Skewness	11.070	6.401	5.182
	Median	0.048	0.061	0.067
Correlation	Mass and Area	0.849	0.906	0.875
	Mass and Flying Distance	-0.153	-0.231	-0.217
	Area and Flying Distance	-0.310	-0.346	-0.197
Sample Size		269	257	686

A lower standard deviation value indicates that observations were closer to the expected value (mean). Variance for a probability normal distribution is defined as the square of the average distance between each observation and expected value.

Table 4-3. Summary of the Measured Firebrand Parameters for Saw Palmetto

Physical Quantity	Statistical Quantity	Constant Wind	Variable Wind (Avg. & Gust Peak)	
		Idle (5.36-m/s)	Medium (11.17 & 14.30-m/s)	High (17.88 and 23.00-m/s)
Flying Distance (m)	Mean (μ)	3.354	2.981	3.227
	Standard Deviation (σ)	3.212	3.305	3.412
	Skewness	1.499	1.666	1.611
	Median	2.101	1.587	1.687
Projected Area (cm^2)	Mean (μ)	1.255	1.789	2.346
	Standard Deviation (σ)	1.497	2.209	1.731
	Skewness	4.932	11.006	3.865
	Median	0.888	1.310	1.825
Mass (g)	Mean (μ)	0.018	0.020	0.081
	Standard Deviation (σ)	0.071	0.048	0.101
	Skewness	8.886	10.378	6.511
	Median	0.004	0.008	0.036
Correlation	Mass and Area	0.781	0.679	0.590
	Mass and Flying Distance	-0.106	-0.197	-0.129
	Area and Flying Distance	-0.186	-0.141	-0.148
Sample Size		938	1289	1230

Table 4-4. Summary of the Measured Firebrand Parameters for Loblolly Pine Tree

Physical Quantity	Statistical Quantity	Constant Wind	Variable Wind (Avg. & Gust Peak)	
		Idle (5.36-m/s)	Medium (11.17 & 14.30-m/s)	High (17.88 and 23.00-m/s)
Flying Distance (m)	Mean (μ)	1.493	2.998	4.093
	Standard Deviation (σ)	1.139	2.760	3.747
	Skewness	2.016	2.119	1.509
	Median	1.587	2.022	2.540
Projected Area (cm^2)	Mean (μ)	1.787	0.611	0.960
	Standard Deviation (σ)	3.569	0.879	1.096
	Skewness	6.687	3.808	3.520
	Median	0.915	0.329	0.613
Mass (g)	Mean (μ)	0.185	0.030	0.055
	Standard Deviation (σ)	0.845	0.073	0.134
	Skewness	11.646	6.941	5.707
	Median	0.038	0.008	0.019
Correlation	Mass and Area	0.915	0.891	0.905
	Mass and Flying Distance	-0.140	-0.236	-0.143
	Area and Flying Distance	-0.220	-0.306	-0.138
Sample Size		381	575	167

Figure 4.3 shows a standard distribution (where $\mu = 0\ and\ \sigma = 1$) and the 68-95-99.7 rule, also known as the *Empirical Rule*. Employing this rule shows the percentage of observations in a dataset that lie within a band around the expected value (mean). The Empirical Rule can assist in determining the characteristic physical properties of firebrands in different testing conditions. These values can then be used in further statistical analysis studies, input to design or optimize experiments, and input for developing standard testing

methods in the future. The physical characteristics of firebrands by vegetation type using a 95% confidence interval ($\mu + 2\,\sigma$) are summarized in Tables 4.7 to 4.9.

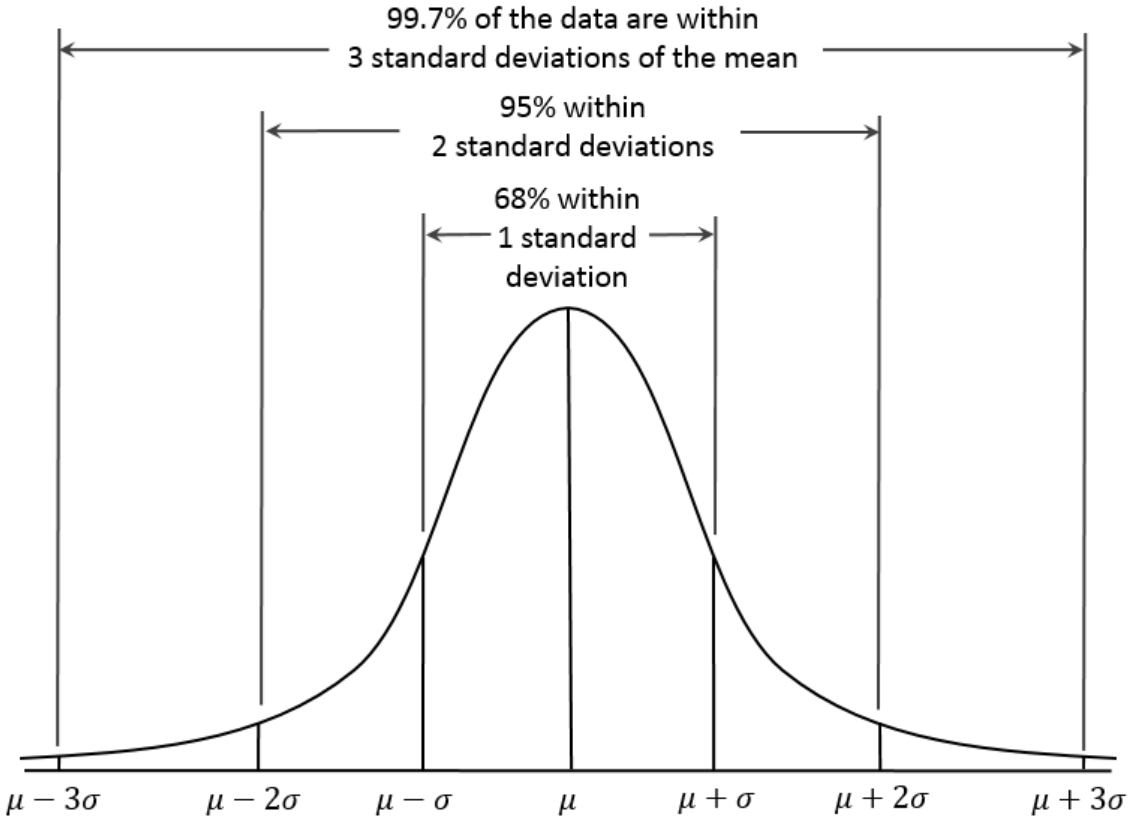

Figure 4.3. Empirical Rule (68–95–99.7 Rule) (Kernler 2018)

The importance of developing a distribution function for firebrands was mentioned earlier. Hedayati (2018) suggested that a PDF can be employed to calculate the critical heat flux of accumulated firebrands. Physical properties of firebrands, including, mass and projected area, were parameters of interest in this suggested model. A detailed methodology to facilitate firebrand characterization and employing a predictive model can be reviewed in (Hedayati et al. 2019).

Physical Quantity	Statistical Quantity	Green Tree			Dry Tree		
		Constant Wind	*Variable Wind (Avg. & Gust Peak)*		*Constant Wind*	*Variable Wind (Avg. & Gust Peak)*	
		Idle (5.36-m/s)	Medium (11.17 & 14.30-m/s)	High (17.88 and 23.00-m/s)	Idle (5.36-m/s)	Medium (11.17 & 14.30-m/s)	High (17.88 and 23.00-m/s)
Flying Distance (m)	Mean (μ)	1.883	2.446	4.129	2.827	2.247	6.446
	Standard Deviation (σ)	1.326	1.769	3.835	2.559	1.553	6.147
	Skewness	0.813	1.675	1.461	1.907	1.923	1.189
	Median	1.470	2.028	2.762	2.028	2.028	3.353
Projected Area (mm^2)	Mean (μ)	118.756	120.591	123.238	109.768	96.712	91.861
	Standard Deviation (σ)	107.344	112.514	167.580	88.526	102.823	91.457
	Skewness	2.260	1.877	3.975	2.188	3.079	2.860
	Median	77.352	83.378	67.928	72.722	66.150	62.968
Mass (g)	Mean (μ)	0.063	0.045	0.056	0.056	0.048	0.170
	Standard Deviation (σ)	0.090	0.047	0.161	0.081	0.075	1.636
	Skewness	3.243	3.243	8.254	2.607	4.110	12.516
	Median	0.032	0.030	0.021	0.021	0.025	0.025
Correlation	Mass and Area	0.732	0.836	0.415	0.700	0.910	0.123
	Mass and Flying Distance	-0.345	-0.235	-0.117	-0.384	-0.222	-0.177
	Area and Flying Distance	-0.302	-0.313	-0.152	-0.312	-0.174	-0.272
Sample Size		64	94	92	87	71	157

[*] *Data obtained from this experiment (Phase II- 2017) was combined with data from Leyland Cypress tests in Phase 1 (2016) for data analysis. Specimen preparation and moisture content monitoring techniques were similar in phases I and II of experiments.*

Table 4- 6. Summary of the Measured Firebrand Parameters for Green Leyland Cypress Tree-Phase I

Physical Quantity	Statistical Quantity	Constant Wind	Variable Wind (Avg. & Gust Peak)	
		Idle (5.36-m/s)	Medium (11.17 & 14.30-m/s)	High (17.88 and 23.00-m/s)
Flying Distance (m)	Mean (μ)	1.238	2.040	3.928
	Standard Deviation (σ)	0.739	1.989	2.657
	Skewness	1.327	2.529	1.099
	Median	0.938	1.587	2.474
Projected Area (cm^2)	Mean (μ)	1.881	1.745	2.371
	Standard Deviation (σ)	3.518	1.255	2.733
	Skewness	14.635	3.693	8.412
	Median	1.352	1.414	1.631
Mass (g)	Mean (μ)	0.191	0.108	0.283
	Standard Deviation (σ)	1.729	0.197	0.828
	Skewness	21.928	7.727	16.443
	Median	0.052	0.054	0.099
Correlation	Mass and Area	0.915	0.886	0.911
	Mass and Flying Distance	-0.068	-0.258	-0.300
	Area and Flying Distance	-0.147	-0.331	-0.333
Sample Size		529	883	1013

Two other values also play an essential role in moving forward with understanding the variability of data: median and mode. Comparing median and mode values of firebrand data from a population or sample set with their mean value shows whether the distribution is symmetric or not. The number of occurrences of a given data value (or mode) also defines the shape of the distribution of data. If *n* different peaks (or modes) appears in the data set, then the data set is multimodal. For instance, if two different modes appear in a data set, then the data set is bimodal, and two peaks will be observed while plotting the

distribution. Various types of data distribution regarding the mode value are shown in Figure 4.4 (Doanne and Seward 2011).

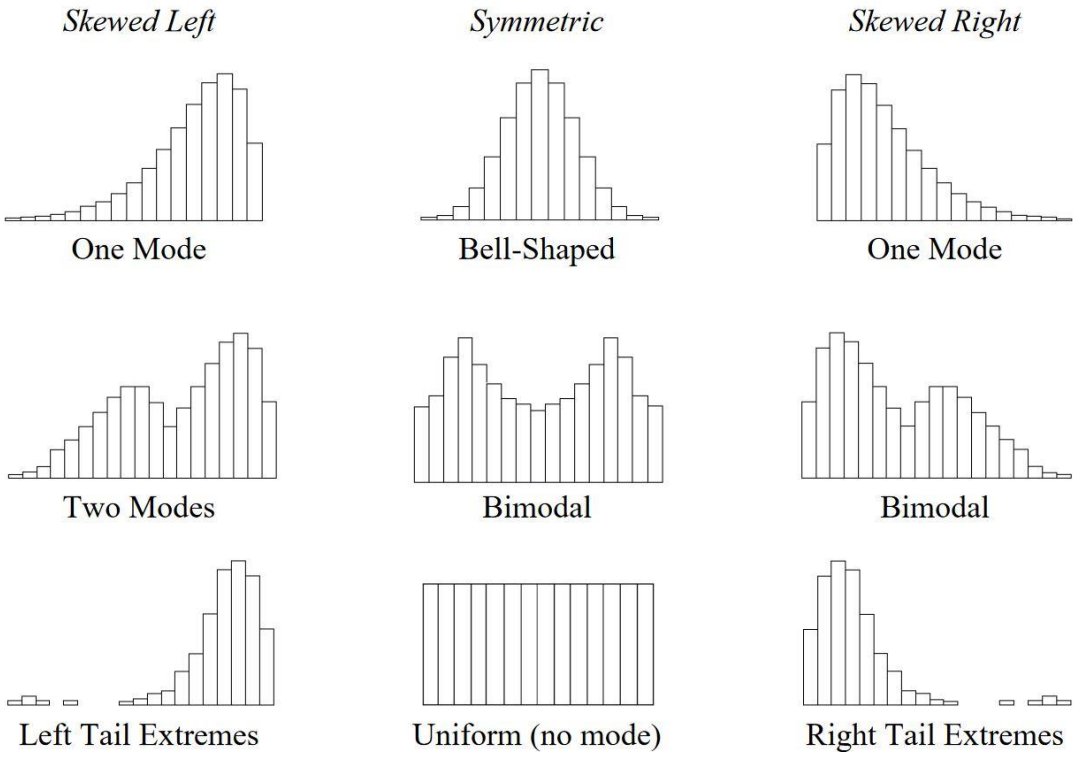

Figure 4.4. Prototype Histograms Illustrating Multimodal Distributions

Skewness is defined as the degree of asymmetry (or distortion) from the distribution around its expected value (mean). As illustrated in Figure 4.5, positive and negative skewness indicates the tendency of a tail extending toward the right or left side of the mean, respectively.

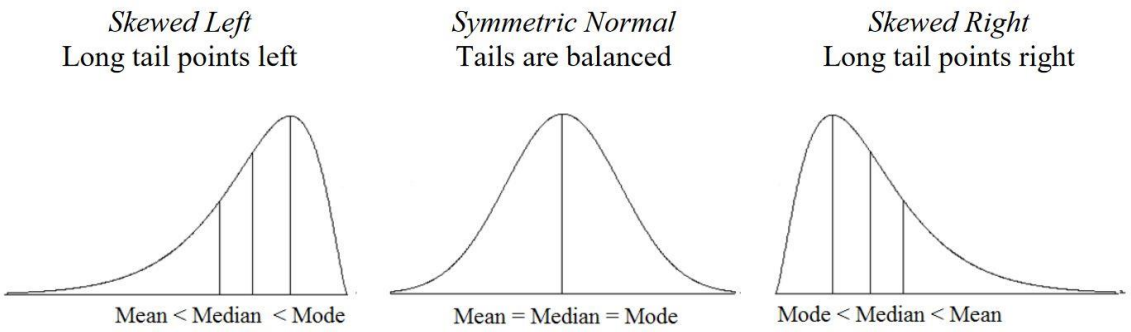

Figure 4.5. General Position of Mean, Median, and Mode and their Effect on Skewness of Data (Doanne and Seward 2011)

Distribution of mass and projected area of firebrands with the three vegetation types, grass, shrub, and tree, and three wind speed levels, idle, medium, and high, are plotted in Figures 4.6 and 4.7. Distributions in all nine sub-levels are right-skewed, and similarities in distributions were observed in the projected area and mass. As noted in Figure 4.5, a right-skewed histogram indicates that the mode and median values of a dataset are smaller than its mean value. It also shows that the dataset is unimodal. Histograms plotted in Figures 4.6 and 4.7 verifies this statement. Besides, this histogram shape might reveal the presence of potential outliers in the dataset. Visual inspection of distributions indicates the following results:

1) Most of the firebrands (~88%) in this study had projected area values < 3-cm^2,
2) Most of the firebrands (~98%) in this study had mass values < 1-g,
3) The similarity of distributions in two various physical properties, mass and projected area, shows a potential correlation among them.

The potential correlation between mass and area of firebrands was proposed in some of the previous studies (Manzello et al. 2017; Suzuki et al. 2016; Tohidi et al. 2015). The right-skewed distribution of firebrand mass and area in this study is in agreement with

previous studies on vegetative firebrands (Manzello et al. 2009; Manzello et al. 2008; Manzello et al. 2007). Given the fact that all the values for the physical properties of firebrands are positive, a right-skewed distribution was expected.

Skewness in all sub-levels is calculated using Equation 4.2, and results are summarized in Tables 4-1 to 4-6. It can be calculated as:

$$Skewness = \frac{n}{(n-1)(n-2)} \sum \left(\frac{x_i - \mu}{\sigma} \right)^3 \quad \text{(Eq. 4.2)}$$

Where n is the number of observations, and μ and σ are the mean and standard deviation of a population, respectively.

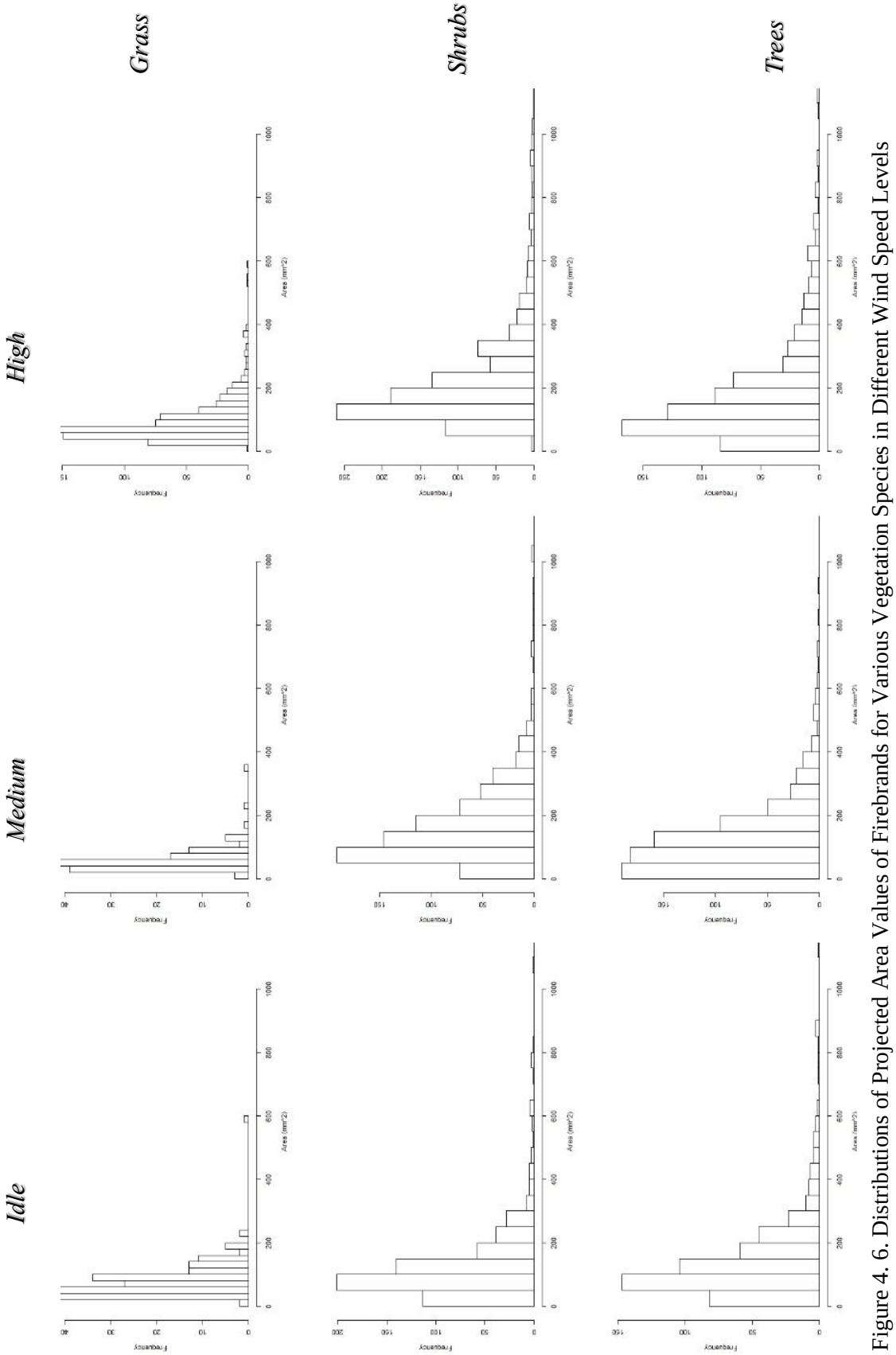

Figure 4. 6. Distributions of Projected Area Values of Firebrands for Various Vegetation Species in Different Wind Speed Levels

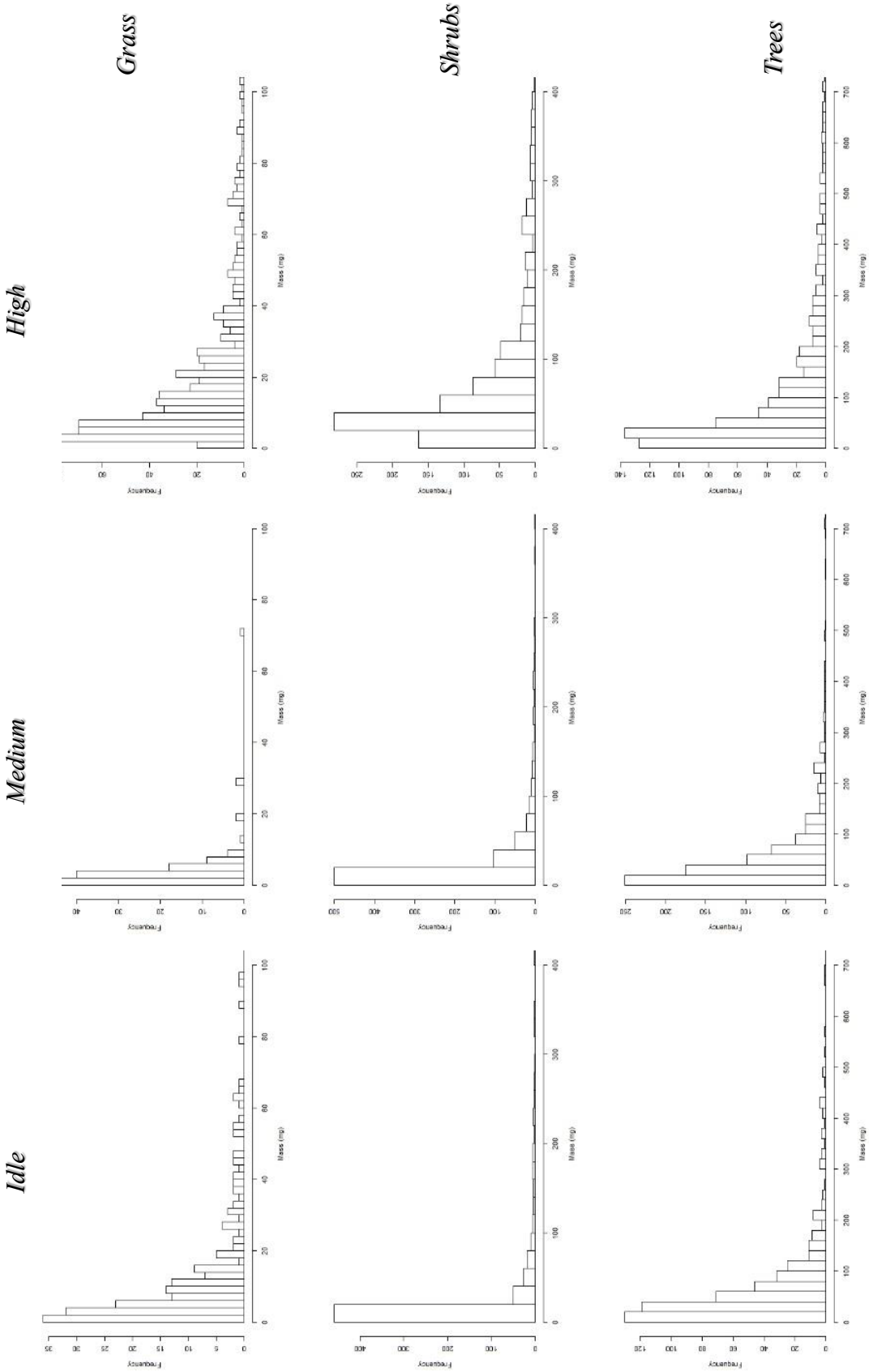

Figure 4. 7. Distributions of Mass Values of Firebrands for Various Vegetation Species in Different Wind Speed Level

4.1.5 Probability Distributions

The probability density functions were plotted using the whole population to find the best fit. PDFs were selected based on common distributions used in statistical analysis since all PDFs cannot be examined separately due to a large number of them. The four PDFs chosen for this study were based on the general shape of the distribution of the physical properties of firebrands, where values were positive, and distributions were moderate to heavily right-skewed. As a result, distributional choices were Exponential, Weibull, Gamma, and Log-Normal distribution. The Normal (Gaussian) distribution was also utilized as a basis for comparison (Mun 2008, Damodaran 2011).

To select a model among a finite set of models for this dataset, the *Bayesian Information Criterion* (BIC), also known as the *Schwarz Information Criterion* (SIC, SBC, SBIC), was employed. BIC was built based on the maximum likelihood estimate measure named the *Akaike Information Criterion* (AIC). The BIC score values could be used as useful criteria to prevent overfitting a model while increasing the likelihood and choosing between different distribution models (Schwarz 1978). BIC can mathematically be defined as:

$$BIC = \ln(n)\, k - 2\ln(\hat{L}) \qquad \text{(Eq. 4.3)}$$

Where:

- $\hat{L}$ → Maximized value of the likelihood function for the model
- n → Number of datapoints
- k → number of free parameters to be estimated

Schwarz introduced a penalty term for the number of parameters to prevent the trade-off between the model's accuracy and its complexity (Analyttica Datalab 2019). Selected PDFs can be tested using their corresponding BIC score values, where the lowest BIC score

can present the most probable function for a dataset (Posada and Buckley 2004). The BIC scores for the five previously mentioned PDFs are summarized in Table 4-7.

Table 4-7. Bayesian Information Criterion (BIC) Scores for Various Distributions

Distribution Name	***BIC Score***	
	Mass	***Projected Area***
Gaussian	27,424	21,833
Exponential	23,551	20,749
Gamma	13,350	11,778
Weibull	10,879	11,878
Log-Normal	10,393	10,553

As observed, the Log-Normal distributions reported the lowest BIC score among other PDFs. As a result, this PDF is the most probable fit for this dataset. Distributions of three PDFs, including Inverse Normal (Wald), Normal (Gaussian), and Log-Normal, are plotted for mass and projected area of the population in Figures 4.8 and 4.9, respectively. Visual inspection of distributions for firebrand mass values indicates that Log-normal distribution did not represent the best estimate for this parameter.

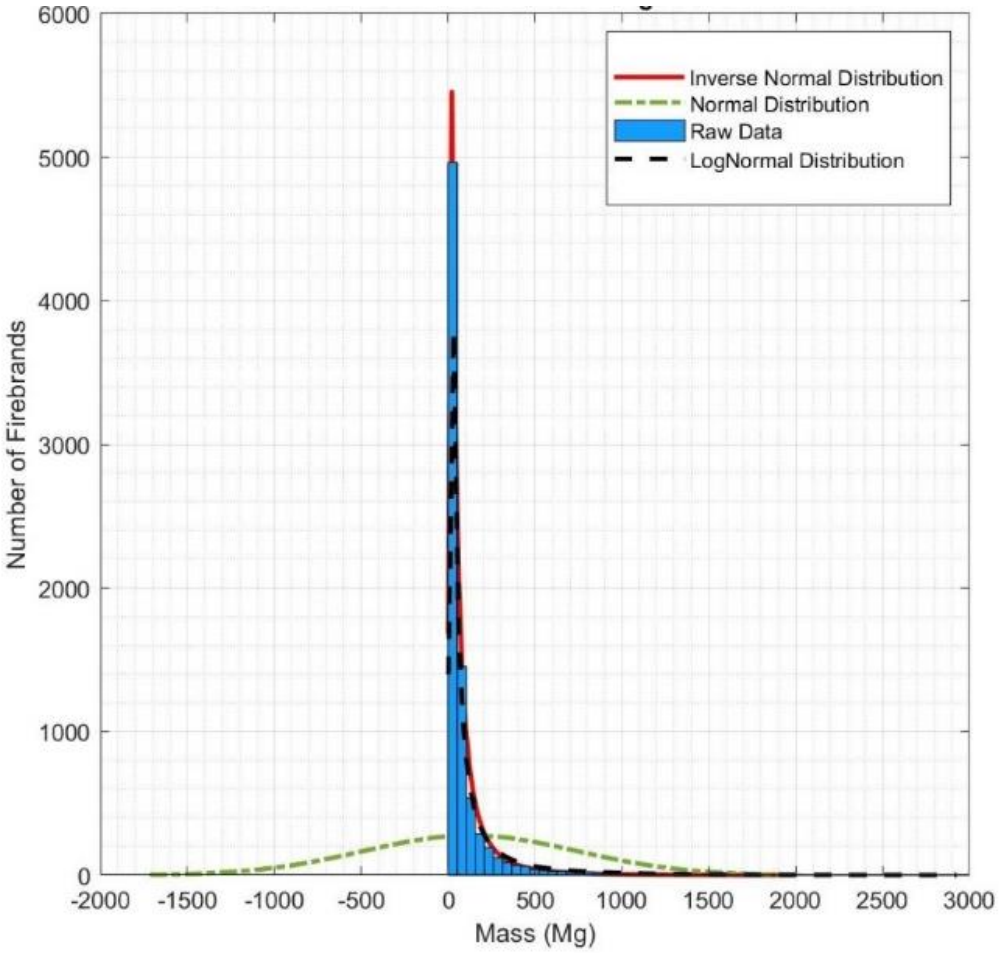

Figure 4.8. Various Probability Distributions Fitted
on the Entire Mass Values of the Vegetative Firebrand Dataset

A similar inspection for the projected area of firebrands, however, indicated that Log-Normal distribution was the PDF with the best fit for this parameter. Various tests can be performed to examine the normality and goodness-of-fit for potential distributions and to examine the appropriate PDF for a dataset. Examples of normality tests are D'Agostino's K-squared test, Anderson–Darling test, Kolmogorov–Smirnov test, Shapiro–Wilk test, and Pearson's chi-squared test. A study showed that the Shapiro–Wilk, and Anderson-Darling tests could be adopted for both symmetric and asymmetric distributions for large datasets (>100 observations) (Razali et al. 2011). However, the Shapiro–Wilk test is less powerful

in datasets with a small sample size. Thus, the Anderson-Darling normality test was utilized as the statistical test to examine the hypothesis of normality for vegetative firebrands.

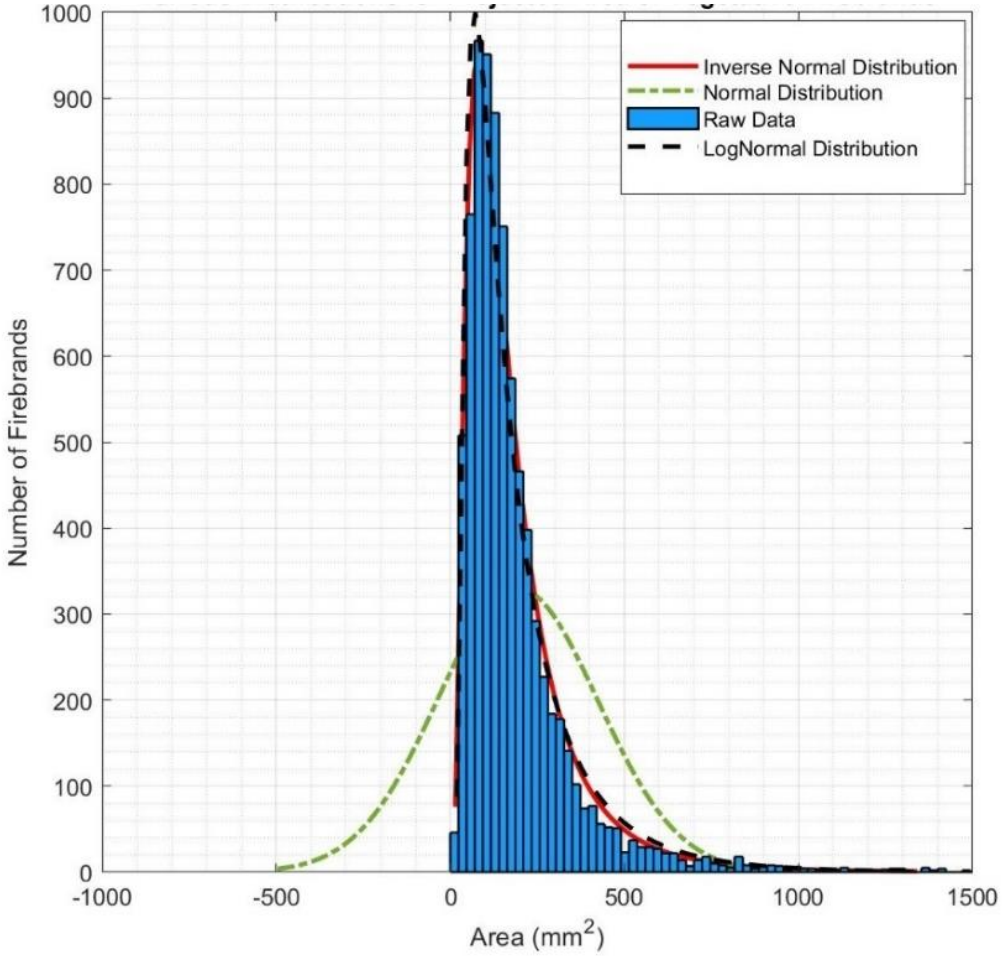

Figure 4.9. Various Probability Distributions Fitted
on the Entire Projected Area Values of the Vegetative Firebrand Dataset

Various PDFs were plotted using the vegetation type firebrand data in Figure 4.10. Visual inspection of Figures 4.8 and 4.9 indicates that no specific PDF can precisely predict the best distribution model for the vegetation type. However, as stated in Table 4-7, statistical tests for BIC scores are demonstrating that the Log-Normal distribution can be used to proceed with data analysis. To better examine the practicality of this distribution, statistical tests such as normality and goodness-of-fit can be employed during the regression analysis.

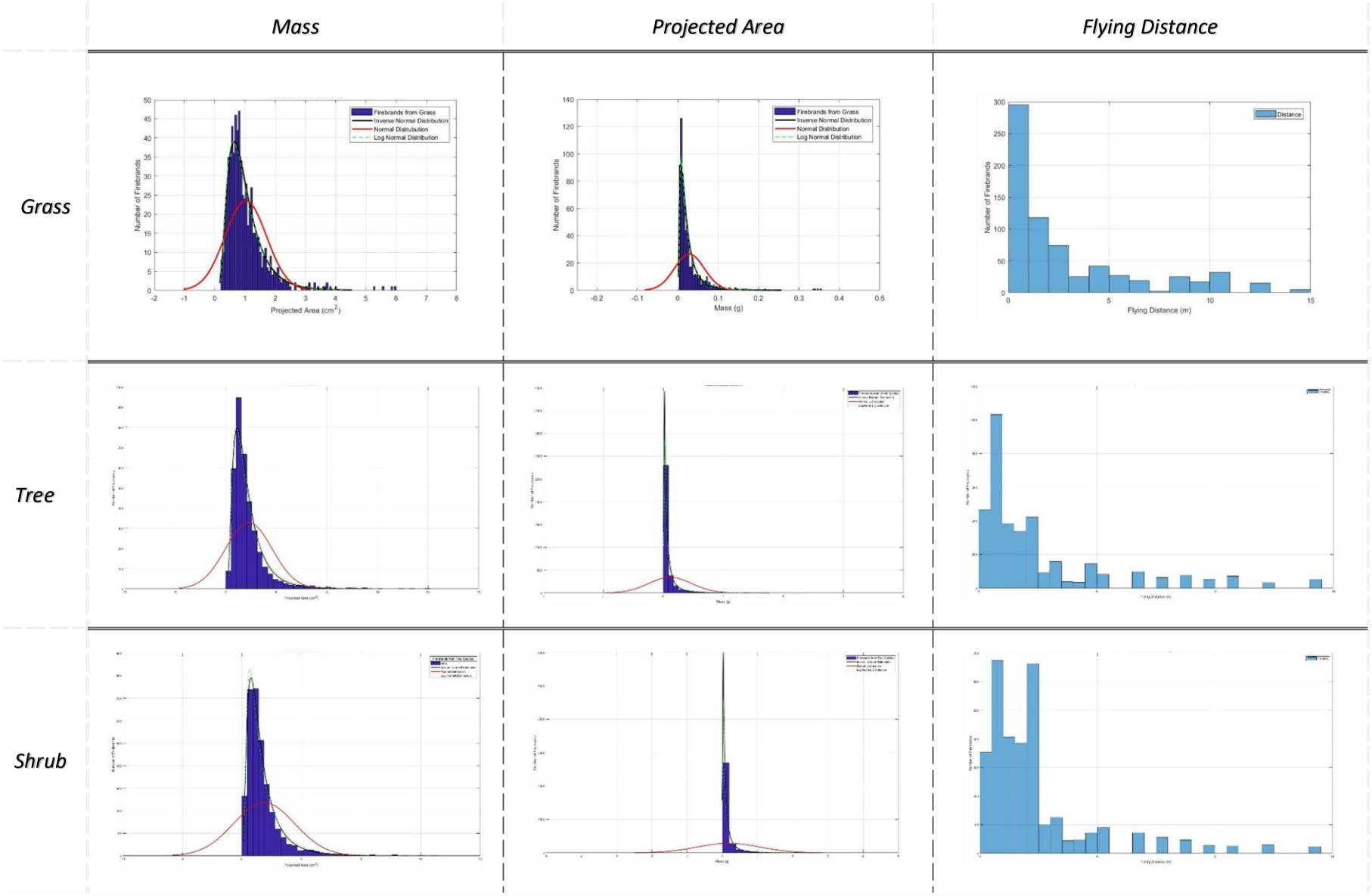

Figure 4.10. Various Probability Distributions Fitted to Different Types of Vegetative Fuels

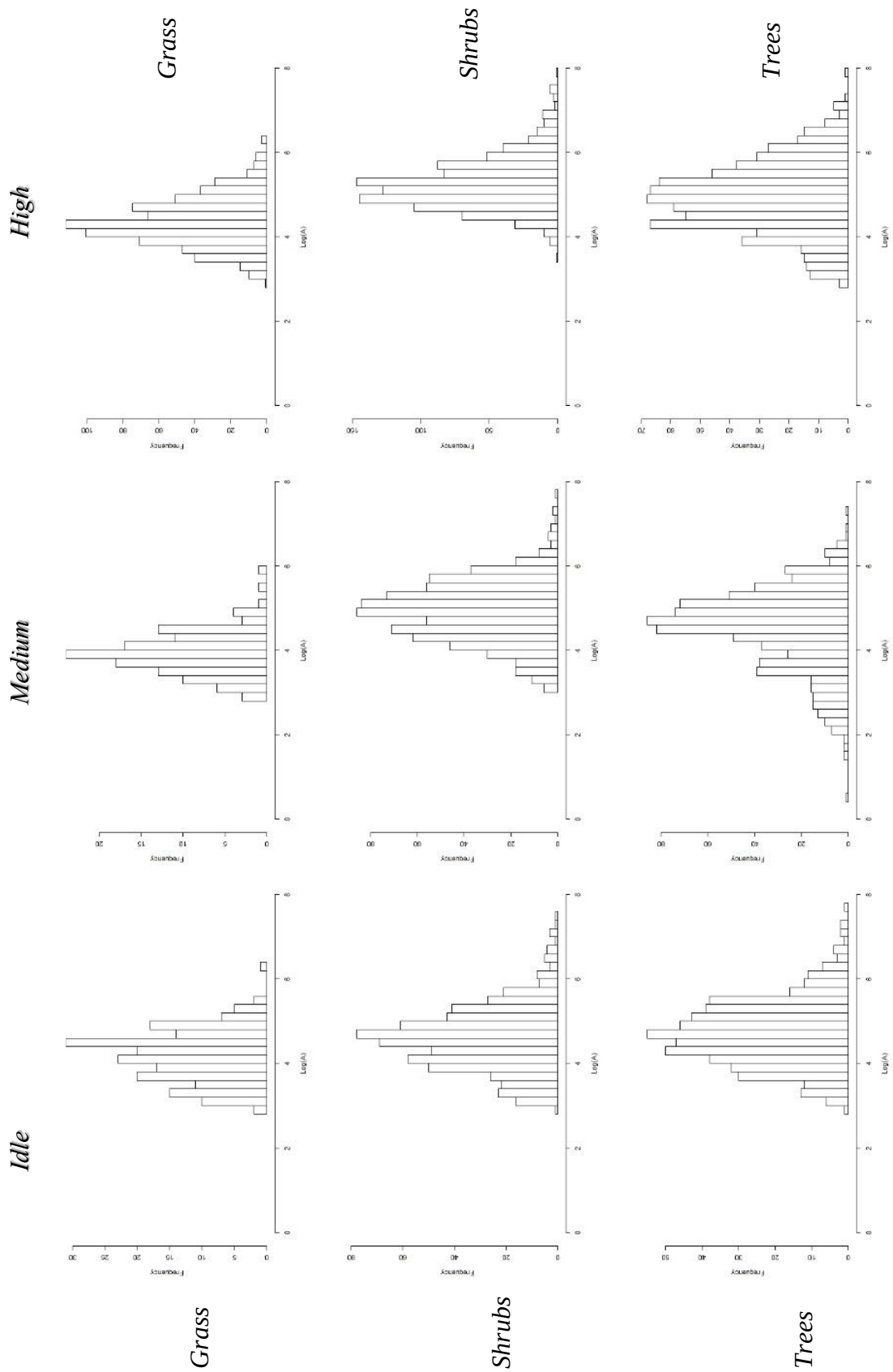

Figure 4.11. Histograms of Projected Area Values of Firebrands after Log Transformation for Various Vegetation Species in Different Wind Speed Levels

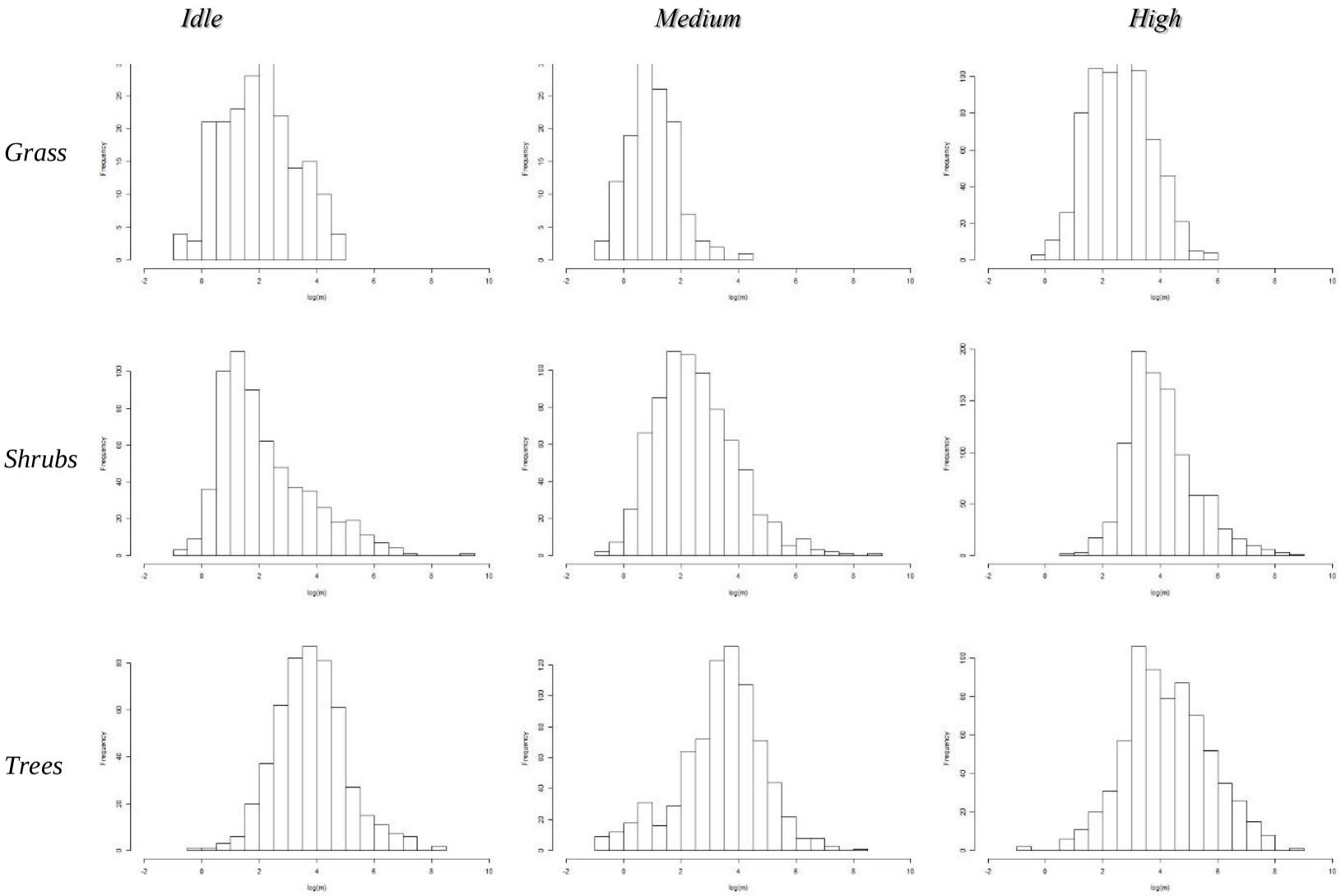

Figure 4.12 . Histograms of Mass Values of Firebrands after Log Transformation for Various Vegetation Species in Different Wind Speed Levels

Log-transformed firebrand data for mass and projected area by vegetation type level are plotted in Figures 4.11 and 4.12. As can be seen, none of the distributions were multimodal, and log-transformation was clearly one crucial step toward a more symmetric and Gaussian-like distribution to continue with meeting the requirements of the regression analysis. However, visual inspection is not sufficient, and statistical tests are required to examine the hypothesis of normality, both for vegetation type and the whole vegetative population.

Anderson-Darling test is written as:

$$A = -n - \frac{1}{n}\sum_{i=1}^{n}[2i-1][\ln(p_{(i)}) + \ln(1 - p_{(n-i+1)})] \quad \text{(Eq. 4.4)}$$

Where:

$$p_{(i)} = \Phi[x_{(i)} - \bar{x}]/s \quad \text{(Eq. 4.5)}$$

Φ: $Cumulative\ distribution\ function\ (CDF) of\ the\ standard\ normal\ distribution$

$\bar{x}$: $Mean\ of\ Data$

$\bar{x}$: $Standard\ Deviation\ of\ Data$

The p-value for this test is calculated as Equation 4.6, according to Table 4-10 in (D'Agostino et al. 1986).

$$Z = A(1.0 + 0.75/n + 2.25/n^2) \quad \text{(Eq. 4.6)}$$

A set of statistical processes needs to be performed on the data set to estimate any potential relationship among predictor(s) (independent variables) and outcome (dependent variable) before employing the normality and goodness-of-fit test. This set of processes is called *regression analysis*. By performing a linear predictor function on log values of mass and projected area of firebrands and employing the Anderson-Darling test for each sub-level of data and the whole population, a set of p-values were derived that can assist in

understanding whether or not a specific group or a subgroup's distribution behaves similar to the Gaussian regression.

Anderson-Darling (AD) test is a goodness-of-fit test that measures how well the data fits the desired probability distribution. The null hypothesis in the AD test is that observations are normally distributed. Results from this test in vegetation-level are summarized in Tables 4-8 and 4-9 and were used to determine the normality of data.

Table 4-8. Maximum Likelihood Estimation of Parameters for Lognormal Distribution- Area

Species	***Wind Speed***	***Mean Value***	***Standard Deviation***	***p-Value***
Grass	Idle	4.17	0.61	0.43
	Medium	3.93	0.52	0.88
	High	4.35	0.58	0.14
Shrub	Idle	4.59	0.77	0.13
	Medium	4.90	0.74	0.29
	High	5.25	0.62	9.91×10^{-4}
Tree	Idle	4.72	0.79	0.58
	Medium	4.50	0.96	4.73×10^{-4}
	High	4.93	0.85	0.93

As observed, p-values of only two sub-groups for the projected area and four sub-groups for mass, both out of nine sub-groups, were less than 0.05. For instance, shrub species' mass data shows strong evidence in rejecting the null hypothesis; referring to the Anderson-Darling test results, mass distribution of shrub species were not normally distributed under any wind level condition.

Table 4-9. Maximum Likelihood Estimation of Parameters for Lognormal Distribution- Mass

Species	***Wind Speed***	***Mean Value***	***Standard Deviation***	***p-Value***
Grass	Idle	1.99	1.25	0.55
	Medium	1.02	0.85	0.68
	High	2.58	1.09	0.27
Shrub	Idle	2.16	1.54	9.71×10^{-7}
	Medium	2.51	1.39	9.6×10^{-3}
	High	4.02	1.17	3.55×10^{-6}
Tree	Idle	3.78	1.23	0.21
	Medium	3.39	1.48	9.97×10^{-4}
	High	4.24	1.44	0.35

Interestingly, the p-value of the Anderson-Darling test for log-values of data was 0.033, meaning that the test weakly rejects the normality of distribution after log-transformation. The rejection indicated that the relationship between predictor and outcome might not be linear, and further analysis or transformation would be required. Figure 4.13 illustrates the distribution of residuals after log-transformation and linear regression analysis. Visual inspection of this figure showed that the distribution is closer to a Gaussian distribution after the logarithmic transformation. However, statistical tests are necessary to determine whether data is behaving like a normal distribution or not.

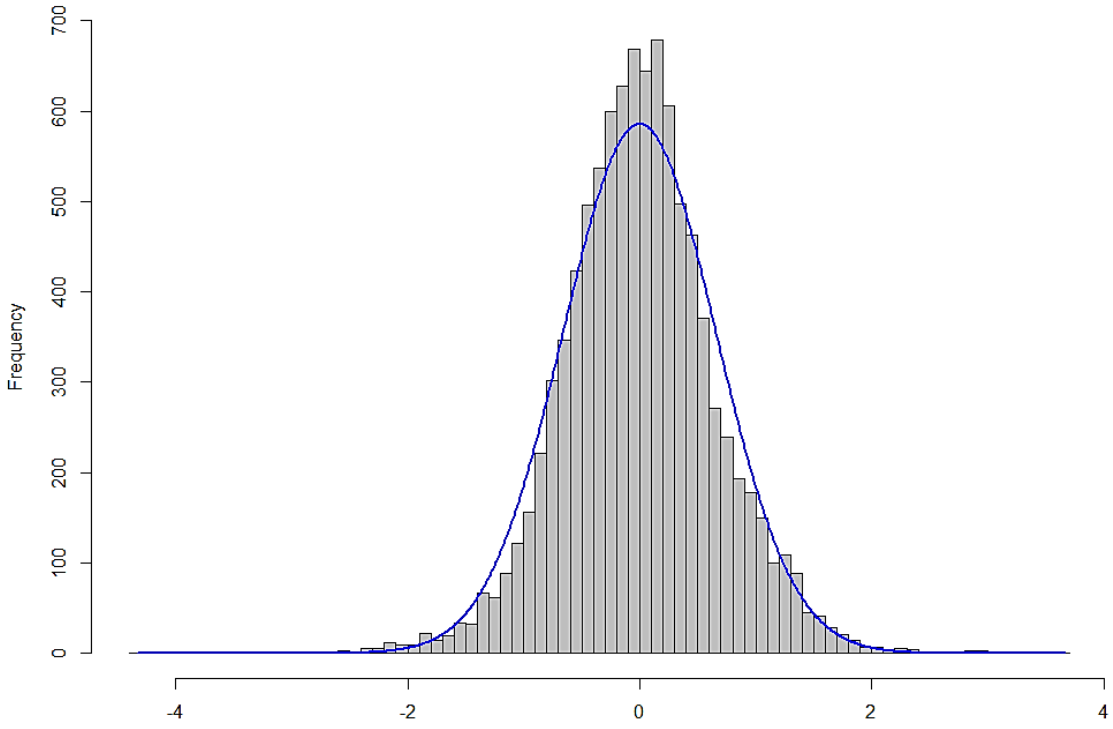

Figure 4.13. Distribution of Residuals after Log-Transformation

Another assumption in linear regression is the absence of heteroscedasticity in the data. Heteroscedasticity means that error terms in an independent variable are not normally distributed, and one or more of the independent variables have a statistically significant relationship with residuals. A statistical test known as the Breusch-Pagan Test or Non-Constant Variable test was employed (Pagan 1979) to examine heteroscedasticity in a data set. The null hypothesis in this test is that the variance remains constant during regression analysis. Using the non-constant variable test on log-transformed firebrand data results in a p-value of 22×10^{-16}, indicating that the test rejects the null hypothesis, and consequently, the data still did not show homoscedasticity after log-transformation. The fact that the p-value was significantly smaller than 0.05 showed that there were potential, influential outliers present in the dataset, and further treatment of the regression model was necessary, including the use of statistical methods to eliminate outliers.

4.1.6 Potential Correlations among Variables

The potential correlations among variables were examined to proceed with statistical analysis. Understanding the correlation is essential since such a relationship among independent variables can alter the results from the regression analysis. Correlation is calculated using the following equation:

$$Correl(X,Y) = \frac{\sum(x-\bar{x})(y-\bar{y})}{\sqrt{(x-\bar{x})^2.\sum(y-\bar{y})^2}} \quad \text{(Eq. 4.7)}$$

Where $\bar{x}$ and $\bar{y}$ are the average values for the first and second parameters, respectively.

Correlation shows the strength of the relationship between two variables and can vary between -1 and 1. Positive correlation values indicate that two parameters are moving in tandem, where a negative correlation shows that the two variables move in opposite directions. The closer the correlation value to 1, the stronger the relationships of variables are.

Correlation among the physical properties of firebrands has been previously observed in the literature. Scatter plots can assist in visual inspection and generating potential trendlines among variables to examine the correlation. Figures 4.14 and 4.15 illustrate the scatterplots of mass vs. projected area for all vegetative firebrands. A linear regression trend for all dataset shows a correlation of 0.77 between the mass and projected area.

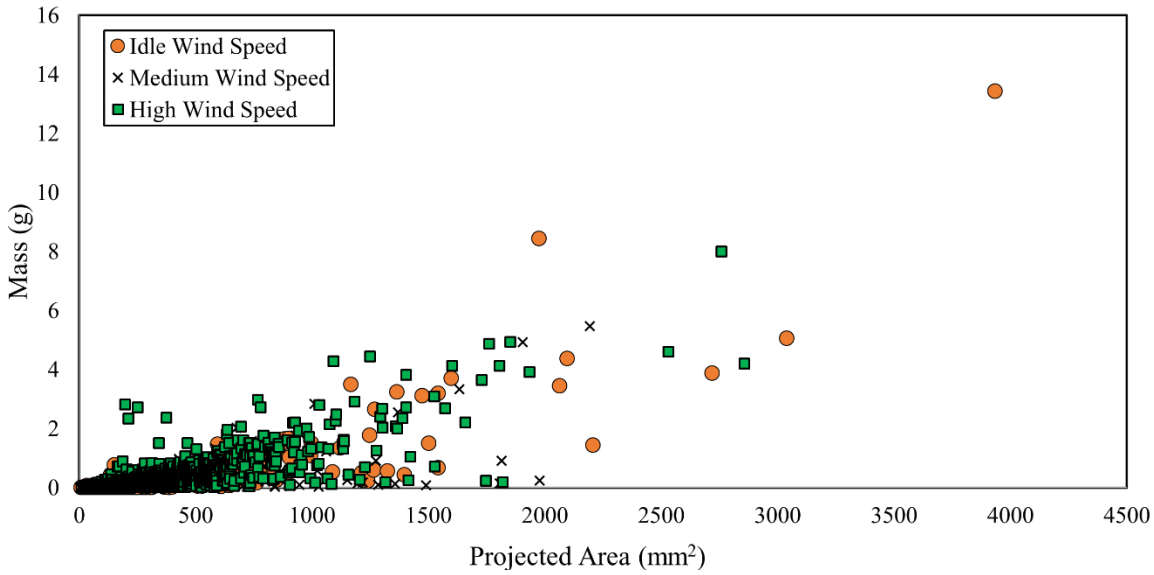

Figure 4.14. Scatterplot of All Vegetative Firebrands in Various Wind Speed Levels

Reviewing photos of firebrands indicated that the four largest firebrands in this study should be considered as outliers (see Figure 4.16). Reasons for this decision are:

- Daily notes showed that two large branches were detached from the Leyland cypress during the experiment run at the high wind speed. Further examination showed that these branches were only charred and not burned, and could not become a source of firebrand production after detachment
- All four specimens were collected from the first row on pans. In other words, the second sub-process of firebrand phenomena, transportation, did not occur for these samples
- The average projected area of these samples was 30 times larger than the average of 45% of the data. A rule of thumb to eliminate outliers from a data set is to remove the data above $\mu + 2\sigma$ or below $\mu - 2\sigma$, where μ is the mean and σ is the standard deviation of the dataset.

Figures 4.14 and 4.15 represent all data points before the removal of outliers and utilizing any statistical tests.

The sources of uncertainly in measurement and the importance of defining the firebrand are discussed in depth in section 4.1.7.

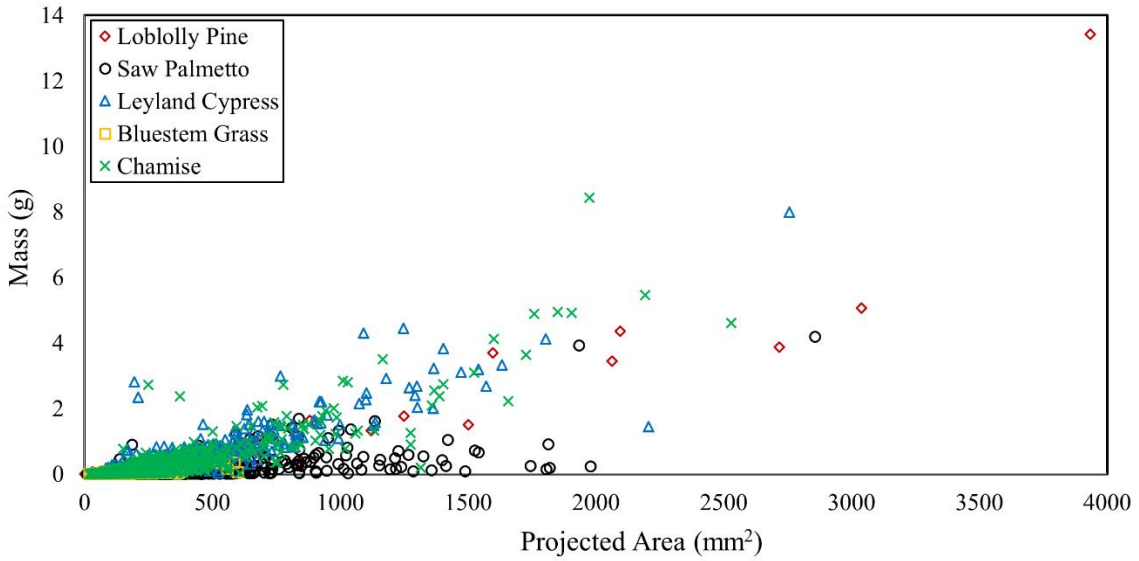

Figure 4.15. Scatterplot of All Vegetative Firebrands Grouped by Species

The correlation values between mass and projected area in all species were positive and larger than 0.50, whereas flying distance had negative correlation values between both mass and projected area. The negative correlation values indicated that the farther firebrands were being transported from their generation source, the smaller their mass and projected area values were.

Tables 4.10 to 4.14 show the correlation values and the strength of association among various physical properties of vegetative firebrands in this study. As shown, the correlation between mass and projected areas in all species is positive and higher than 0.50. Tree species show the highest correlation among these two variables (> 0.89 in all wind speeds).

No specific pattern was observed while considering the effect of wind speed changes on the correlation values. In other words, higher wind speed levels did not necessarily increase the correlation values between mass and projected areas.

As observed in the tables, there is a consistent positive relationship between mass and projected area, and a negative relationship between both flying distance and projected area, and flying distance and mass. This fact indicated that larger firebrands were more likely to have higher mass values. On the other hand, negative correlation implied that firebrands landed farther were more likely to be smaller. Although correlation is a parameter to measure the linear association between two variables, it does not imply the causation, especially if the relationship is not linear. Further analysis is required to find the relationships between the physical properties of firebrands. This topic is discussed in detail in section 4.1.8 of this dissertation.

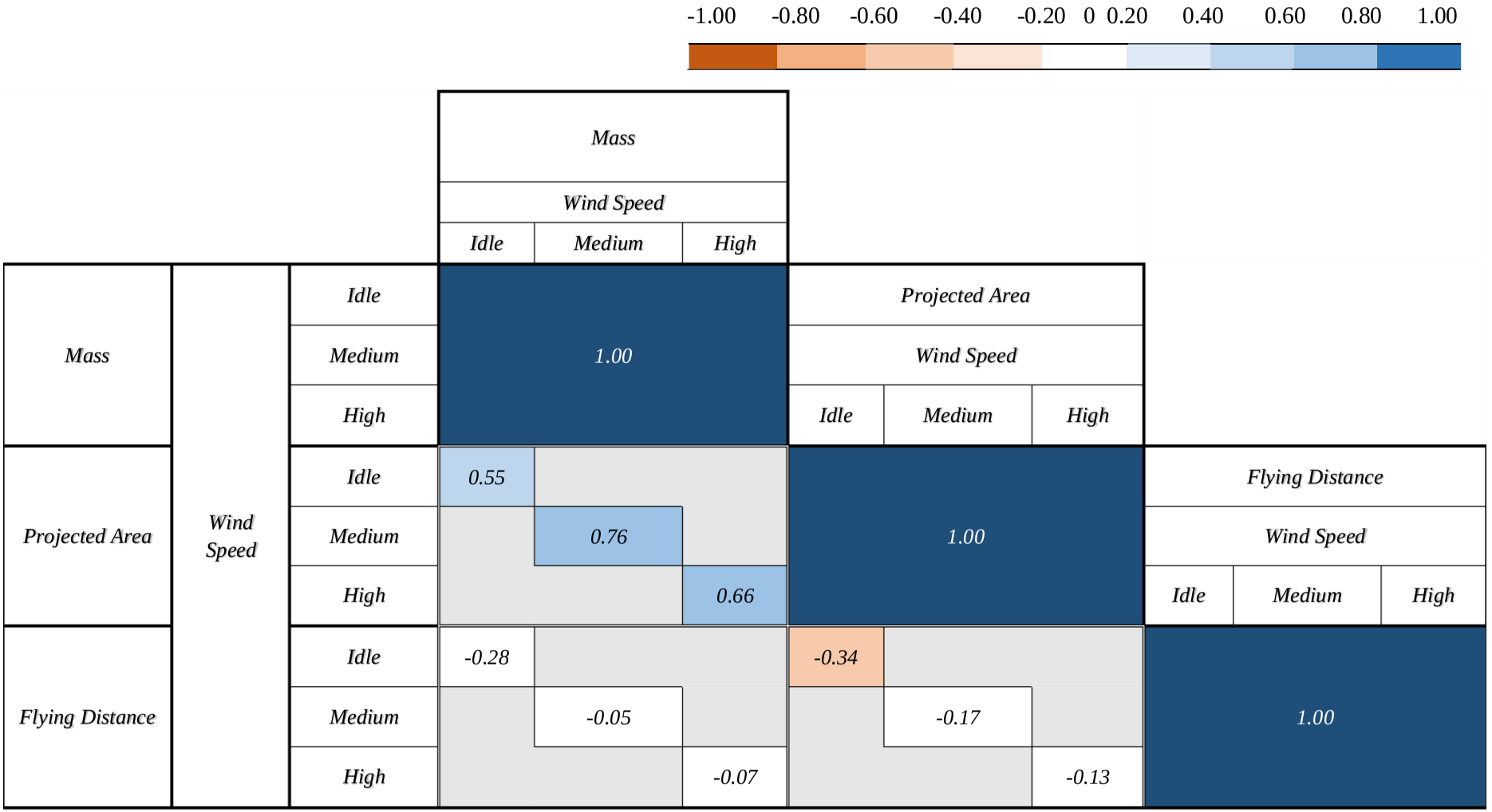

Table 4-10. Correlogram for Physical Properties of Little Bluestem Grass in Different Wind Speed Levels

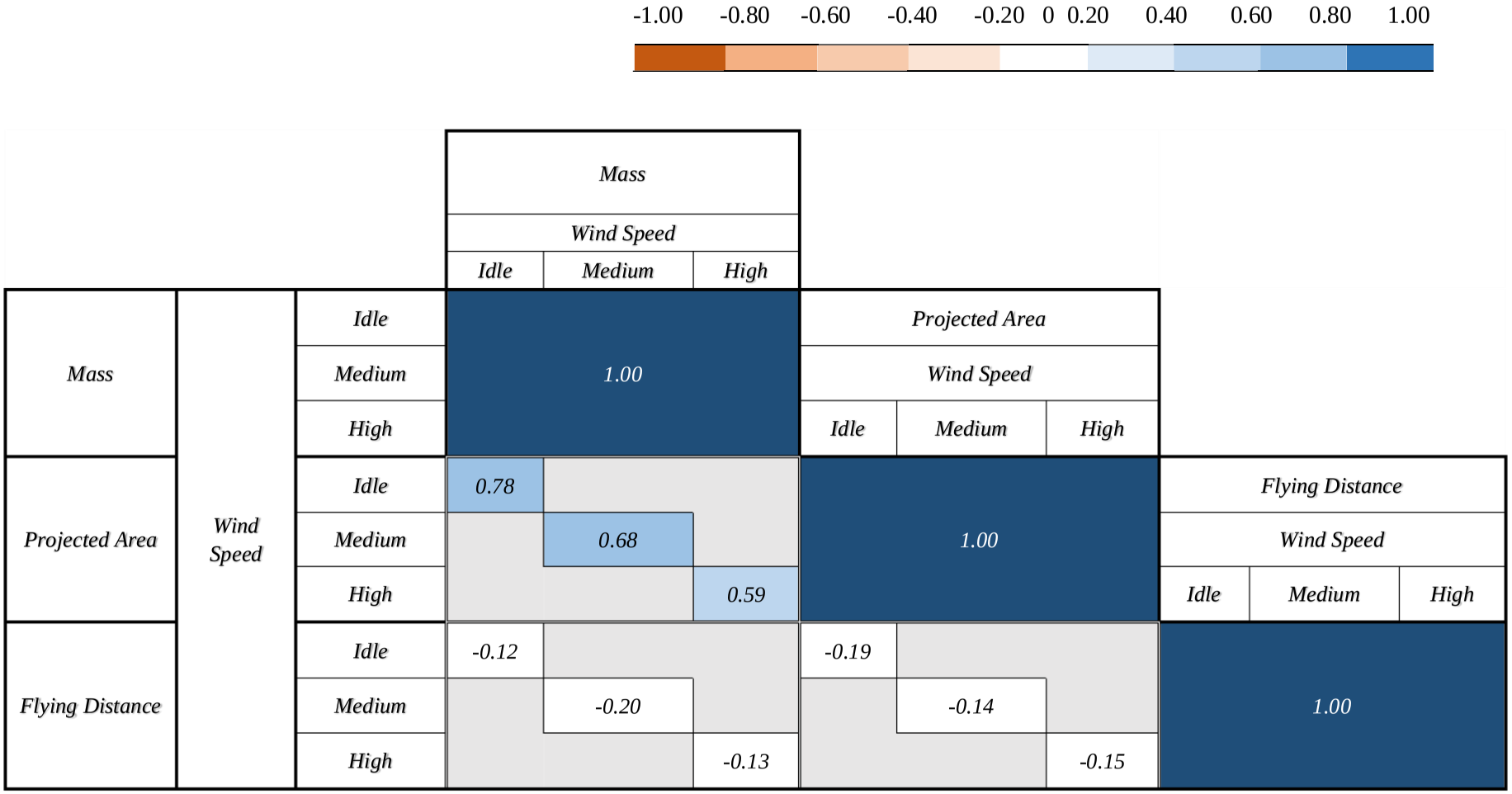

Table 4-11. Correlogram for Physical Properties of Saw Palmetto in Different Wind Speed Levels

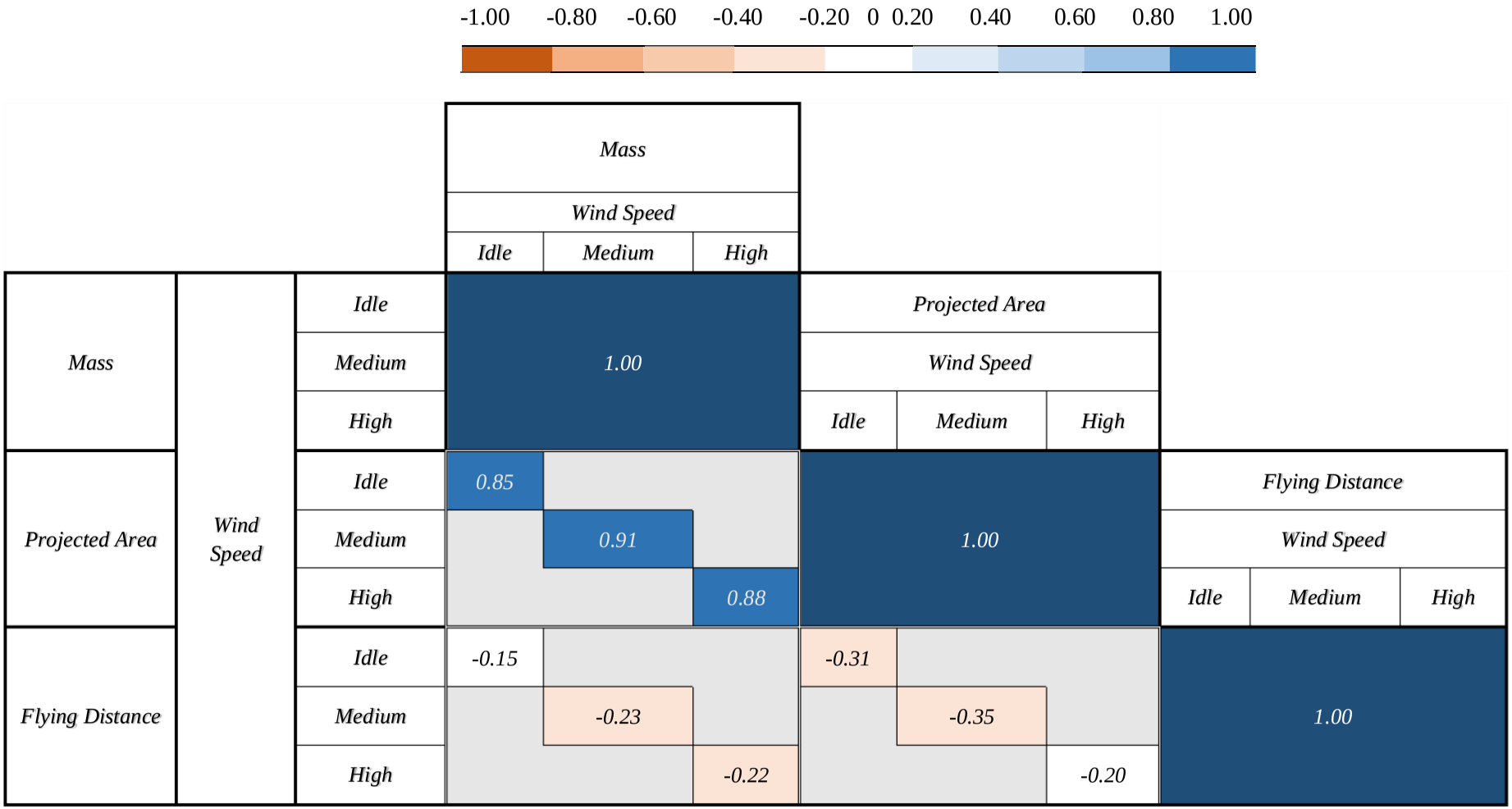

Table 4-12. Correlogram for Physical Properties of Chamise in Different Wind Speed Levels

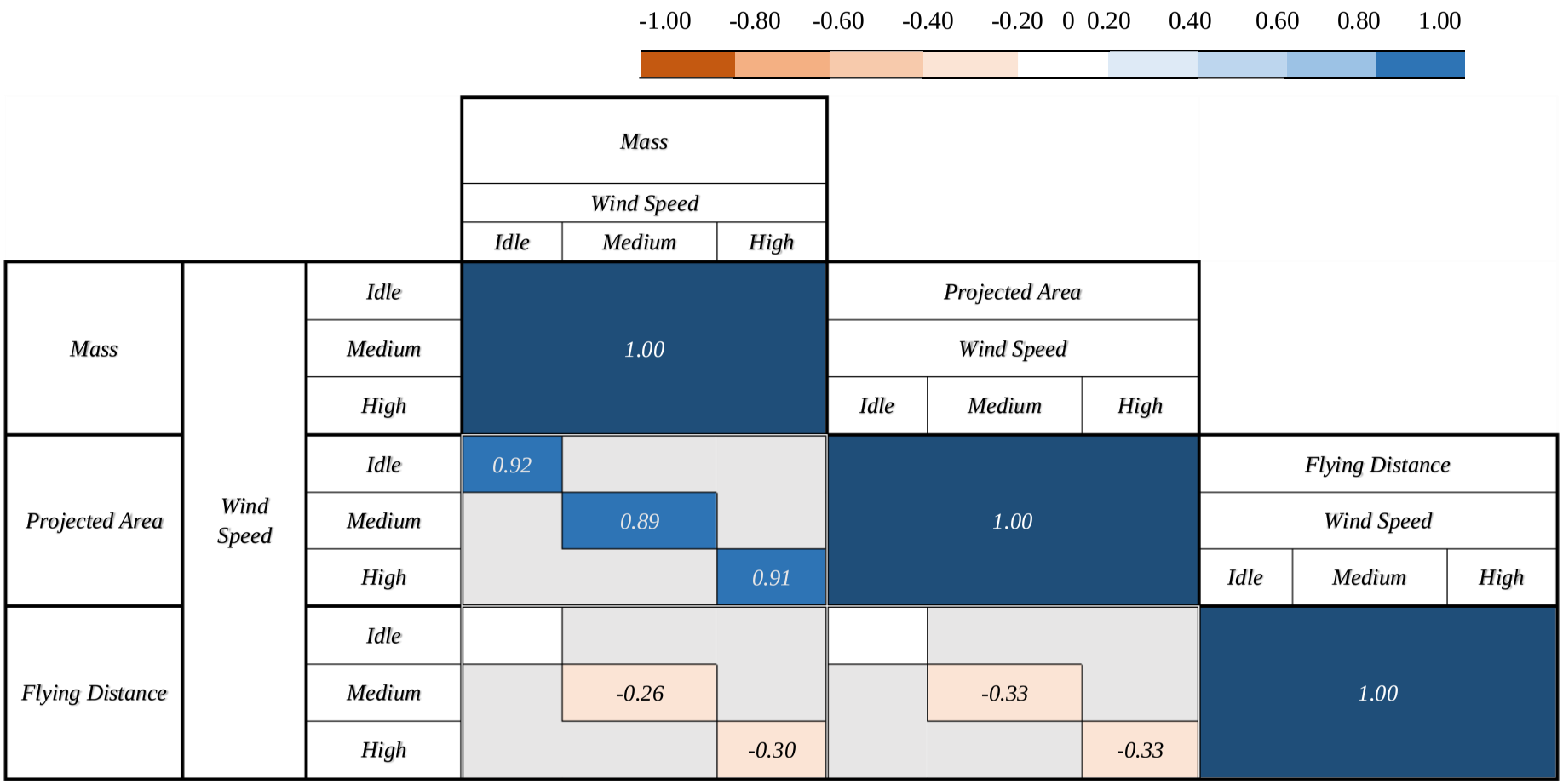

Table 4-13. Correlogram for Physical Properties of Leyland Cypress in Different Wind Speed Levels

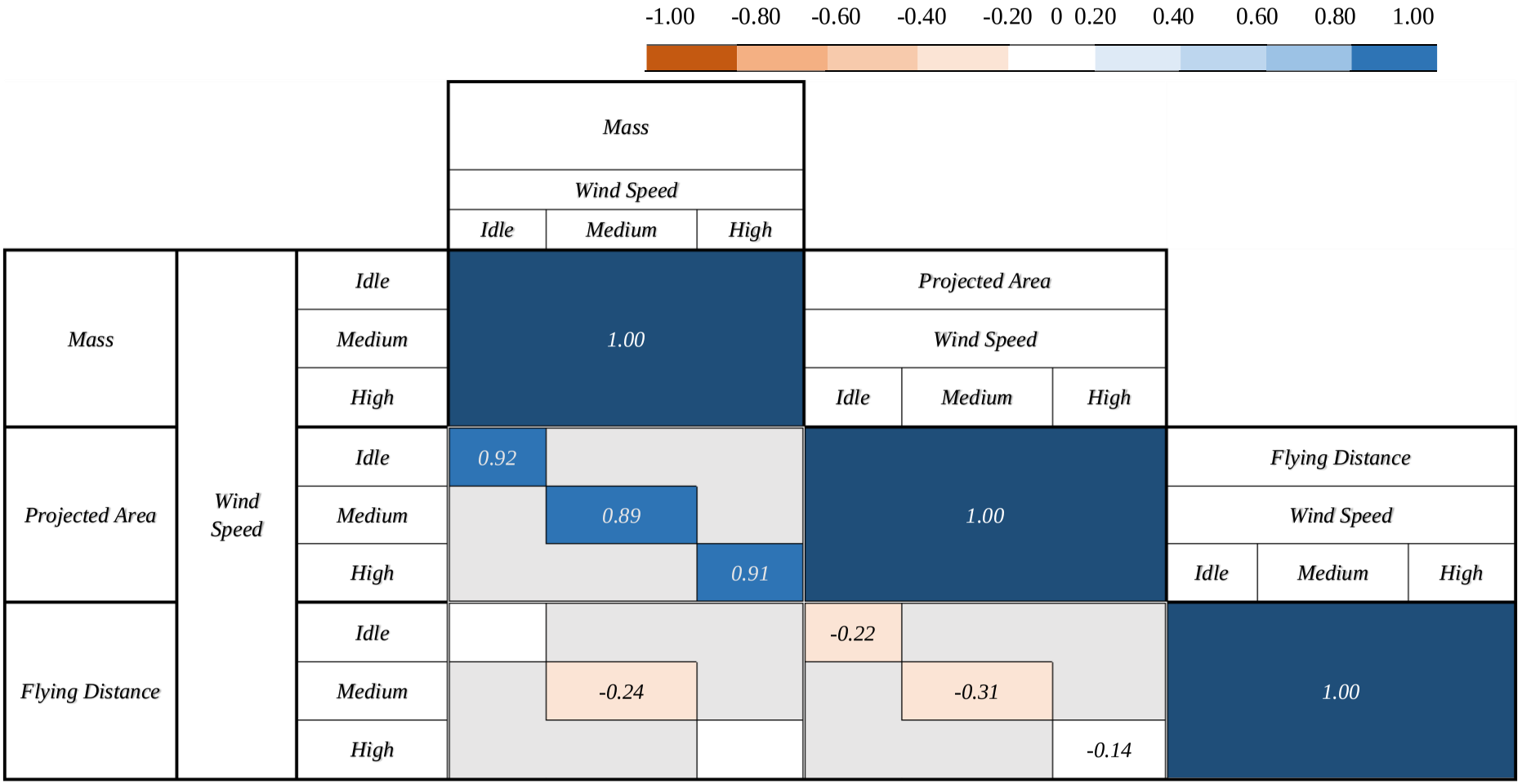

Table 4-14. Correlogram for Physical Properties of Loblolly Pine in Different Wind Speed Levels

4.1.7 Sources of Uncertainty in Measurement

The strong correlation between mass and projected area of firebrands in this study means that only one should be used as the independent variable. The uncertainty of measurement in projected area values compared to the measurement of mass was more considerable, considering the sampling method and initial characterization. There are numerous sources of uncertainty when computing the projected area of firebrands, including, but not limited to, the thresholding technique and related error, and quality of the captured photo for image analysis. Detailed uncertainty analysis of the firebrand projected areas can be found in (Hedayati et al. 2019). The current image analysis approach utilized a 2-D image of the firebrands (i.e., projected area). Due to the non-uniform nature of firebrand shapes, they can have several thickness values in different cross-sections. Measuring the thickness of firebrands is a time-consuming and complicated process. Some of the previous studies utilized semi-precision calipers and reported an average value of 3 to 10 measurements from different locations in cross-sections of firebrands (Manzello and Maranghides 2007; Manzello et al. 2008; Manzello and Foote 2014; Manzello and Suzuki 2014; Filkov et al. 2017). Multiple sources of error are present in measuring a firebrand thickness using a caliper:

1) Observational (measurement) error: Indicates the difference between the measured value and the actual value.
2) Measurement method error: There is no standard or guideline published to date for the measurement of firebrand thickness. Consequently, different measurement procedures were suggested and used in previous papers.

3) The error resulting from the nature of measured object: In the case of firebrands, non-uniform thickness and irregular shape of edges are sources of error in measurement. Although some of the previous studies suggested a cylindrical shape for vegetative firebrands to simplify the post-experiment measurements and modeling (Anthenien et al. 2006; Atreya et al. 2017b; Manzello et al. 2008; Mell et al. 2009), photos of near 10,000 firebrands in this study strongly support the non-uniform nature of firebrands and their various shapes. Different shapes can be formed due to combustion mode, fuel characteristics, and environmental conditions. The firebrand generation process may cause numerous sources of uncertainty for the measurand, result in neither precise nor accurate measurements.
4) Instrument error: The precise measurement of the thickness of tiny firebrands depends on the resolution of the caliper. Also, the calibration of semi-precision measuring equipment was another source of uncertainty.

The sampling method plays a vital role in the further statistical analysis of a sample set or population. Early firebrand studies used plastic sheets as collection methods (Vodvarka 1969, 1970), while more recent experiments at the National Institute of Standard and Technology (NIST) and other locations used water pans to collect landed firebrands. Due to financial and design restrictions, collection pans are not continuous and are mostly arranged in semi-circular or rectangular shapes. There are two reasons for damaging the randomness of firebrand collection process:

1) Non-continuous pans result in the partial collection. In other words, only those firebrands will be collected that landed in one of the pans.

2) There are no criteria for size, shape, and mass of firebrands. Some of the landed firebrands could be relatively large or small. The problem with larger pieces generated from vegetation is that there are still no clear criteria to distinguish firebrand and fire debris from one another. Figure 4.16 shows some of the large pieces, mostly twigs and branches, collected in this study. According to daily experimental notes in Tables 3.3 to 3.7, some of these pieces are unburned and/or detached during the 10-s direct flame impingement from the tree trunk and fell into the first row of collection pans.

Figure 4.16. Various Shape, Size, and Mass of Firebrands Collected from Generation Experiments of Three Vegetation Species

Such big pieces generated during experiments can raise several questions in the sampling method:

- The first sub-process of the firebrand phenomenon is firebrand generation. Generated firebrands have two combustion modes: flaming or smoldering. While some of these specimens are not entirely burned or only charred/ partially-charred, should they be considered as a firebrand? Note that an ignition potential from a smoldering firebrand is still existed, depending on the conditions of the receptive fuel bed.
- The second sub-process of the firebrand phenomenon is lofting by wind and/or fire plume, and transportation with wind or in a convection column. Since these pieces are detached and fell without horizontal transportation, should they be considered as a firebrand?
- The third sub-process in the firebrand phenomenon is the landing and potential ignition of recipient fuel. These samples are detached and have not been transported. Their combustion mode is also neither flaming nor smoldering. The other question is the falling location of these pieces, where due to larger size, they may fall on two or more adjacent collection pans. The collection of such pieces can then be only based on the judgment of the collector, which later determines the flying/ landing distance of the sample.
- During some of the experiments on firebrand generation from structural fuels (see (Hedayati et al. 2019)), detachment and falling of big pieces of structural assemblies were observed mainly in at lower wind speeds. The author of this study recorded 500-fps video footage using a high-speed camera of some of these experiments. Reviewing these videos and comparing them to captured high-speed videos of generated firebrands

from vegetative fuels, as seen in Figure 4.17, detached debris from a structural assembly stayed typically in the flaming or smoldering condition. It was observed to be a source of firebrand generation itself.

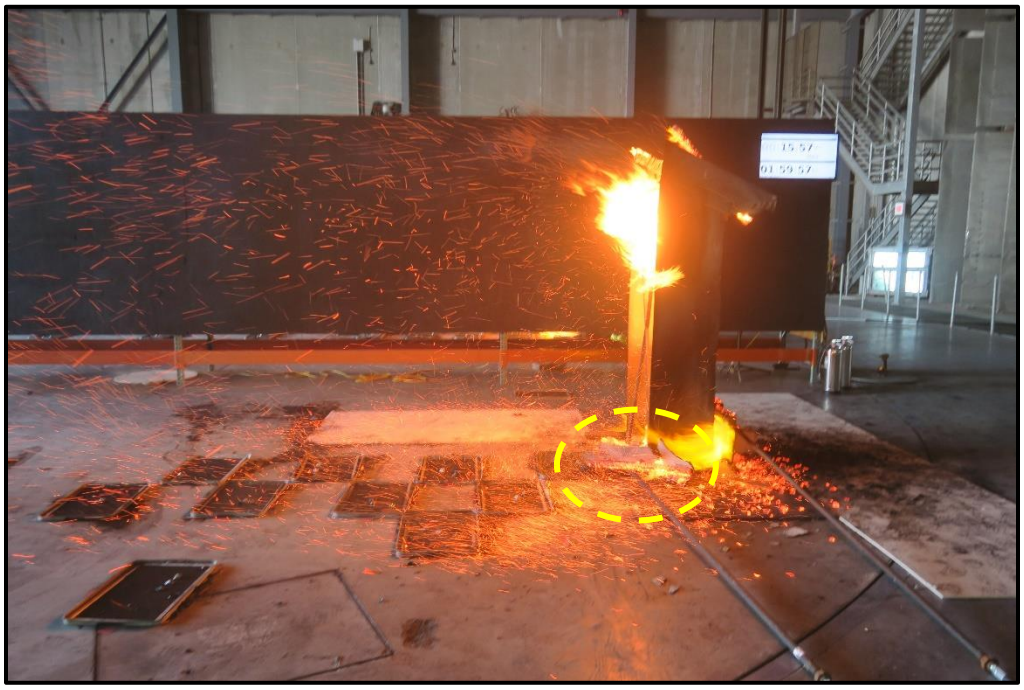

Figure 4.17. A Structural Assembly constructed from Oriented Strand Board (OSB) Siding, Sheathing, and Roof w/ Gypsum Board in Medium Wind Speed. Fallen Fire Debris is Generating Firebrands during the Test (Photo Courtesy of IBHS)

On the contrary, detached sections from a vegetative specimen during experiments, either twig, branch, or bark, were not observed to generate further firebrands during the tests due to their combustion mode or small size.

In summary, the firebrand collection process is a non-probability method known as the *consecutive sampling method*, where only samples/ observations of interest or available ones are collected (Suresh 2014). The collected samples were to be representatives of the whole samples. During the firebrand collection process, samples were selected that were more accessible compared to other firebrands. The selection of minimum size was also subjective and based on the collector's judgment or the experimental protocol. Landed

firebrands could also be broken during the collection and processing of firebrands, including lifting the screen mesh out of the pan and sliding it into a rack before transportation to ovens. This process was another source of uncertainty in the firebrand characterization process (Zhou et al. 2019).

(a) Saw Palmetto and Pine Needle Bed Tested in High Wind Speed

(b) Leyland Cypress Tested in Idle Wind Speed

(c) Chamise and Pine Needle Bed Tested in High Wind Speed

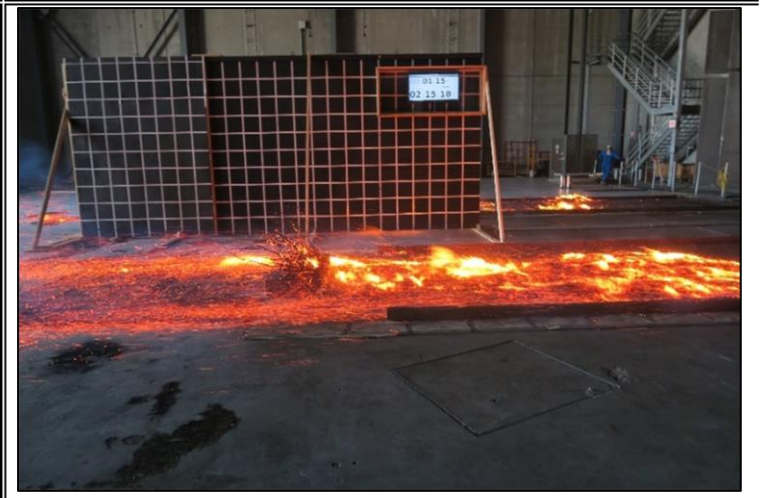

(d) Chamise and Pine Needle Bed Tested in High Wind Speed

Figure 4.18. Firebrand Generation in Various Vegetative Fuels and Wind Speed Levels (Photo Courtesy of IBHS)

4.1.8 Development of Regression Models

4.1.8.1 Lognormal Transformation

As observed in Figures 4.14 and 4.15, scatterplots showed that data were centralized around a point (i.e., the pattern of scatterplots was somewhat linear). A logarithmic transformation assisted in spreading the data points and decreasing the curve-like trend of plotted data. In other words, log-transformation reduced the skewness of the dataset. Data transformation was a deterministic mathematical function applied to observations so that they better meet the assumptions of a statistical model.

Figures 4.19 and 4.20 illustrate the difference in data trend when one of the variables, mass or projected area, is transformed to a logarithmic scale. This trend can assist in meeting the requirements of the assumptions of normality in descriptive statistics.

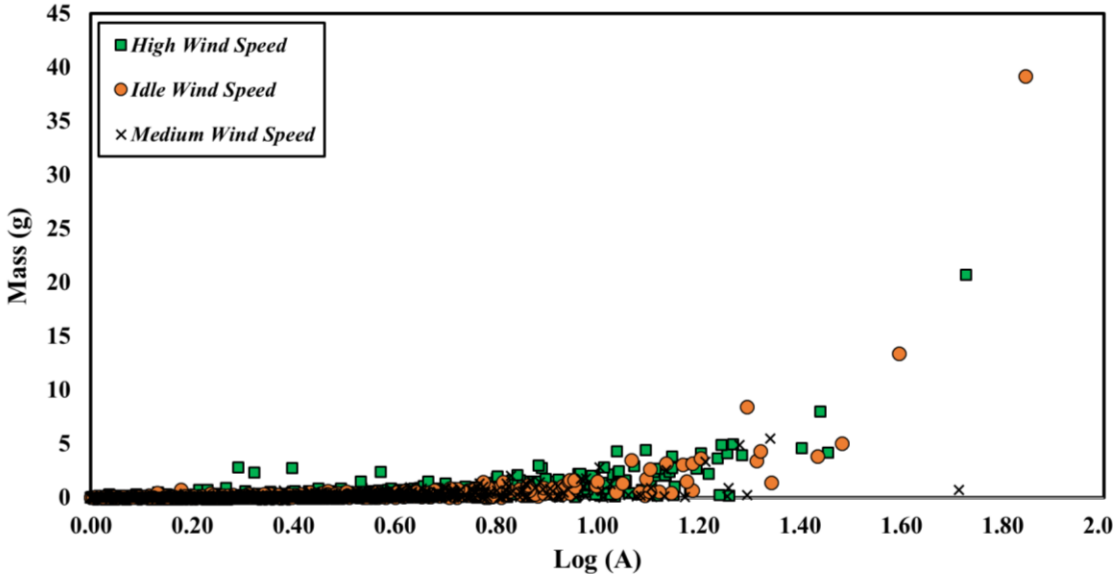

Figure 4.19. Scatter Plot of Mass vs. the Logarithm of Projected Area
Values of all Vegetative Firebrands

Following the discussion after Figure 4.16, the four marked detached pieces were considered as outliers during data analysis; however, they can still be observed in plots after the log transformation in Figures 4.19 and 4.20.

The lognormal distribution is defined as:

$$f(x) = \frac{1}{\sqrt{2\pi}\sigma x} e^{-(\log(x)-\mu)^2/2\sigma^2} \quad \text{(Eq. 4.8)}$$

Where:μ is the mean, and σ is the standard deviation of the logarithm.

Mean is calculated as:

$$E(x) = \exp\left(\mu + \frac{1}{2\sigma^2}\right) \quad \text{(Eq. 4.9)}$$

Median is calculated as:

$$med(X) = \exp(\mu) \quad \text{(Eq. 4.10)}$$

Variance is calculated as:

$$Var(X) = \exp\,(2\mu + \sigma^2)(\exp(\sigma^2) - 1) \quad \text{(Eq. 4.11)}$$

The Coefficient of Variation is calculated as $\sqrt{\exp(\sigma^2) - 1}$, which approximately equals σ when $\sigma < 0.5$ (or considered small) (Johnson et al. 1964).

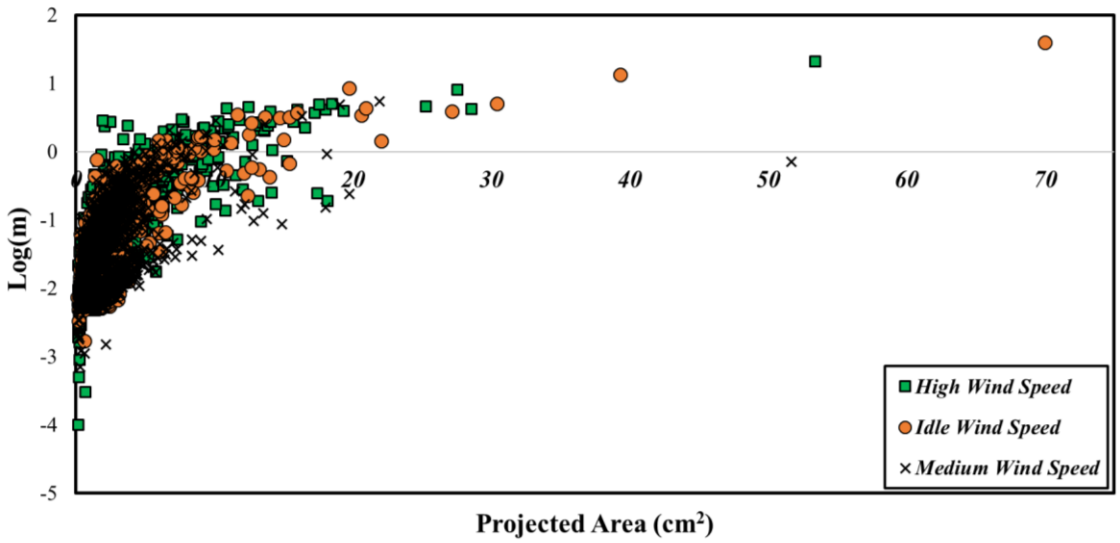

Figure 4.20. Scatter Plot of the Logarithm of Mass vs. Projected Area
Values of all Vegetative Firebrands

The likelihood function is defined as the estimation of parameters for particular PDFs for a sample data set. The Likelihood functions assist in a better understanding of how the data

is summarizing such parameters. Maximizing a likelihood function gives a maximum likelihood estimation (MLE) that estimates the parameters of the probability distribution so that the observed data values occurrence is most probable (Myung 2003).

The log-log transformation data for all vegetative firebrands is shown in Figure 4.21. Linear regression of data after transformation was plotted for three wind speed levels.

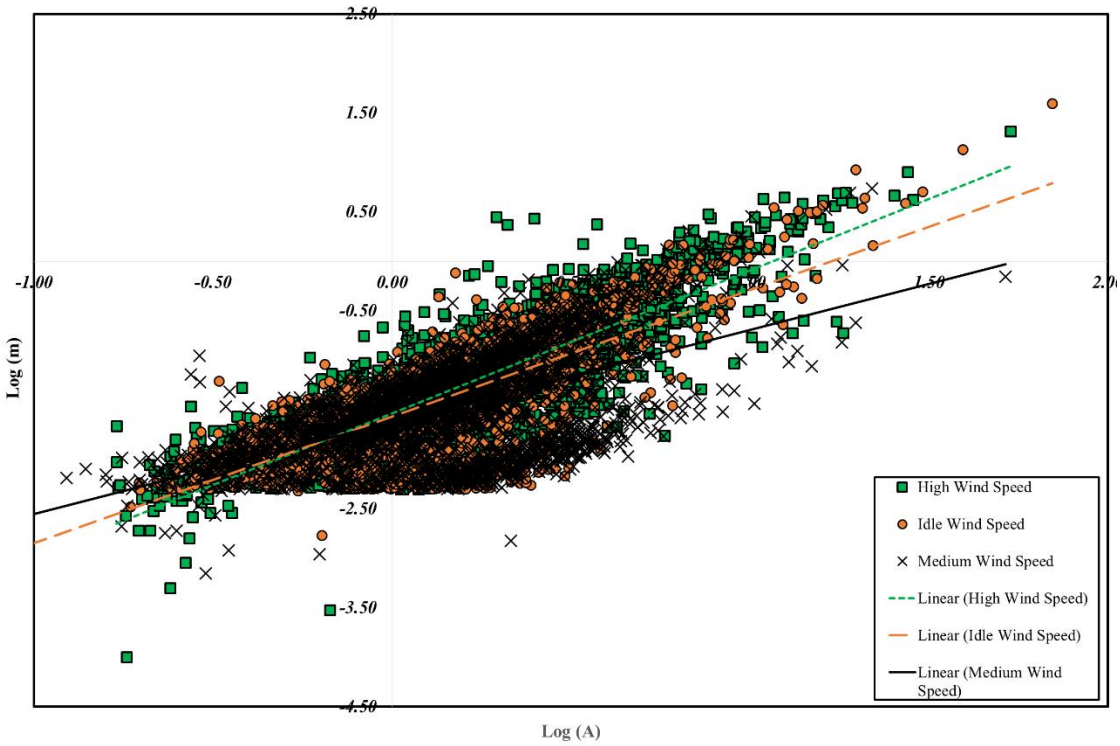

Figure 4.21. Scatter Plot of the Logarithm of Mass vs. the Logarithm of Projected Area Values of all Vegetative Firebrands (Log-Log Plot)

The difference in slopes in linear regression trendlines indicated that wind speed levels had a different effect on the physical properties, mass and projected area of the firebrands. The difference value can be obtained by interpreting the slope of the logarithmic regression model for vegetative firebrands in Equation 4.12.

$$\log(m) = \beta_{0,i} + \beta_1 \log(A_{FB}) + \varepsilon \qquad \text{(Eq. 4.12)}$$

Where $\beta_{0,i}$ is the slope, β_1 is the intercept, and ε is the estimated error.

As discussed in section 4.2.7.1, the projected area measurement of firebrands comes with various sources of uncertainty. By comparison, firebrand mass is relatively more straightforward, accompanied by fewer uncertainty factors. Thus, the mass was chosen as the outcome (dependent variable) and projected area, vegetation species, and wind speed level was used as predictors (independent variables). Estimates of the coefficients are summarized in Table 4-15.

Table 4-15. An estimate of Coefficients for Linear Regression of Firebrand Mass after Log-Transformation

Species	***Wind Speed***	***Total Generated Firebrands***	***Estimated Intercept Coefficient (β)***	***Estimated Slope Coefficient (β_1)***
Little Bluestem Grass	Idle	202	-3.87	1.41
	Medium	138	-3.05	1.04
	High	692	-2.76	1.23
Saw Palmetto	Idle	938	-3.65	1.17
	Medium	1289	-3.10	1.08
	High	1230	-3.66	1.43
Chamise	Idle	269	-3.84	1.62
	Medium	257	-3.44	1.49
	High	686	-4.22	1.64
Loblolly Pine	Idle	381	-3.12	1.49
	Medium	575	-3.11	1.46
	High	167	-3.05	1.44
Leyland Cypress	Idle	680*	-3.02	1.43
	Medium	1048*	-3.27	1.47
	High	1262*	-3.58	1.59

* *Leyland Cypress was tested in two phases: Phase I in 2016 and Phase II in 2017. The number in the cell shows the total generated firebrands for both phases. Generated firebrands separated by phases and based on various wind speeds are: Idle: 529 (phase I) and 151 (phase II), Medium: 883 (phase I) and 165 (phase II), and High: 1013 (phase I) + 249 (phase II)*

The p-values for all estimated coefficients were between 2×10^{-16} and 2×10^{-11}, which were less than 0.05 and consequently rejected the null hypothesis of the estimated intercept

coefficient (β) equal to zero. The rejection shows a significant statistical relationship among variables in this logarithmic regression model. The coefficient of determination (R^2) for this regression model was 0.967. Results from the Anderson-Darling test for log-transformation were summarized in Table 4-8 and 4-9. They showed that the test rejects the null hypothesis, and the data does not show homoscedasticity after log-transformation. Thus, further treatment of this regression model is required.

4.1.8.2 Power Transformation

The current dataset of firebrands showed a variance-on-mean relationship even after log-transformation. This relationship means that different data points have different variability values. In such cases, a variance-stabilizing transformation was required to remove this relationship and allow the application of regression analysis (Bartlett 1947). For regression purposes, a power transform known as Box-Cox transformation was suggested to create a monotone dataset utilizing power functions (Box 1964); to stabilize variance and assist in reshaping the distribution in a way that presents more symmetry (i.e., closer to Gaussian distribution).

The Box-Cox power transformations are defined as below for a random variable X:

$$Y = \frac{X^{\lambda}-1}{\lambda} \quad , \quad \lambda \neq 0 \qquad \text{(Eq. 4.13)}$$

Note, all values should be positive in the distribution, and Y is assumed to come from a normal distribution. This transformation is continuous in λ.

$$y_i = \frac{x_i^{\lambda}-1}{\lambda} \quad , \quad \lambda \neq 0 \qquad \text{(Eq. 4.14)}$$

Where *i=1 to n* form a random sample from a normal distribution (Box 1964).

Box-Cox transformation suggested that the value of λ should be chosen based on maximizing the likelihood function. Alternatively, goodness-of-fit tests can be used (Box 1964; Kowarik, 2019). The log-likelihood function of transformed observations can be re-written as (Stoline 1991) employing the change of variable formula:

$$\log[L(\lambda,\mu,\sigma)] = -\frac{n}{2}\log(2\pi) - \frac{n}{2}\log(\sigma^2) - \frac{1}{2\sigma^2}\sum_{i=1}^{n}(y_i-\mu)^2 + (\lambda-1)\sum_{i=1}^{n}\log(x_i) \quad \text{(Eq. 4.15)}$$

Where y_i is defined in Equation 4.14. To maximize the log-likelihood function, mean (μ) and standard deviation (σ) should be replaced by their maximum likelihood estimators (for a fixed value of λ):

$$\hat{\mu} = \frac{1}{n}\sum_{i=1}^{n} y_i \quad \text{(Eq. 4.16)}$$

$$\hat{\sigma} = \left[\frac{1}{n}\sum_{i=1}^{n}(y-\bar{y})^2\right]^{1/2} \quad \text{(Eq. 4.17)}$$

The value for λ is calculated as 1.1 after employing the Box-Cox power transformation, where λ is the power value in the regression model. The final model for vegetative firebrands in this study can then be written in Equation 4.18.

$$(log(m))^{1.1} = \beta_{0,i} + \beta_1\, log(A_{FB}) + \varepsilon \quad \text{(Eq. 4.18)}$$

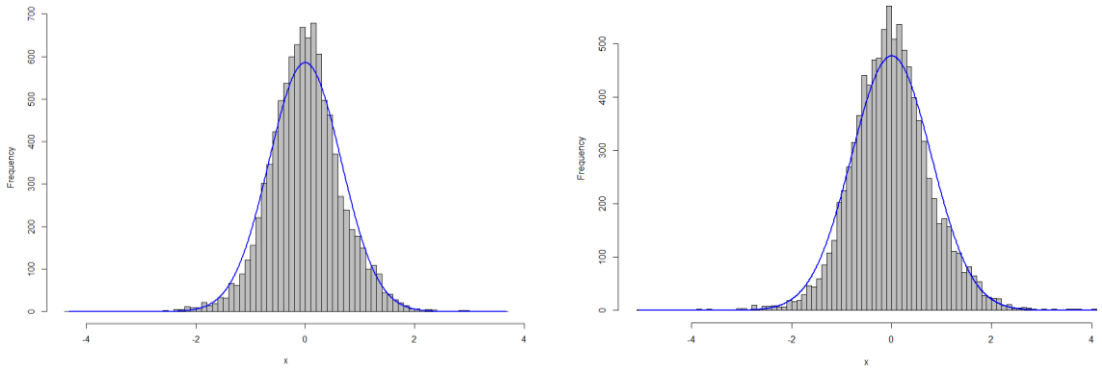

Figure 4.22. Log-Normal Histogram (Left) and Power Transformed Histogram (Right) of Mass Residuals for all Datapoints

The p-value of the Anderson-Darling test for log-values of data was 0.289, which meant that the test failed to reject the normality of distribution after power-transformation. Figure 4.22 compares the distribution of residuals after log-transformation and power-transformation. Non-Constant Variable test after power-transformation computed a p-value of 0.568. The null hypothesis in this test was that the variance remained constant during regression analysis, and this p-value indicated that the test failed to reject the null hypothesis, and consequently, data shows homoscedasticity after the power-transformation.

Estimates of the coefficients after power-transformation are summarized in Table 4-16. The p-values for all estimated coefficients were between 2×10^{-16} and 5.49×10^{-8}, which is 10^{-6} times less than 0.05, and consequently, the null hypothesis of the estimated intercept coefficient (β) equal to 0 is rejected. This fact shows a significant relationship among variables in this logarithmic regression model. The coefficient of determination (R^2) for this regression model was 0.964, indicating a strong correlation between predictors and our response variables.

Table 4-16. An estimate of Coefficients for Linear Regression of Firebrand Mass after Power-Transformation

Species	Wind Speed	Total Generated Firebrands	Estimated Intercept Coefficient (β)	Estimated Slope Coefficient (β_1)
Little Bluestem Grass	Idle	202	-4.28	1.56
	Medium	138	-3.13	1.09
	High	692	-3.49	1.46
Saw Palmetto	Idle	938	-4.38	1.37
	Medium	1289	-3.74	1.26
	High	1230	-5.09	1.81
Chamise	Idle	269	-5.27	2.05
	Medium	257	-4.97	1.92
	High	686	-5.98	2.10
Loblolly Pine	Idle	381	-4.32	1.87
	Medium	575	-3.56	1.67
	High	167	-4.13	1.79
Leyland Cypress	Idle	680*	-4.24	1.80
	Medium	1048*	-4.49	1.85
	High	1262*	-4.86	1.99

* *Leyland Cypress was tested in two phases: Phase I in 2016 and Phase II in 2017. The number in the cell shows the total generated firebrands for both phases. Generated firebrands separated by phases and based on various wind speeds are: Idle: 529 (phase I) and 151 (phase II), Medium: 883 (phase I) and 165 (phase II), and High: 1013 (phase I) + 249 (phase II)*

4.2 Characteristic Parameters of Vegetative Firebrands

To better understand the range of generated firebrands from different vegetation types in this study, the main physical properties of firebrands are summarized using a 95% confidence interval in Tables 4-17 to 4-19.

Table 4-17. Characteristic Physical Properties (Mass and Projected Area) of Firebrands Generated from Grass Specimen

Wind Speed	Idle	Medium	High
Mass [g]	(0.02 – 0.03)	(0.01 – 0.02)	(0.21 – 0.33)
Projected Area [cm^2]	(0.89 – 1.17)	(0.71 – 1.20)	(0.97 – 1.09)

Table 4-18. Characteristic Physical Properties (Mass and Projected Area) of Firebrands Generated from Shrub Species

Wind Speed	Idle	Medium	High
Mass [g]	(0.07 – 0.13)	(0.01 – 0.09)	(0.13 – 0.16)
Projected Area [cm^2]	(1.78 – 2.09)	(2.17 – 2.47)	(2.28 – 2.49)

Table 4-19. Characteristic Physical Properties (Mass and Projected Area) of Firebrands Generated from Tree Species

Wind Speed	Idle	Medium	High
Mass [g]	(0.10 – 0.29)	(0.08 – 0.10)	(0.21 – 0.30)
Projected Area [cm^2]	(1.65 – 2.12)	(1.47 – 1.61)	(2.05 – 2.35)

Figure 4.23 illustrates the comparison among results from various firebrand studies and the characteristic mass and projected area of those using a 95% confidence interval. Note, these data are only firebrands generated from vegetative fuels, A dataset from generation studies at IBHS in 2013 was also added to the graph. Results from studies at NIST (Zhou et al. 2015; Manzello and Suzuki 2017) showed no agreement with generated firebrands in this study.

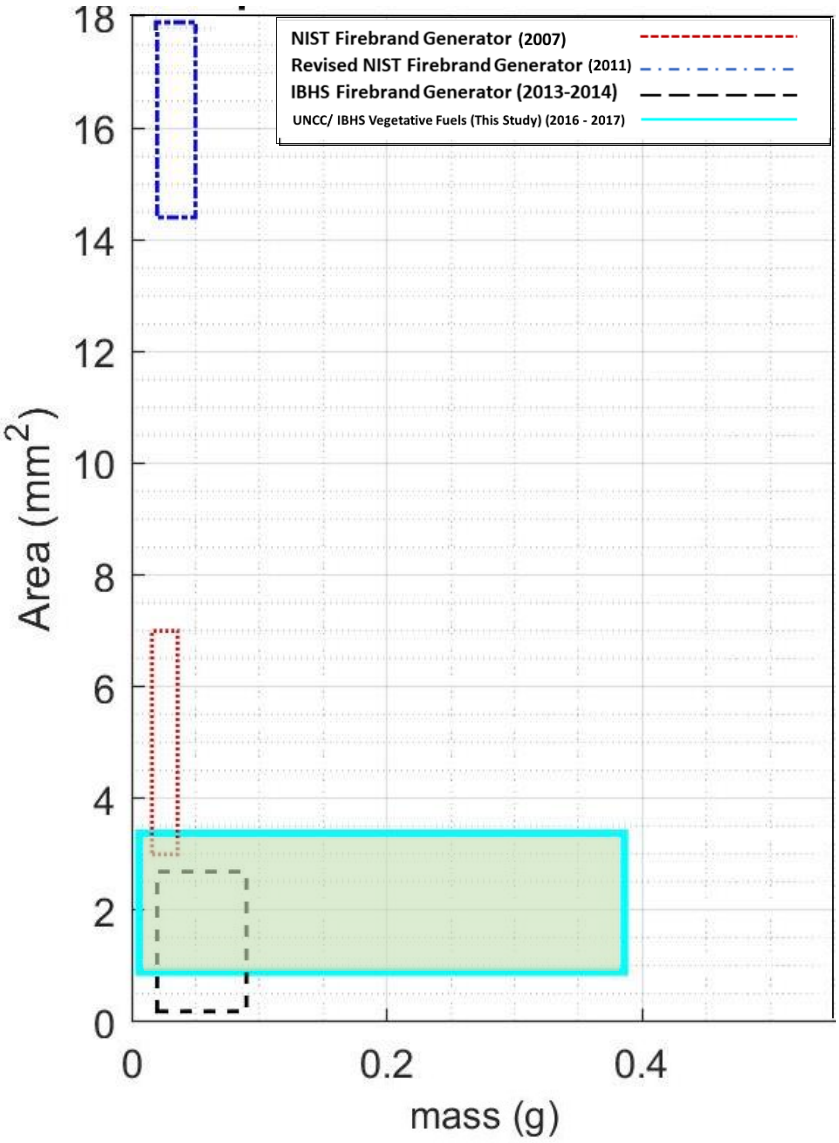

Figure 4.23. Comparison of Characteristic Values of Mass and Projected Area of Firebrands from various Experiments with 95% Confidence Interval

* Data are obtained from the following sources: 1) NIST Firebrand Generator (2007) from [60], 2) Revised NIST Firebrand Generator (2011) from [90], 3) IBHS Firebrand Generator (2013 – 2014) provided by IBHS Research Staff

Studies focused on vegetative firebrand reported average area values between 10 – 33 mm^2 (Blunck et al. 2019), and 120 – 212 mm^2 (Manzello et al. 2007).

4.3. Results and Discussion

Full-scale experiments were conducted to generate firebrands from burning vegetative in a controlled laboratory environment. More than 10,000 firebrands were produced, and a

total of 9,814 vegetative firebrands were analyzed during the experiments for this study, including 1,032 firebrands from grass specimens, 4,669 firebrands from shrub species, and 4,113 firebrands from tree species. To date, this is the largest firebrand dataset for vegetative fuels.

Characterization was performed on five species and three wind speed levels. Results from regression analysis conducted on individual and mutual effects of all sub-levels. In regression with multiple independent variables, the coefficient(s) indicates how much the expected positive and negative variation in a dependent variable while the independent variable increases by a certain percentage, holding all the other independent variables constant. The number of generated firebrands at various factor levels is summarized in Figure 4.24.

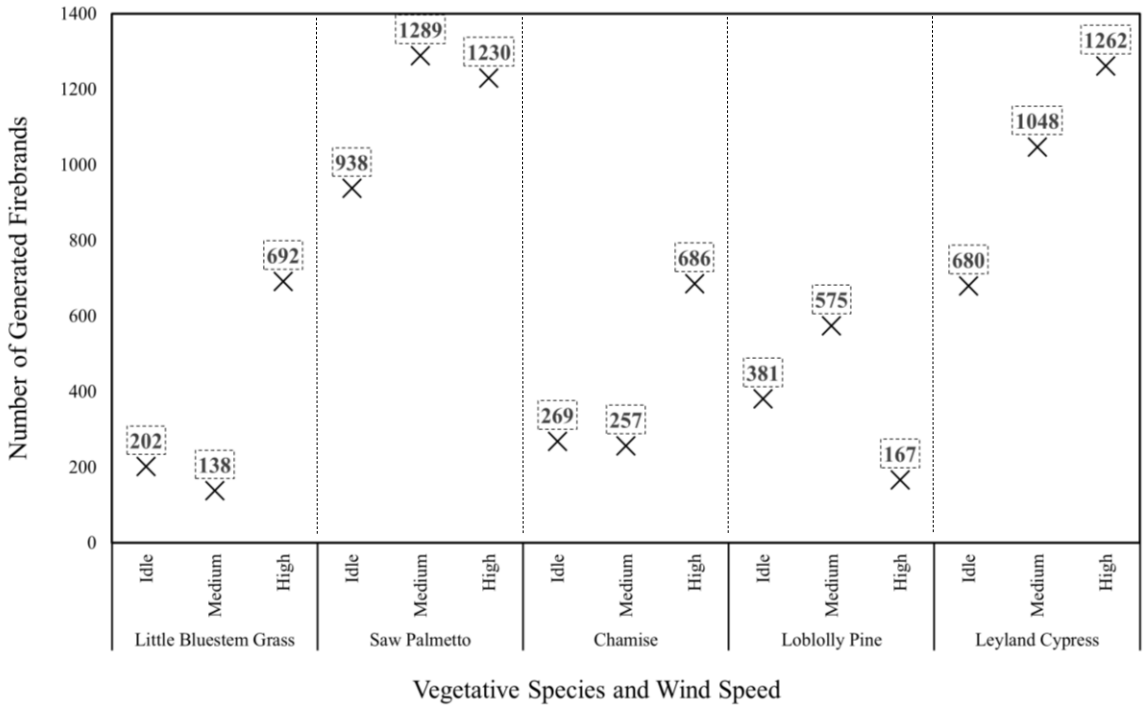

Figure 4.24. Effect of Vegetation Species and Wind Speed on Generation of Firebrands

4.3.1 Effect of Wind Speed and Vegetation Type on the Amount of Firebrand Generated

As seen in Figure 4.24, there was no consistent trend in terms of the number of generated firebrands for all species. Some species generated more firebrands at higher wind speeds relative to others. Reviewing of the whole dataset indicated that 41% of all firebrands were generated during experiments at the high wind speed level, followed by 34% and 25% for medium and idle wind speed levels, respectively.

On vegetation type level, increasing wind speed levels resulted in greater firebrand generation for shrub and tree samples. However, more firebrands were collected after idle wind speed experiments from grass samples compared to medium wind speed. It should be noted that high wind speed was responsible for the generation of 67% of firebrands in grass samples.

On the species level, still, no uniform trend is observed. The number of firebrands in high wind speed in Little Bluestem Grass is 5 and 3.5 times higher comparing to the medium and idle wind speed levels, respectively. In shrub species, Chamise followed a similar trend as Little Bluestem Grass. Note that Chamise whole plants were collected on the field, were taken apart, and shipped to IBHS, where they were reconstructed by inserting the shipped parts into wire cages (Figure 3.4). This process could affect the firebrand production process from reconstructed Chamise specimens comparing to a whole-plant Chamise. The number of generated firebrands from Saw Palmetto was also less than 5% different at medium and high wind speed levels.

For tree species, very different results were observed. While increasing the wind speed from idle in Leyland Cypress increased the firebrand generation process 1.5 and 1.9 times in the medium and high wind speeds, respectively, 51% of the firebrands generated from

the Loblolly pine were collected during medium wind speed level. It is worthy to remind that branches were spaced apart closer in Leyland cypress comparing to in Loblolly pine trees.

4.3.2 Effect of Wind Speed and Vegetation Type on Physical Properties of Firebrands

To better understand the effect of wind speed on mass and projected area of generated firebrands, a statistical test, *two-sample z-test*, was employed in vegetation type and species level based on the following criteria:

- the large population of the dataset (>30)
- known standard deviation
- the necessity to test a hypothesis
- data is normally distributed (after logarithmic and power transformation)

The z-Score indicates the distance between the standard deviation and the mean value of a datapoint. This statistical test is based on Gaussian distribution and determines if there is a statistically significant difference between two sets of scores when the population variance is known. The null hypothesis (H_0) in this test states that mean values in two groups are identical, alternatively (H_a) $\mu_1 \neq \mu_2$.

Results from the z-test for vegetation type are summarized in Table 4-19. If p-value > 0.05, the null hypothesis fails to be rejected, indicating there is no statistically significant difference in values of physical properties between two wind speed levels. If p-value < 0.05, the null hypothesis is rejected, meaning that wind speed level has had a significant effect in values of mass and/or projected area of firebrands.

Table 4-20. z-Test Results for Different Vegetation Types

Vegetation Type	*Physical Parameter*	*Wind Speed Level Change*	*p-Value*
Grass	Mass	Idle to Medium	1.00
		Idle to High	4.46×10^{-6} *
		Medium to High	2.2×10^{-16} *
	Projected Area	Idle to Medium	0.99
		Idle to High	0.001*
		Medium to High	1.71×10^{-14} *
Shrub	Mass	Idle to Medium	0.62
		Idle to High	2.22×10^{-10} *
		Medium to High	2.05×10^{-12} *
	Projected Area	Idle to Medium	2.18×10^{-7} *
		Idle to High	2.2×10^{-16} *
		Medium to High	4.48×10^{-9} *
Tree	Mass	Idle to Medium	0.99
		Idle to High	0.21
		Medium to High	1.01×10^{-9} *
	Projected Area	Idle to Medium	0.99
		Idle to High	0.28
		Medium to High	8.75×10^{-11} *

* There is a statistically significant difference between two wind speed levels

The following results can be extracted from Table 4-20:

- Grass: Higher wind speed significantly affected the mass and projected area values of firebrands, where the average mass values were reduced 1.6 and 6 times in the idle and medium wind speeds, respectively. A similar trend was observed for the projected area as the decrease was 1.2 and 1.6 for the idle and medium wind speed levels, respectively. The average value for firebrand mass was higher at high, idle, and medium wind speed levels, respectively. Regarding the correlation between mass and projected area, a similar trend was observed for average values of the projected area of firebrands is grass

species. This association indicated that firebrands generated from grass samples in high wind speed have a higher potential of initiating a spot fire.

- Shrubs: Increasing wind speed level resulted in higher values of mass and projected area of firebrands. In Chaparral specimens, the projected area was increased by 1.4 and 1.5 times when increasing the wind from idle and medium to high, respectively. A similar trend was observed for the average mass values. In Palmetto firebrands, the projected area was increased by 1.4 and 1.3 times when changing the wind speed from idle and medium to high, respectively.

  The average values of firebrand mass were less than 20% different in idle and medium wind speed levels for shrub species. This trend indicated that higher wind speeds resulted in larger and more massive firebrands, and consequently, potential lethality increased with increasing wind speed.

- Trees: A similar trend was observed in both species, where the average values for mass and projected area decreased from idle to medium wind speed and increased from medium to high wind speed levels. While this trend was similar, changes in the values of the physical properties of firebrands did not follow the same pattern. Firebrands generated from the Loblolly pine trees were 3 and 2 times larger in idle and medium wind speed comparing to high wind speed, respectively. The largest firebrands generated from the Leyland cypress were those at high speed, where the firebrands were 1.4 and 1.3 times larger than those at medium and idle wind speeds, respectively.

  High wind speed produced larger and heavier firebrands from Leyland cypress; thus, high wind speed can potentially initiate a spot fire when this species is dominant in a region during a wildfire.

CHAPTER 5: SUMMARY AND CONCLUSION

5.1 Summary

The firebrand phenomenon is one of the three main mechanisms in wildfire spread. There are three main sub-processes in the firebrand phenomenon: generation, lofting and transportation by fire plume or wind, and landing and potential ignition of recipient bed. Firebrands can be generated from both wildland (vegetative) and structural fuels. Studies showed that many factors in the firebrand phenomenon, including lofting height, flying distance, combustion rate, and ignition potential, are related to the physical properties of firebrands such as their mass and shape. Although there have been numerous field and laboratory studies on firebrand generation, the characterization and statistical analysis of firebrands to understand better the significance of impacts of various parameters (such as fuel classification and environmental conditions) have not been comprehensively studied.

To begin filling this gap, the main objectives of this study were to 1) develop a robust statistical framework considering both fuel characteristics and environmental conditions, and 2) perform a comprehensive statistical analysis so that the outcomes can benefit whoever is dealing with wildland and WUI problems such as homeowners, community and property managers, and standards-making committees.

A total of 51 full-scale laboratory experiments at three different wind speed levels, idle, medium, and high, representing the fluctuating velocity in atmospheric boundary layer flow, were conducted at the Insurance Institute for Business & Home Safety (IBHS) research center to observe, collect, and measure the vegetative firebrands generated from burning wildland fuels. The three average wind speed levels were: idle non-fluctuating (5.36-m/s or 12-mph), medium fluctuating (11.17-m/s or 25-mph), and high fluctuating

(17.88-m/s or 40-mph). Where the idle wind velocity was constant, the 3-s gust peaks for the fluctuating wind speeds were 14.3-m/s (32-mph), and 23-m/s (51-mph) for the fluctuating medium and high wind velocity record, respectively.

Three vegetation types, including trees, shrubs, and grass, representing various spatially distributed vegetative fuels, were evaluated. These types included five vegetation species including *Little Bluestem Grass (*grass*)*, *Saw Palmetto (*shrub*)*, *Chamise (*shrub*)*, *Loblolly Pine (*tree*)*, and *Leyland Cypress* (tree) were selected based on two criteria:

1) representative of vegetative fuels prone to ignition and contribution to firebrand generation in wildfires, and

2) availability and accessibility to research teams

Three replicates were used at each wind speed level. A consecutive sampling method was developed to collect landed firebrands after landing and being quenched in one of the 46 aluminum pans that were filled with water. Firebrands were then dried for at least 24-hours under standard conditions at 103°C in ovens. Physical properties of all firebrands, including mass, projected area, and flying distance, were measured or computed.

A thorough statistical analysis was performed to characterize the vegetative firebrands. Descriptive and inferential statistics were employed, a regression model was developed, and multiple statistical tests were utilized to evaluate the effect of wind speed, vegetation type, and vegetation species on the generation and physical properties of firebrands. A parametric model was developed to predict the value for firebrands mass using coefficients from a physical property (projected area), environmental conditions, and fuel characteristics.

5.2 Results and Conclusions

Outcomes of statistical tests in this study showed that higher wind speed affected the firebrand generation in grass specimens, although the magnitude of the effect differed by vegetation species. On vegetation-type level, increasing wind speed levels resulted in greater firebrand generation for shrub and tree samples. However, more firebrands were collected after idle wind speed experiments from grass samples compared to medium wind speed. The number of generated firebrands varied in shrub and tree specimens regarding different species. Out of near 10,000 characterized firebrands, 1,032 firebrands were generated from grass specimens, 4,669 firebrands from shrub species, and 4,113 firebrands from tree species. On the species level, still, no uniform trend was observed. While the number of generated firebrands were increased in Little Bluestem grass while increasing the wind speed and Chamise, it was not significantly (<5%) different in Saw Palmetto. Tree species showed a different behavior against the increase of wind speed, where most of the generated firebrands from Loblolly pine were at the medium wind speed. Firebrand production followed the same trend with the increase of wind speed in Cypress tree samples.

Statistical comparison of physical properties of firebrands showed that more massive and larger firebrands were generated at higher wind speeds as. Besides, the higher wind speeds did not have a consistent effect of generation in all species, where some species generated more firebrands in higher wind speeds compared to others. Reviewing of the whole dataset indicated that 41% of all firebrands were generated during experiments at the high wind speed level, following by 34% and 25% for medium and idle wind speed levels, respectively.

The BIC scores calculated for the four probability density functions, exponential, lognormal, gamma, and Weibull, indicated that the lognormal distribution resulted in the lowest value. No specific PDF can precisely predict the best distribution model for a dataset, however, the lowest BIC score indicated that the likelihood of fitting a lognormal distribution over this dataset was the highest, and this PDF was the best fit for this dataset. Data were investigated, transformed to logarithmic and power scale, and statistical tests were conducted to assure the model met the requirements of linear regression. Multiple statistical tests such as normality, non-constant variance, lack of fit, goodness-of-fit, and transformations were employed so that the dataset could be treated as it is following the Gaussian distribution to proceed with building the parametric model.

The correlation between mass and projected area in all species were positive and higher than 0.50. Tree species show the highest correlation among these two variables (> 0.89 in all wind speeds). No specific pattern was observed while considering the effect of wind speed changes on the correlation values. In other words, higher wind speed levels did not necessarily increase the correlation values between mass and projected areas.

Correlation among the physical properties of firebrands, especially mass and shape, was observed in previous experimental studies. However, it was seldom examined within a statistical framework. Correlation study in vegetation type and species level in this dataset showed a strong relationship between mass and projected area of firebrands regardless of fuel characteristics and environmental conditions of the experiment. It also indicated that higher wind speeds generated firebrands having greater mass and projected area. This was an important takeaway as the accumulation of firebrands on a recipient fuel may start a spot fire, depending on numerous parameters of landed firebrands, recipient bed, and

environmental factors. Nevertheless, it can be concluded that firebrands generated in higher wind speeds are potentially more lethal. Note that larger firebrands are being only one of the extreme weather factors that make wildfires more dangerous.

In regression with multiple independent variables, the coefficient(s) indicates how much the expected positive and negative variation in a dependent variable while the independent variable increases by a certain percentage, holding all the other independent variables constant.

Results also showed that with 95% confidence, the mass values of firebrands were between 0.02 and 0.33-gr, and values for the projected area were between 0.71 and 2.49-cm^2.

5.3 Significance and Implications of this Study

Sample sets of firebrands in the field and laboratory-controlled experiments are usually large, and characterization of various parameters can be a time-consuming and expensive process. A reliable statistical framework is an asset to facilitate the characterization of such data sets. This study has the most extensive sample set of vegetative firebrands to date, including almost 10,000 data points. The number of generated firebrands in each test is summarized in tables 4.1 to 4.6.

Predictive models based on physical properties, environmental conditions, and characteristics of vegetative fuels were developed in this study. The statistical analysis method developed in this study can be used in future firebrand characterization studies, so that interpretation of data achieves acceptable statistical reliability.

5.4 Future Study Suggestions

Developed methods in this study brought new knowledge in understanding the firebrand phenomenon (particularly firebrand generation). Findings in this study can be expanded to wildfire preparedness strategies in locations with dominant vegetative species similar to those in this study. Recommendations for future studies, especially in firebrand generation field, are as follow:

- As discussed in chapter four, a clear definition of firebrand and distinguishing between firebrand and fire debris is necessary for further characterization studies. This definition could assist in developing wildfire spread and spotting risk.
- A lack of physical and empirical models, specifically for the generation of firebrands, is noticeable. Similar models have been previously developed for lofting and transportation. However, ignition, detachment, and production of firebrands requires further investigation to parameterize the characteristics of vegetative firebrands successfully.
- There are limited data available from collected firebrands during the post-fire investigation of prescribed fires and wildfires, which make it challenging to validate the current parametric models developed based on laboratory experiments. Future studies should focus on experimental data from real wildfires, where firebrands are collected in the field, to assist with modeling efforts.
- There is a limited coupling between standards, codes, and guidelines with the firebrand exposure problem in wildfires. The quantification of firebrand exposure in this study can contribute to the WUI Fire Hazard Scale developed by (Maranghides and Mell 2013).

- Further supervised and unsupervised techniques can be developed to predict the characteristic physical properties of firebrands

BIBLIOGRAPHY

[1] Abatzoglou, John T., and A. Park Williams. 2016. “Impact of Anthropogenic Climate Change on Wildfire Across Western US Forests.” *Proceedings of the National Academy of Sciences* 113(42): 11770–75. http://www.pnas.org/lookup/doi/10.1073/pnas.1607171113.

[2] Abt, Robert, David Kelly, and Mike Kuypers. 1987. “The Florida Palm Coast Fire: An Analysis of Fire Incidence and Residence Characteristics.” *Fire Technology* 23(3): 230–52. http://link.springer.com/10.1007/BF01036938.

[3] Albini, Frank A., 1979. *Spot Fire Distance from Burning Trees: A Predictive Model*. Ogden, Utah: Intermountain Forest and Range Experiment Station, Forest Service, U.S. Dept. of Agriculture. file://catalog.hathitrust.org/Record/007421892.

[4] Albini, Frank A., 1981. *Spot Fire Distance from Isolated Sources -Extensions of a Predictive Model*. Ogden, Utah.

[5] Albini, Frank A. 1983a. “Potential Spotting Distance from Wind-Driven Surface Fires.” *United States Department of Agriculture* (April): 30.

[6] Albini, Frank A.1983b. “Transport of Firebrands by Line Thermals †.” *Combustion Science and Technology* 32(5–6): 277–88. http://www.tandfonline.com/doi/abs/10.1080/00102208308923662.

[7] Alessio Farcomeni, Luca Greco. 2016. *Robust Methods for Data Reduction*. CRC Press.

[8] Alexander Maranghides, William Mell. 2013. *Framework for Addressing the National Wildland Urban Interface Fire Problem--Determining Fire and Ember Exposure Zones Using a WUI Hazard Scale (NISTTN 1748) (No. Technical Note (NIST TN)-1748)*. https://www.nist.gov/publications/framework-addressing-national-wildland-urban-interface-fire-problem-determining-fire.

[9] Anderson, Roger C., 2006. “ Evolution and Origin of the Central Grassland of North America: Climate, Fire, and Mammalian Grazers 1 .” *The Journal of the Torrey Botanical Society*.

[10] Anthenien, Ralph A., Stephen D. Tse, and Carlos A. Fernandez-pello. 2006. “On the Trajectories of Embers Initially Elevated or Lofted by Small Scale Ground Fire Plumes in High Winds.” *Fire Safety Journal* 41: 349–63.

[11] Atreya, Arvind, Pawel Olszewski, Yawei Chen, and Howard R. Baum. 2017a. “The Effect of Size, Shape, and Pyrolysis Conditions on the Thermal Decomposition of Wood Particles and Firebrands.” *International Journal of Heat and Mass Transfer* 107: 319–28. http://dx.doi.org/10.1016/j.ijheatmasstransfer.2016.11.051.

[12] Barr, B. W., and O.A. Ezekoye. 2013. “Thermo-Mechanical Modeling of Firebrand Breakage on a Fractal Tree.” *Proceedings of the Combustion Institute* 34(2): 2649–56. http://dx.doi.org/10.1016/j.proci.2012.07.066.

[13] Bartlett, M. S., 1947. “The Use of Transformations.” *Biometrics* 3(1): 39–52. URL: https://www.jstor.org/stable/3001536.

[14] Baum, H., and Arvind Atreya. 2014. “A Model for Combustion of Firebrands of Various Shapes.” *Fire Safety Science* 11: 1353–67. http://www.iafss.org/publications/fss/11/1353.

[15] Bennett, Lauren T., Cristina Aponte, Thomas G. Baker, and Kevin G. Tolhurst. 2014. "Evaluating Long-Term Effects of Prescribed Fire Regimes on Carbon Stocks in a Temperate Eucalypt Forest." *Forest Ecology and Management*.

[16] Benzahra Belkacem, Fatima Zahra, Noureddine Zekri, and Mekki Terbeche. 2015. "Statistical Characterization of a Small World Network Applied to Forest Fires." In, 27–37. http://link.springer.com/10.1007/978-3-319-16619-3_3.

[17] Bland, J M., and D. G Altman. 1996. "Statistics Notes: Measurement Error." *BMJ* 312(7047): 1654–1654. http://www.bmj.com/cgi/doi/10.1136/bmj.312.7047.1654.

[18] Blunck, David L., Butler, Bret, Bailey, John, Wagenbrenner, Natalie. 2019. *Multi-Scale Study of Ember Production and Transport under Multiple Environmental and Fuel Conditions*. https://www.firescience.gov/projects/15-1-04-9/project/15-1-04-9_final_report.pdf.

[19] Boonmee, N., and J.G. Quintiere. 2002. "Glowing and Flaming Autoignition of Wood." *Proceedings of the Combustion Institute* 29(1): 289–96. https://linkinghub.elsevier.com/retrieve/pii/S1540748902800396.

[20] Box, G. E. P. Cox, and D. R. 1964. "An Analysis of Transformations." *Journal of the Royal Statistical Society* 26(2): 211–52. www.jstor.org/stable/2984418.

[21] CAL FIRE. 2019. California Department of Forestry and Fire Protection *Emergency Fund Fire Suppression Expenditures*. http://www.fire.ca.gov/fire_protection/downloads/SuppressionCostsOnepage.pdf.

[22] CAL FIRE. 2018. "Top 20 Most Destructive California Wildfires." (December 1). http://www.fire.ca.gov/communications/downloads/fact_sheets/Top20_Destruction.pdf.

[23] Calkin, David E., et al., 2011. USDA Forest Service - General Technical Report RMRS-GTR *A Comparative Risk Assessment Framework for Wildland Fire Management: The 2010 Cohesive Strategy Science Report*. https://www.fs.usda.gov/treesearch/pubs/38717.

[24] Calkin, David E., Jack D. Cohen, Mark A. Finney, and Matthew P. Thompson. 2014. "How Risk Management Can Prevent Future Wildfire Disasters in the Wildland-Urban Interface." *Proceedings of the National Academy of Sciences* 111(2): 746–51. http://www.pnas.org/cgi/doi/10.1073/pnas.1315088111.

[25] Center for Disaster Philanthropy. 2020. "2019-2020 Australian Bushfires." https://disasterphilanthropy.org/disaster/2019-australian-wildfires/ (February 20, 2020).

[26] "Chapter 3: Statistical Treatment." 1961. *Acta Physiologica Scandinavica* 51: 16–20.

[27] Climate Central. 2012. "The Age of Western Wildfires." *Western Wildfires*: 1–23. https://www.climatecentral.org/wgts/wildfires/Wildfires2012.pdf.

[28] Climate Signals. 2018. "Western Wildfire Season 2018." https://www.climatesignals.org/events/western-wildfire-season-2018

[29] Cohen, J D., 2008. "The Wildland-Urban Interface Fire Problem: A Consequence of the Fire Exclusion Paradigm." *Forest History Today* 2008: 20–26.

[30] D'Agostino, Ralph B., and Stephens, Michael A., 1986. "Tests Based on EDF Statistics." In *Goodness-of-Fit Techniques*, Marcel Dekker Inc., 97–185.

[31] Damodaran, Aswath. 2011. "Probabilistic Approaches: Scenario Analysis, Decision Trees, and Simulations." : 1–61. http://people.stern.nyu.edu/adamodar/pdfiles/papers/probabilistic.pdf.

[32] Datalab, Analyttica. 2019. “Akaike Information Criterion(AIC).” https://medium.com/@analyttica/akaike-information-criterion-aic-7a4b58bce206 (February 15, 2020).

[33] Deeming, John E. et al., 1974. “The National Fire-Danger Rating System.” *Fort Collins, CO: Rocky Mountain Forest and Range Experiment Station, Forest Service, U.S. Department of Agriculture* Res. Pap.

[34] Doanne, D.P, and L. E Seward. 2011. “Measuring Skewness.” *Journal of Statistics* 19(2): 1–18.

[35] Fernandez-Pello, A. C. et al., 2015. “Spot Fire Ignition of Natural Fuel Beds by Hot Metal Particles, Embers, and Sparks.” *Combustion Science and Technology* 187(1–2): 269–95. http://dx.doi.org/10.1080/00102202.2014.973953.

[36] Filkov, Alexander, et al., 2017. “Investigation of Firebrand Production during Prescribed Fires Conducted in a Pine Forest.” *Proceedings of the Combustion Institute* 36(2): 3263–70. http://linkinghub.elsevier.com/retrieve/pii/S1540748916301833.

[37] Fire Executive Council. 2009. *Guidance for Implementation of Federal Wildland Fire Management Policy*. Washington, DC, USA. https://www.nifc.gov/policies/policies_documents/GIFWFMP.pdf.

[38] Ganteaume, Anne, et al., 2011. “Laboratory Characterization of Firebrands Involved in Spot Fires.” *Annals of Forest Science* 68(3): 531–41. http://link.springer.com/10.1007/s13595-011-0056-4.

[39] Garfin, Gregg M., et al., 2018. *Chapter 25 : Southwest. Impacts, Risks, and Adaptation in the United States: The Fourth National Climate Assessment, Volume II*. Washington, DC. https://nca2018.globalchange.gov/chapter/25/.

[40] GeoMAC. 2019. “GeoMAC Wildland Fire Support.” https://www.geomac.gov/viewer/viewer.shtml.

[41] Gordon, DA. 2000. “Structure Survival in the Urban/Wildland Interface: A Logistic Regression Analysis of the 1991 Oakland/Berkeley Tunnel Fire.” University of California, Berkeley.

[42] Hakes, Raquel S.P., Hamed Salehizadeh, Matthew J. Weston-Dawkes, and Michael J. Gollner. 2019. “Thermal Characterization of Firebrand Piles.” *Fire Safety Journal* 104(June 2018): 34–42. https://doi.org/10.1016/j.firesaf.2018.10.002.

[43] Hargrove, W.W et al., 2000. “Simulating Fire Patterns in Heterogeneous Landscapes.” *Ecological Modelling* 135(2–3): 243–63. https://linkinghub.elsevier.com/retrieve/pii/S0304380000003689.

[44] Hedayati, Faraz, Bahrani, Babak, Zhou, Aixi, Quarles, Stephen L., Gorham, Daniel J. 2019. “A Framework to Facilitate Firebrand Characterization.” *Frontiers in Mechanical Engineering* 5(July): 1–14.

[45] Hedayati, Faraz. 2018. “Generation and Characterization of Firebrands from Selected Structural Fuels.” The University of North Carolina at Charlotte. https://librarylink.uncc.edu/login?url=https://search.proquest.com/docview/2036863709?accountid=14605.

[46] Hernandez, C., C. Keribin, P. Drobinski, and S. Turquety. 2015. “Statistical Modelling of [47]

Wildfire Size and Intensity: A Step toward Meteorological Forecasting of Summer Extreme Fire Risk." *Annales Geophysicae* 33(12): 1495–1506. https://www.ann-geophys.net/33/1495/2015/.

[47] Holmes, J.D., C.J. Baker, and Y. Tamura. 2006. "Tachikawa Number: A Proposal." *Journal of Wind Engineering and Industrial Aerodynamics* 94(1): 41–47. https://linkinghub.elsevier.com/retrieve/pii/S0167610505001121.

[48] Holmes, Thomas P., Jeffrey P. Prestemon, and Karen L. Abt. 2008. "An Introduction to the Economics of Forest Disturbance." In, 3–14. http://link.springer.com/10.1007/978-1-4020-4370-3_1.

[49] El Houssami, Mohamad, et al. 2016. "Experimental Procedures Characterising Firebrand Generation in Wildland Fires." *Fire Technology* 52(3): 731–51.

[50] Hudson, Tyler R., and David L. Blunck. 2019. "Effects of Fuel Characteristics on Ember Generation Characteristics at Branch-Scales." *International Journal of Wildland Fire*: 941–50.

[51] Jay, A et al. 2018. "Overview. In Impacts, Risks, and Adaptation in the United States: Fourth National Climate Assessment, Volume II." *U.S. Global Change Research Program, Washington*.

[52] Johnson, Norman L., Kotz, Samuel, Balakrishnan, N., 1964. "Continuous Univariate Distributions (Vol. 1)." In Wiley-Interscience, 207–59.

[53] Jolly, W. Matt et al., 2015. "Climate-Induced Variations in Global Wildfire Danger from 1979 to 2013." *Nature Communications* 6(1): 7537. http://dx.doi.org/10.1038/ncomms8537.

[54] Kernler, Dan. 2018. "Normal Distribution." https://en.wikipedia.org/wiki/File:Empirical_Rule.PNG.

[55] Koo, Eunmo, Patrick J. Pagni, David R. Weise, and John P. Woycheese. 2010. "Firebrands and Spotting Ignition in Large-Scale Fires." *International Journal of Wildland Fire* 19(7): 818. http://www.publish.csiro.au/?paper=WF07119.

[56] Kowarik, Alexander. 2019. "Boxcox Power Transformation." https://www.rdocumentation.org/packages/EnvStats/versions/2.3.1/topics/boxcox.

[57] Liu, Yongqiang, Scott L. Goodrick, and John A. Stanturf. 2013. "Future U.S. Wildfire Potential Trends Projected Using a Dynamically Downscaled Climate Change Scenario." *Forest Ecology and Management* 294: 120–35. http://dx.doi.org/10.1016/j.foreco.2012.06.049.

[58] Manzello, Samuel. L., Maranghides, Alexander, Shields, Jogm R., and Mell, william E.. 2007. "Measurement of Firebrand Production and Heat Release Rate (HRR) from Burning Korean Pine Trees." *Fire Safety Science 7*: 108–16.

[59] Manzello, Samuel L., et al., 2008. "Experimental Investigation of Firebrands: Generation and Ignition of Fuel Beds." *Fire Safety Journal* 43(3): 226–33. https://linkinghub.elsevier.com/retrieve/pii/S0379711207000811.

[60] Manzello, Samuel L. et al. 2008. "On the Development and Characterization of a Firebrand Generator." *Fire Safety Journal* 43(4): 258–68.

[61] Manzello, Samuel L. et al., 2009. "Mass and Size Distribution of Firebrands Generated from Burning Korean Pine (Pinus Koraiensis) Trees." *Fire and Materials* 33(1): 21–31. http://doi.wiley.com/10.1002/fam.977.

[62] Manzello, Samuel L., 2014. "Special Issue on Wildland–Urban Interface (WUI) Fires." *Fire Technology* 50(1): 7–8. http://link.springer.com/10.1007/s10694-012-0319-0.

[63] Manzello, Samuel L., and Ethan Foote. 2014. “Characterizing Firebrand Exposure from Wildland-Urban Interface (WUI) Fires: Results from the 2007 Angora Fire.” *Fire Technology* 50(1): 105–24.

[64] Manzello, Samuel L., and Maranghides, Alexander. 2007. “Measurement of Firebrand Production and Heat Release Rate (HRR) from Burning Korean Pine Trees.” *Fire Safety Science 7*: 108–16.

[65] Manzello, Samuel L., Maranghides, Alexander, and Mell, Willaim E.. 2007. “Firebrand Generation from Burning Vegetation.” *International Journal of Wildland Fire* 16(4): 458–62.

[66] Manzello, Samuel L., and Sayaka Suzuki. 2014. “Exposing Decking Assemblies to Continuous Wind-Driven Firebrand Showers.” In *Fire Safety Science*.

[67] Manzello, Samuel L., and Sayaka Suzuki. 2017. “Generating Wind-Driven Firebrand Showers Characteristic of Burning Structures.” *Proceedings of the Combustion Institute* 36(2): 3247–52. https://linkinghub.elsevier.com/retrieve/pii/S1540748916302656.

[68] Manzello, Samuel L., Sayaka Suzuki, Michael J. Gollner, and A. Carlos Fernandez-Pello. 2020. “Role of Firebrand Combustion in Large Outdoor Fire Spread.” *Progress in Energy and Combustion Science* 76: 100801. https://doi.org/10.1016/j.pecs.2019.100801.

[69] Maranghides, Alexander, and William Mell. 2011. “A Case Study of a Community Affected by the Witch and Guejito Wildland Fires.” *Fire Technology* 47(2): 379–420.

[70] McArthur, A.G., 1967. *Fire Behaviour in Eucalypt Forests*. Canberra : Forestry and Timber Bureau. https://trove.nla.gov.au/version/26402708.

[71] Mell, William E., et al., 2010. “The Wildland - Urban Interface Fire Problem - Current Approaches and Research Needs.” *International Journal of Wildland Fire* 19(2): 238. http://www.publish.csiro.au/?paper=WF07131.

[72] Mell, William E., Alexander Maranghides, Randall McDermott, and Samuel L. Manzello. 2009. “Numerical Simulation and Experiments of Burning Douglas Fir Trees.” *Combustion and Flame* 156(10): 2023–41. http://dx.doi.org/10.1016/j.combustflame.2009.06.015.

[73] MNP LLP. 2017. *A Review Of the 2016 Horse River Wildfire*. Edmonton, AB. https://www.alberta.ca/assets/documents/Wildfire-MNP-Report.pdf.

[74] Mun, Johnathan. 2008. “Understanding and Choosing the Right Probability Distributions.” : 899–917. https://onlinelibrary.wiley.com/doi/pdf/10.1002/9781119197096.app03.

[75] Muraszew, A, and J. B. Fedele. 1976. *Statistical Model for Spot Fire Hazard*. El Segundo, Calif.: Engineering Science Operations, The Aerospace Corp.

[76] Myung, In Jae. 2003. “Tutorial on Maximum Likelihood Estimation.” *Journal of Mathematical Psychology* 47(1): 90–100.

[77] National Interagency Fire Center (NICC). 2019. *Wildland Fire Summary and Statistics Annual Report 2019*. https://www.predictiveservices.nifc.gov/intelligence/2019_statssumm/2019Stats&Summ.html (February 15, 2020).

[78] NASA. 2018. “Southeastern U.S. Sees Wildfire Activity.” https://www.nasa.gov/image-feature/goddard/2018/southeastern-us-sees-wildfire-activity/

[79] Pagan, A. R., and Breusch, T. S., 1979. “A Simple Test for Heteroscedasticity and Random

Coefficient Variation." *Econometrica* 47(5): 1287–94.

[80] Peter J. Huber. 2004. *Robust Statistics*. Wiley.

[81] Poole, Michael A., and Patrick N. O'Farrell. 1971. "The Assumptions of the Linear Regression Model." *Transactions of the Institute of British Geographers*.

[82] Porterie, Bernard, Nouredine Zekri, Jean-Pierre Clerc, and Jean-Claude Loraud. 2007. "Modeling Forest Fire Spread and Spotting Process with Small World Networks." *Combustion and Flame* 149(1–2): 63–78. https://linkinghub.elsevier.com/retrieve/pii/S0010218006002896.

[83] Posada, David, and Thomas R. Buckley. 2004. "Model Selection and Model Averaging in Phylogenetics: Advantages of Akaike Information Criterion and Bayesian Approaches over Likelihood Ratio Tests." *Systematic Biology* 53(5): 793–808.

[84] Ramsay, G.C., N.A. McArthur and V.P. Dowling. 1986. "Building Survival in Bushfires." In *Fire Science 186: The 4th Australian National Biennial Conference*, 17.

[85] Razali, Nornadiah Mohd, Yap Bee Wah, and Mathematical Sciences. 2011. "Power Comparisons of Shapiro-Wilk, Kolmogorov-Smirnov, Lilliefors, and Anderson-Darling Tests." *Journal of Statistical Modeling and Analytics* 2(1): 21–33.

[86] Schwarz, Gideon. 1978. "Estimating the Dimension of a Model." *Annals of Statistics* 6(2): 461–64.

[87] Service, National Part. 2017. *Chimney Tops 2 Fire Review- Individual Fire Review Report*. Boise, Idaho. https://wildfiretoday.com/documents/ChimneyTops2Report.pdf.

[88] Stoline, Michael R., 1991. "An Examination of the Lognormal and Box and Cox Family of Transformations in Fitting Environmental Data." *Environmetrics* 2(1): 85–106.

[89] Suresh, Sharma. 2014. *Nursing Research and Statistics*. Elsevier Health Sciences.

[90] Suzuki, S., and S. Manzello. 2011. "On the Development and Characterization of a Reduced Scale Continuous-Feed Firebrand Generator." *Fire Safety Science* 10(1): 1437–48. http://www.iafss.org/publications/fss/10/1437.

[91] Suzuki, Sayaka, and Samuel L. Manzello. 2016. "Firebrand Production from Building Components Fitted with Siding Treatments." *Fire Safety Journal* 80: 64–70. https://linkinghub.elsevier.com/retrieve/pii/S0379711216300091.

[92] Suzuki, Sayaka, Samuel L. Manzello, and Yoshihiko Hayashi. 2013. "The Size and Mass Distribution of Firebrands Collected from Ignited Building Components Exposed to Wind." *Proceedings of the Combustion Institute* 34(2): 2479–85. https://linkinghub.elsevier.com/retrieve/pii/S1540748912001691.

[93] Suzuki, Sayaka, Samuel L. Manzello, Matthew Lage, and George Laing. 2012. "Firebrand Generation Data Obtained from a Full-Scale Structure Burn." *International Journal of Wildland Fire* 21(8): 961. http://www.publish.csiro.au/?paper=WF11133.

[94] Tachikawa, M., 1988. "A Method for Estimating the Distribution Range of Trajectories of Wind-Borne Missiles." *Journal of Wind Engineering and Industrial Aerodynamics* 29(1–3): 175–84. https://linkinghub.elsevier.com/retrieve/pii/0167610588901560.

[95] Thomas, Jan C., et al., 2017. "Investigation of Firebrand Generation from an Experimental Fire: Development of a Reliable Data Collection Methodology." *Fire Safety Journal* 91(April): 864–71. http://dx.doi.org/10.1016/j.firesaf.2017.04.002.

[96] Tohidi, Ali, Nigel Kaye, and William Bridges. 2015. “Statistical Description of Firebrand Size and Shape Distribution from Coniferous Trees for Use in Metropolis Monte Carlo Simulations of Firebrand Flight Distance.” *Fire Safety Journal* 77: 21–35. http://dx.doi.org/10.1016/j.firesaf.2015.07.008.

[97] Tompkins, F., Deconcini, C., 2014. “Western U.S. Wildfires and the Climate Change Connection.” *World Resource Institute* (September): 1–6. http://www.wri.org/sites/default/files/WRI14_Factsheets_Western_US_Wildfires.pdf.

[98] ToolBox, Engineering. 2012. “Moisture Content.” https://www.engineeringtoolbox.com/moisture-content-d_1821.html.

[99] Vodvarka, Frank J., 1969. *Firebrand Field Studies- Final Report*. IIT Research Institute. Chicago, IL.

[100] Vodvarka, Frank J., 1970. *Urban Burns - Full-Scale Field Studies*. IIT Research Institute. Chicago, IL.

[101] Westerling, Anthony Le Roy. 2016. “Increasing Western US Forest Wildfire Activity: Sensitivity to Changes in the Timing of Spring.” *Philosophical Transactions of the Royal Society B: Biological Sciences* 371(1696).

[102] Wilson, A.A.G, and I.S. Ferguson. 1986. “Predicting the Probability of House Survival during Bushfires.” *Journal of Environmental Management* 23: 259–70. http://hdl.handle.net/102.100.100/273966?index=1.

[103] Yoshioka, Hideki, Yoshihiko Hayashi, Hideaki Masuda, and Takafumi Noguchi. 2004. “Real-Scale Fire Wind Tunnel Experiment on Generation of Firebrands from a House on Fire.” *Fire Science and Technology* 23(2): 142–50.

[104] Zhou, Aixi, Quarles, Stephen L. Weise, David R., 2019. *Fire Ember Production from Wildland and Structural Fuels*. JFSP 15-1-04-4 Final Report. https://www.firescience.gov/projects/15-1-04-4/project/15-1-04-4_final_report.pdf

[105] Zhou, Kuibin, Sayaka Suzuki, and Samuel L. Manzello. 2015. “Experimental Study of Firebrand Transport.” *Fire Technology* 51(4): 785–99. http://dx.doi.org/10.1007/s10694-014-0411-8.